ÉCOLE DE TECHNOLOGIE SUPÉRIEURE
UNIVERSITÉ DU QUÉBEC

THESIS PRESENTED TO
ÉCOLE DE TECHNOLOGIE SUPÉRIEURE

IN PARTIAL FULFILLEMENT OF THE REQUIREMENTS FOR
THE DEGREE OF DOCTOR OF PHILOSIPHY
PH. D.

BY
Francis PELLETIER

POWER PERFORMANCE EVALUATION AND IMPROVEMENT OF OPERATIONAL WIND POWER PLANTS

MONTREAL, APRIL 4, 2014

BOARD OF EXAMINERS

THIS THESIS HAS BEEN EVALUATED

BY THE FOLLOWING BOARD OF EXAMINERS

Mr. Christian Masson, Thesis Supervisor
Department of Génie Mécanique at École de technologie supérieure

Mr. Antoine Tahan, Thesis Co-supervisor
Department of Génie Mécanique at École de technologie supérieure

Mr. Simon Joncas, President of the Board of Examiners
Department of Génie de la production automatisée at École de technologie supérieure

Mr. Louis Lamarche, Member of the jury
Department of Génie Mécanique at École de technologie supérieure

Mr. Hussein Ibrahim, External Evaluator
TechnoCentre éolien

THIS THESIS WAS PRENSENTED AND DEFENDED

BEFORE A BOARD OF EXAMINERS AND PUBLIC

MARCH 21, 2014

AT ÉCOLE DE TECHNOLOGIE SUPÉRIEURE

ACKNOWLEDGMENT

It goes without saying that a project of this scope could not have been completed without the precious collaboration of a number of individuals and companies.

Firstly, I would like to thank my director and co-director for their financial and technical support throughout this long endeavour. Without the confidence of my director Dr. Masson, this project would never have been completed. I also thank Dr. Masson for providing the opportunity to gain invaluable experience and contacts in the research sector. A special thanks to my co-director Dr. Tahan as well for always being there to answer my questions and for supporting me at every step of the elaboration of this project.

Several individuals from within various companies have also made this project possible. My sincere thanks to Martin Jetté of OSIsoft for the financial and priceless technical support he and all of his team offered. Thanks also to Normand Bouchard, Robert Guillemette, and all the technicians at Cartier, without whose help this project would not have been possible. Special acknowledgement goes to GL GH for its financial assistance and specifically to Bouaziz Ait-Driss and Dariush Faghani for the technical support they so graciously provided. Thanks to Philippe Giguère and Peter Gregg of GE for their support without which this project would have been unfeasible.

I also express my gratitude to the IT technicians (Mamadou Gueye, Martin Gauthier) at ETS for their great work in installing and maintaining the PI system. Martin Boulay from Ohméga and his team also provided vital assistance in the installation and follow-up of the PI system. I also thank all the trainees who supported me throughout this project.

Lastly and most importantly, I thank my partner Katia for her unconditional support, her trust and her complete confidence in me throughout this project. I am not able to thank her enough for giving us our two beautiful girls as well: Élia and Sofia. Thanks to my little girls for being so proud of me.

POWER PERFORMANCE EVALUATION AND IMPROVEMENT OF OPERATIONAL WIND POWER PLANTS

Francis PELLETIER

RESUME

L'exploitation de centrales éoliennes à une échelle industrielle est plutôt récente. Avec cette nouvelle ère industrielle, les exploitants sont parfois enclins à appliquer à l'éolien les mêmes méthodes d'évaluation et d'amélioration de performance (économique, énergétique, environnementale, etc.) que celles utilisées pour leurs centrales électriques dites conventionnelles. L'évaluation de la performance énergétique est sans contredit le paramètre le plus étudié par les exploitants. La comparaison entre la production énergétique réelle d'une centrale (habituellement l'électricité) et l'apport énergétique nécessaire à cette centrale (ex. : charbon, pétrole, vent, etc.) permet d'évaluer sa performance énergétique. Cette évaluation ne représente habituellement pas un défi technique important pour les centrales dites conventionnelles. Cependant, la nature complexe du vent et de son interaction avec les éoliennes rend cette évaluation ardue et laborieuse pour le domaine éolien.

À l'heure actuelle, seule la norme CEI 61400-12-1 est acceptée par l'industrie. Cependant, cette méthode est onéreuse et permet l'évaluation de la performance énergétique d'une seule éolienne à la fois. De plus, l'utilisation de cette norme par l'industrie depuis plus de 15 ans a permis d'établir clairement ses limites d'applicabilité et sa précision relative, conséquence des hypothèses simplificatrices qui ont été retenues.

Le premier objectif de ce projet consiste donc à tenter d'améliorer les méthodes présentement utilisées pour l'évaluation de la performance énergétique des éoliennes et des centrales éoliennes en phase d'exploitation. Ainsi, l'élaboration d'un modèle à l'aide de réseau de neurones à six entrées (*inputs*) et selon une technique à plusieurs étapes a permis d'obtenir une modélisation minutieuse de la courbe de puissance de deux éoliennes. Les résultats de ce modèle ont été comparés à plusieurs autres techniques de modélisation et sa précision accrue a été démontrée pour les cas analysés.

Le deuxième objectif de ce projet consiste à tenter d'améliorer la production énergétique de projets éoliens déjà en exploitation. À la suite de l'identification d'un modèle affichant une précision accrue, des essais sur deux éoliennes en exploitation ont été réalisés sur une période de presque deux ans. La méthode choisie afin de tenter d'améliorer la production énergétique consiste à optimiser l'orientation des girouettes nacelles. Les résultats obtenus ont permis d'anticiper des gains énergétiques potentiels de l'ordre de 1% à 3 %.

Finalement, plusieurs résultats provenant de ce projet de recherche ont été appliqués dans divers contextes industriels. Plus spécifiquement, un propriétaire de projet éolien ayant fait

l'acquisition d'une option d'amélioration de performance a fait appel à l'auteur de ce document afin de quantifier les gains énergétiques y étant associés. Une méthode de comparaison « Side-by-side » a été utilisée sur deux éoliennes ayant reçu l'option d'amélioration de performance. Divers tests statistiques ont été développés afin de quantifier les gains énergétiques ainsi que leur niveau de précision.

Mots clefs : éolienne, test de performance, amélioration de performance, réseau de neurone, erreur d'orientation, Girouette.

POWER PERFORMANCE EVALUATION AND IMPROVEMENT OF OPERATIONAL WIND POWER PLANTS

Francis PELLETIER

ABSTRACT

The operation of wind farms on an industrial scale is relatively recent. With this new industrial era, wind farm operators are sometimes inclined to apply to wind the same methods of assessment and performance improvement (economic, energy, environmental, etc.) as those used for their so-called conventional power plants. The evaluation of energy performance is unquestionably one of the parameters most analyzed by operators. Energy performance can be evaluated by comparing the energy production of a plant (usually electricity) and the energy intake required for the said facility (e.g. coal, oil, wind, etc.). This assessment does not usually represent a significant technical challenge for so-called conventional plants. However, the complex nature of wind and its interaction with wind turbines makes this evaluation difficult for the wind energy sector.

At present, the IEC 61400-12-1 standard is the only method accepted by the industry and which allows the energy performance of a single turbine to be evaluated. However, this approach is relatively costly. Further, the application of this standard in the industry over the past 15+ years has clearly established a number of associated limits.

Thus, the first objective of this project was to try to improve current methods for assessing the energy performance of operational wind turbines and wind farms. In this context, the power curves of two wind turbines were able to be deducted by means of a model based on a neural network with six inputs and a multi-step technique. The results of this model were compared to several other modelling techniques and an increased accuracy was demonstrated for the cases analyzed.

The second objective of this project consisted of attempting to improve the performance of turbines already in operation. After developing a more accurate method for power performance evaluation, tests on two operational turbines were conducted. The method used in an effort to increase energy production was based on optimizing the orientation of the nacelle-mounted wind vanes. Tests were conducted to assess the effect of wind vane orientation on the energy performance and the results obtained suggested that potential energy gains in the order of 1-3% could be achieved.

Lastly, a number of findings from this project have been applied to various industrial projects in different contexts. Specifically, one wind farm owner has requested the services of the author to analyze the energy gain achieved pursuant to the installation of an improvement package on some of its wind turbines. A side-by-side comparison has been completed on two

turbines fitted with this improvement package. Statistical tests have been developed in order to properly assess and quantify the energy gain and the associated uncertainty level.

Key words : wind turbine, power performance testing, power performance improvement, artificial neural network, yaw error, yaw offset, wind vane.

TABLE OF CONTENTS

Page

LIST OF TABLES

Page

LIST OF FIGURES

Page

LIST OF ABREVIATIONS

AEP	Annual Energy Production
ANN	Artificial Neural Network
GUM	Guide to the Expression of Uncertainty
IEC	International Electrotechnical Commission
IYO	Imposed Yaw Offset
LIDAR	Light Detection and Ranging
MLP	Multi-layer Perceptron
O&M	Operation and Maintenance
PF	Power Factor
PF_n	Normalized Power Factor
PPA	Power Purchase Agreement
PPE	Power Performance Evaluation
PPI	Power Performance Improvement
SODAR	Sonic Detection and Ranging
TCE	TechnoCentre éolien
WPP	Wind Power Plant
WTG	Wind Turbine Generator

LIST OF SYMBOLS

C_p	Coefficient of performance
IYO	Imposed Yaw Offset [^{o}]
P	Active power output [kW]
$\hat{P}$	Estimated power output from the multi-stage ANN model [kW]
PF	Power Factor
PF_n	Normalized Power Factor
R	Rotor Radius [m]
TI	Turbulence Intensity [%]
WS	Wind shear (V_{80m}/V_{40m})
WD	Nacelle orientation [deg]
v	Instantaneous free stream wind speed [m.s^{-1}]
v_{10min}	10-minute average wind speed [m.s^{-1}]
V	10-minute nacelle wind speed [m.s^{-1}]
V40	10-minute average wind speed at 40m agl [m.s^{-1}]
V80	10-minute average wind speed at 80m agl [m.s^{-1}]
V_n	Air density normalized wind speed [m.s^{-1}]
λ	Tip speed ratio
ρ	Air density [kg.m^{-3}]
ρ_0	Reference air density [kg.m^{-3}]
σ_{10min}	10-minute standard deviation of wind speed [m.s^{-1}]
Φ_y	Yaw error angle compared to turbine centre line [^{o}]

Φ_{dev}	Angle given by the anemometer, also referred as the wind deviation [^{o}]
Φ_{turb}	Nacelle orientation angle compared to true north [^{o}]
Φ_{w}	Wind direction angle compared to true north [^{o}]
Φ_{YO}	Yaw Offset angle [^{o}]
ω	Rotor rotational speed [rad.s^{-1}]

INTRODUCTION

Context

Though the generation of wind energy on an industrial scale has been around for several decades, Wind Power Plants (WPP) with installed capacities of more than 100 MW are relatively new, but have been becoming more common in recent years. The objectives established in the framework of the Government of Quebec's energy policy (2006-2015) with regard to wind energy are an illustration of this trend. Indeed, Quebec has established an objective of installing 4,000 MW of wind capacity by the end of 2015. Once in operation, this figure will represent close to 10% of the nominal power output of Hydro-Québec's production capacity. Similar examples of energy policies with high levels of penetration for wind energy can be found in all other Canadian provinces and around the world. Figure 0-1 presents the wind capacity built to date and projected (i.e. with signed Power Purchase Agreements (PPA)) in Quebec (Technocentre Éolien, 2012).

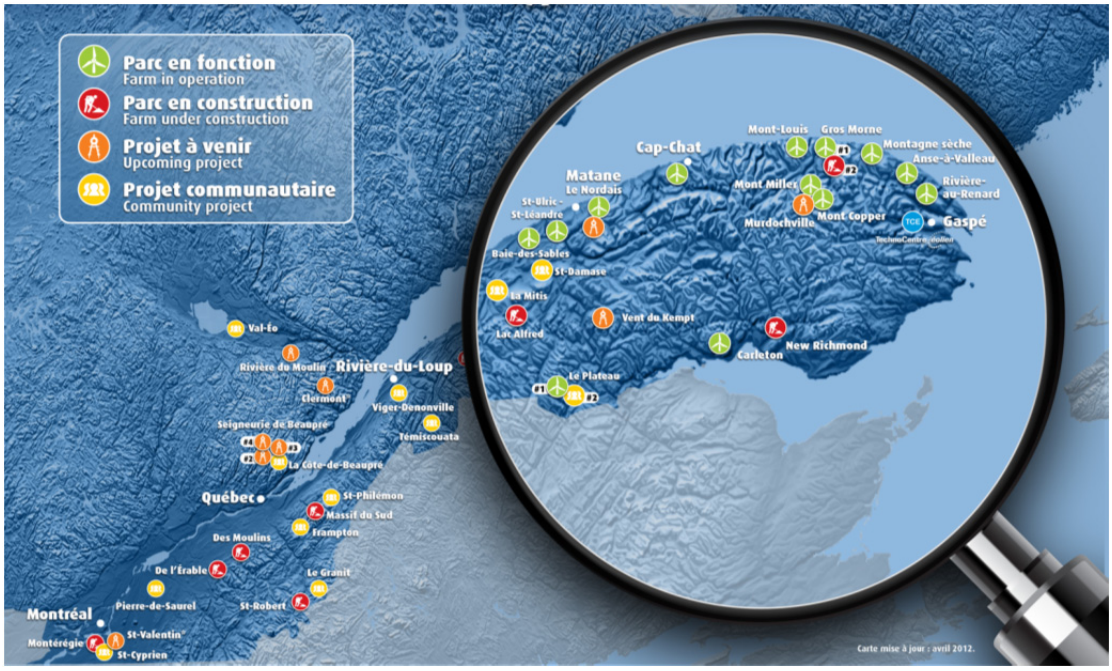

Figure 0-1 Quebec installed and projected wind power plants
(Obtained from TCE, 2012)

In this new context and because the profitability of wind assets is subject to very tight margins, wind farm operators are now paying attention to elements that were not considered significant just a few years ago. Likewise, owners are increasingly interested in investigating new avenues that could optimize their return on investment. New methods, research, tools or services that were not economically viable in the past are now beginning to emerge.

Numerous modern studies (Bell, 2008; Kragh, 2013; Randal, 2008) and even recent specifically dedicated conferences (*Wind Farm Underperformance & Partnerships Conference*, Texas 2012) suggest that operational wind power plants typically exhibit potential for power performance improvement in the order of 1-2% over current output. A good comprehension and improved control of the power performance evaluation (PPE) of the wind assets is therefore crucial to understanding the actual energy inefficiencies and to ensure that proposed mitigation methods are conveniently developed, analyzed, implemented and that their published benefits are valid.

In light of the increased interest of wind farm owners and operators in this field, and because this study is fundamentally focused on improving current methodologies for evaluating and improving power performance outputs of wind assets, several technical and financial partners have agreed to participate in this project.

Technical Challenges and Background

Despite the importance of PPE and the fact that a number of working groups and researchers have been conducting studies in this area for several years, the most widely used methodology, IEC61400-12-1 (International Electrotechnical Commission, 2005), has typically shown an uncertainty level in the order of 5-8% (Pedersen et al., 2002). Although several attempts have been proposed in order to decrease this level of uncertainty (through turbulence intensity normalization (Albers, 2010), wind shear and veer (Wagner, 2010), and numerous other methodologies (Albers, 2004; Anahua et al., 2008; Antoniou et al., 2007; Llombart et al., 2005a; Llombart et al., 2005b; Montes et al., 2009), the level of uncertainty is still typically greater than the 1-2% presented earlier.

The i) stochastic nature of the wind combined with the fact that today's wind turbine rotors are significantly larger than those of the past (>100 m in diameter), ii) the fact that only one wind speed measurement point (at hub height) is generally considered, and iii) the non-linear relationship of power as a function of wind speed or other meteorological variables are all elements that, when combined, represent an important challenge in achieving a proper PPE of individual wind turbines and especially of an entire WPP. This poor level of precision of current PPE techniques renders the detection of underperformance and the evaluation of efficiency improvement measures difficult or unreliable.

Objectives and Methodologies

This study has two main objectives: i) to improve current PPE techniques for individual wind turbines, and ii) to demonstrate a potential improvement in the Annual Energy Production (AEP) of the wind assets under study. Ideally, this increase in AEP would be in the order of 1% or more.

The first objective will mainly focus on the techniques for the PPE of individual WTGs. To date, only the project team PT 61400-12-3 from the IEC Technical Committee 88 (TC 88 / PT 61400-12-3) (TC88WG6, 2004) has proposed to publish a Technical Specification (TS) that will detail a procedure for power performance testing of an entire WPP. This technical specification has not yet been issued nor has the date of publication been determined. Furthermore, no official verification using this proposed methodology has been completed for large WPP located in complex terrain, meaning that the uncertainty level of this method is still unknown. Consequently, PPE for the vast majority of new, large WPP can only be accomplished using partial methodologies, each with their own technical and commercial shortcomings. For this reason, it has been decided that PPE of individual wind turbines would be more relevant in that modelling the behaviour of an individual WTG would be more easily achievable than that of an entire WPP. Additionally, if a significant increase in the precision of a prediction is found through the PPE of individual WTGs, it is expected that by extension this improvement could be applied to an entire WPP.

This first objective will be achieved through testing and comparison of several power performance modelling techniques (old and novel) for wind turbines. In order to do so, real operational data of existing wind turbines will be used. The standard modelling process – data normalization, recoding, reduction and linearization, modelling elaboration, modelling validation (residual analysis) – will be used for this part of the study. Models will be compared by quantifying the error levels of each model.

The second objective will consist of identifying and testing concrete novel methodologies that will increase the energy output of the WTGs under study. This objective will mainly focus on the identification, installation, testing and assessment (through statistical tests) of techniques/methods that would contribute to an increase in AEP. Emphasis will be made on techniques that could be applied to individual WTGs. Ideally, the power performance improvement of the proposed methodology or methodologies would enable an increase in AEP of approximately 1% or greater.

Further, in order to achieve the second objective, a thorough review of literature will be completed and a steering committee will be created in order to identify the most realistic method that could be used in the context, timeframe and logistic possibilities of the actual study. Once such a method has been proposed to and approved by the turbine manufacturer and the wind farm owner, it will be implemented on two selected WTGs. Optimal models developed in the context of the first objective will be used in the pursuit of this second objective in order to perform a continuous monitoring and statistical assessment of the level of improvement of the proposed method.

Thesis Organization

This dissertation is presented in several chapters. Chapter 1 will present a concise review of literature with regard to current methods used for PPE of individual WTGs.

Chapter 2 will present the review of literature and the recommendations received from the steering committee with regard to current methods used for Power Performance Improvement (PPI).

Chapter 3 describes the database provided and installed specifically for this project, which is the foundation for the entire study (and future studies of the *Research Laboratory on the Nordic Environment Aerodynamics of Wind Turbines*, NEAT).

Chapter 4 presents all the steps required to develop a novel technique for modelling WTG power curves, i.e. modelling through Artificial Neural Networks (ANN). The results of this model will be compared with those of discrete, parametric, and non-parametric models.

Chapter 5 and Chapter 6 provide the results obtained using the author's methodology (through ANN) and the Side-by-side methodology for two case studies: i) improvement of AEP through yaw offset optimization and ii) improvement of AEP through aerodynamic component and control algorithm changes.

Lastly, a brief overview of a patent developed during the elaboration of this project is presented in Annex I. This patent enables the *in-situ* calibration of a nacelle-mounted wind vane with a proper degree of accuracy.

CHAPTER 1

LITERATURE REVIEW – POWER PERFORMANCE EVALUATION

The present section presents the succinct results of an extensive review of literature of all available techniques for the PPE of individual WTGs.

1.1 Power Performance Evaluation Methods and Objectives

The theoretical power that can be extracted by a WTG from the wind is expressed by Equation (1.1):

$$P = \frac{1}{2}\rho\pi R^2 C_p v^3 \tag{1.1}$$

where: P is the theoretical power captured by the rotor of a given WTG

ρ is the air density

R is the radius of the rotor

C_p is the power coefficient

v is the wind speed.

ρ, C_p and v all have a significant impact on wind turbine power output. Of these, modelling C_p and v is particularly challenging in that – unlike air density which remains generally constant over a WTG's rotor-swept area – the power coefficient and wind speed can vary substantially across this zone.

Betz (1919) demonstrated that the hypothetical maximum ratio of energy that can be extracted from a given volume of air in movement corresponds to 16/27. This means that the most efficient wind system could extract only 59% of the theoretical kinetic energy. This value corresponds to what is known as the optimal coefficient of performance (C_p).

Figure 1-1 illustrates the C_p value for different types of WTGs as a function of the tip speed ratio (λ), where:

$$\lambda = \frac{Tip\ speed\ of\ blade}{Wind\ speed} = \frac{\omega R}{v} \tag{1.2}$$

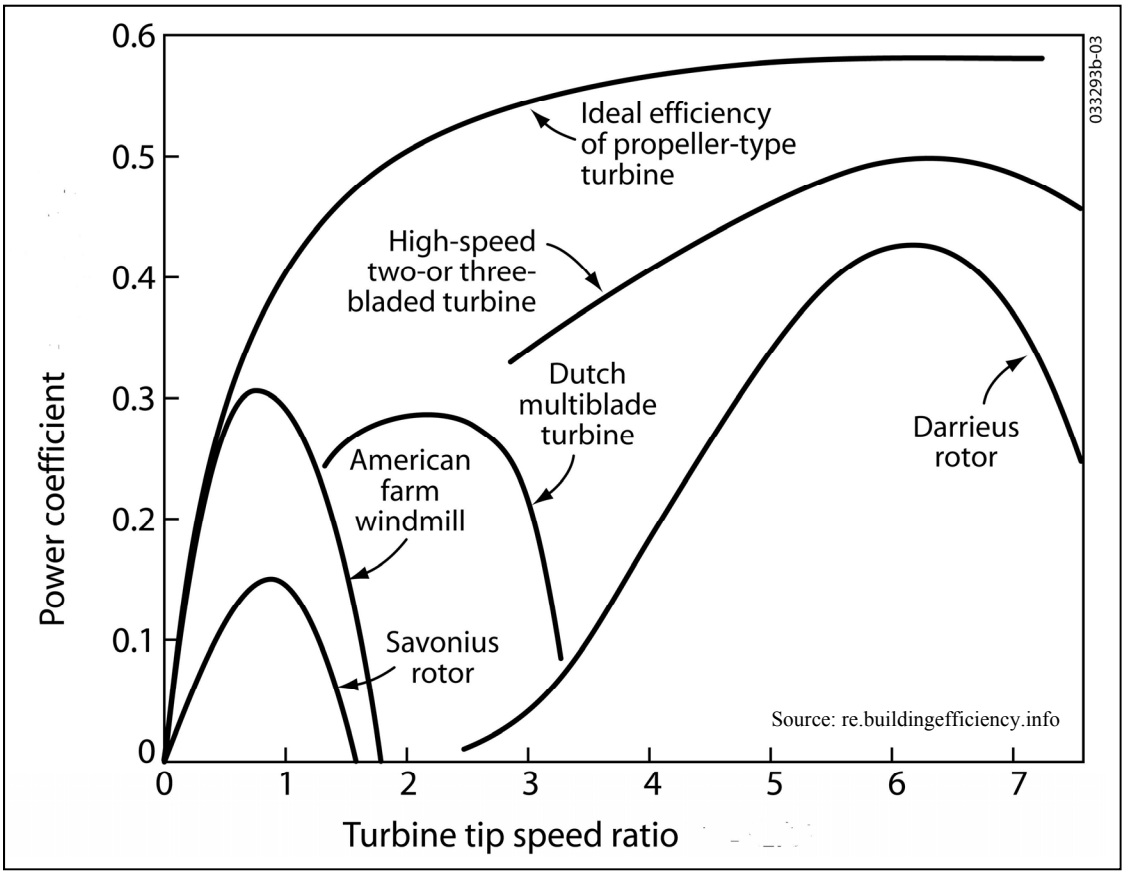

Figure 1-1 Power coefficient for different wind turbine types

As can be seen from Figure 1-1, high-speed two- or three-bladed turbines are the most efficient turbines in terms of extracting energy.

While the C_p is a very good indication of a WTG's performance, the wind industry has developed another metric that is more practical and intuitive to use for power performance evaluation: *the power curve*. The power curve of a WTG shows the net active power output

(in kW) as a function of wind speed measured at hub height (in m/s). Figure 1-2 provides an example of a typical wind turbine power curve (the red line).

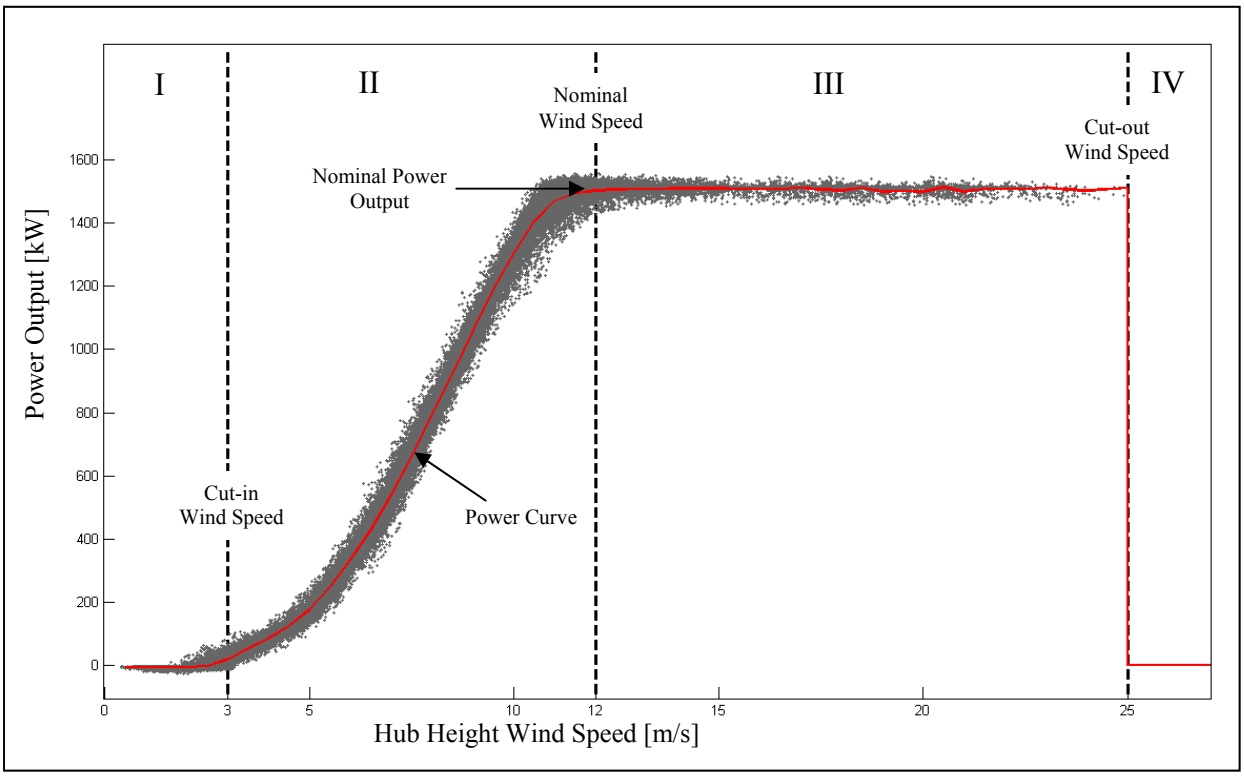

Figure 1-2 Typical wind turbine power curve

The scatter plot depicted in Figure 1-2 is composed of gray dots which represent all 10-minute averaged wind speed and power output data for a typical wind turbine. The red line is referred to as the power curve of a wind turbine. The power curve is obtained by averaging wind speed and power bins (gray dots) which are generally 0.5 m/s wide.

As can be seen from the power curve depicted in Figure 1-2, the expected value of power output has a non-linear relationship with wind speed, i.e. it is not proportional to v. In Zone I this is mainly due to the fact that that WTGs require a minimum wind speed – referred to as the cut-in wind speed – in order to begin producing energy. Zone I in Figure 1-2 represents the wind speeds which are insufficient for energy production. In Zone II this non-linear

character is due to the fact that once a turbine has begun to generate energy, power output is mostly proportional to the cube of the wind speed (v). The first part of this zone is mainly driven by the search of the optimal efficiency C_p (maximum extraction of power output). As the wind speed increases, the turbine needs to regulate the power output in order to protect the WTG's components. At a certain wind speed threshold, the power output is kept constant in order to protect the integrity of the wind turbine equipment. This is known as the nominal wind speed and power. The turbine limits its power throughout Zone III until higher wind speeds induce loads too severe on the turbine and it needs to be shut down. The end of Zone III corresponds with the cut-out wind speed. Beyond the cut-out wind speed (Zone IV) the turbine does not produce energy, but rather remains at a standstill in order to protect itself. It will restart only when the wind speed falls low enough to ensure the structural integrity of the WTG.

The technical and commercial rationale for using a power performance verification strategy based on comparison of WTG power curves – as mentioned by WPP owners or wind energy industry consultants – are numerous and can be summarized as follows:

I. General performance follow-up (Pelletier, 2007),
II. Identification of areas where performance could be improved (Harman et al., 2003; Pelletier, 2007),
III. Identification of changes in power performance (e.g.: pitch control malfunction, blade damage/fouling, control problems, aerodynamic enhancements, etc.) (Harman et al., 2003),
IV. Quantification of discrepancies between actual and forecasted energy production (Graves et al., 2007; Klug, 2007),
V. Diagnosis where production does not meet expectations (Harman et al., 2003),
VI. Improvement and maximization of power plant performance (Pelletier, 2007),
VII. Warranty verification and negotiation (Pelletier, 2007),
VIII. Failure and fault analysis (losses, diagnosis and solution) (Pelletier, 2007),
IX. Minimization of uncertainty in long-term forecast (Graves et al., 2007; Harman et al., 2003; Klug, 2007),

X. Maximization of power plant value (Graves et al., 2007; Klug, 2007),

XI. (Re)evaluation of projects for (re)financing (Harman et al., 2003; Pelletier, 2007).

The more precise the PPE methods are, the more easily the PPI objectives will be achievable, hence showing the importance of improving these methods. The following section will summarize the various groups involved in the improvement of these methods and the techniques that have been applied to date.

1.1.1 Groups Involved in PPE of Individual WTGs and WPP

Before providing the results of the review of literature and in order to give a general view of the main groups involved in PPE, Table 1-1 and Table 1-2 summarize the major groups or institutions that have been involved in PPE of individual WTGs or WPP. For clarity purposes, these groups will be presented in two separate tables, namely normalization institutions and research groups.

Table 1-1 Normalization institutions involved in PPE of WTGs or WPP

International Electrotechnical Commission (IEC) The IEC is an organization that prepares and publishes international standards for all electrical, electronic and related technologies. The IEC has developed a series of standards for WTG systems. More specifically related to this work, the IEC has developed the IEC 61400-12-1 (International Electrotechnical Commission, 2005) standard entitled: *Power performance measurements of electricity producing wind turbines*. This standard is the most widely recognized and used standard in the wind industry. For this reason, further details of this standard will be given in the subsequent sections.
International Energy Agency (IEA) The International Energy Agency (IEA) acts as energy policy advisor to 27 member countries in their effort to ensure reliable, affordable and clean energy for their citizens. The

IEA Wind agreement sponsors cooperative research tasks and provides a forum for international discussion of research and development issues. For this reason, many publications and work related to wind technology have been presented under the IEA group.
The international Measuring Network of Wind Energy Institutes (MEASNET) MEASNET represents a collaboration of institutes which are engaged in the field of wind energy and which strive to ensure high quality measurements, uniform interpretation of standards and recommendations as well as interchangeability of results. In this context, MEASNET has developed four procedures related to wind technology: *Cup Anemometer Calibration Procedure*, *Acoustic Noise Measurement Procedure*, *Power Quality Measurement Procedure*, and *Power Performance Measurement Procedure*. With respect to the latter, it is only quite recently that the MEASNET group has adopted (without modification) the latest version of the IEC61400-12-1.
Canadian Standard Association (CSA) The Canadian Standard Association is a not-for-profit membership-based association that develops standards to enhance public safety and health for multiple areas of expertise. In the 1980-90s, the CSA developed several standards related to renewable energy. The standard entitled *Wind Energy Conversion Systems (WECS) – Performance (CSA-F417M91)* was specifically dedicated to the power performance evaluation of wind turbines. Recently however, the CSA adopted without modification the IEC Standard 61400-12-1.

Table 1-2 Research groups involved in PPE of WTGs or WPP

Risø National Laboratory The Risø National Laboratory from the Technical University of Denmark (DTU) carries out scientific and technical research on society and systems, wind energy, fuel cells and hydrogen, bioenergy, emerging energy technologies and nanobiotechnology. With more than a thousand publications specifically dedicated to wind energy, Risø is inarguably one of the predominant research groups worldwide dedicated to wind energy. Many publications related to the IEC61400-12-1 have been published by Risø. The

following section dedicated to this standard will present the institute's findings and suggestions. A list of all Risø's publications related to wind energy can be found at: http://www.risoe.dk/Risoe_dk/Home/Knowledge_base/publications/VEA.aspx

National Renewable Energy Laboratory (NREL)

The National Renewable Energy Laboratory (NREL) is the primary US laboratory for renewable energy and energy efficiency research and development (R&D). With more than 60 staff and numerous publications related to wind energy research, NREL is an important research group in the wind industry. A list of its publications can be found at: http://www.nrel.gov/wind/publications.html.

Energy research Centre of the Netherlands (ECN)

The aim of ECN Wind Energy is to contribute to the realization of both national and international targets for wind energy through:

I. Long-term R&D work that aims to increase the value-cost ratio of wind energy;
II. Removal of technical barriers for the implementation of wind power, particularly for large-scale wind power plants;
III. Technical assistance for innovative wind energy projects and solutions to technical problems.

ECN has presented several papers related to power performance evaluation of wind turbines (see http://www.ecn.nl/en/wind/publications/).

Centro Nacional de Energías Renovables (CENER)

The Centro Nacional de Energías Renovables (CENER) is a technical centre specialized in the applied research and development of renewable energies. CENER's wind department is mainly involved in applied R&D related to wind energy. Three main areas of research have been identified by CENER:

I. Evaluation of wind potential and wind farm design,
II. Wind turbine certification,
III. Design of wind turbine equipment.

Wind Energy Institute of Canada (WEICan) The WEICan institute was founded 25 years ago with the objective of advancing the development of wind energy through research, testing, innovation, and collaboration. WEICan's location at North Cape, Prince Edward Island with 300° exposure to the Gulf of St. Lawrence is unique and offers a number of characteristics which make it an ideal site for conducting research on wind turbine operations in Nordic conditions, namely: I. IEC Class 1 wind resource with relatively low turbulence, II. A harsh marine environment with high corrosion rates, III. Icing events during winter months, IV. Large winter/summer temperature differences.
Site nordique expérimental en éolien CORUS The TechnoCentre éolien owns an experimental wind energy site, the Site nordique expérimental en éolien CORUS (SNEEC) that features two REpower wind turbines, two 126 m wind measurement masts, a LIDAR (Light Detection and Ranging) unit and a microgrid. Located at an elevation of 350 m in Rivière-au-Renard (Quebec, Canada) this research centre is mainly focused on the impact of icing and complex terrain on wind turbine performance.

Though several other groups worldwide have been involved to varying degrees in wind turbine PPE, the preceding table presents the most renowned and influential groups in this area of research.

1.1.2 Current Methodologies for PPE of Individual WTGs

This section presents the results of a literature review on the different approaches used to estimate the power output of a given WTG. These methods fall into four fundamentally different categories of approaches:

I. Discrete (mainly IEC method),
II. Parametric,
III. Non-parametric,

IV. Stochastic.

The following sections describe each of the above-listed types of PPE methods, their advantages and disadvantages, as well as the techniques associated with each approach.

1.1.2.1 Discrete Methods

Discrete methods consist of modelling a continuous process with discrete approximations. The IEC61400-12-1 (IEC-12-1) (International Electrotechnical Commission, 2005) and IEC61400-12-2 (IEC-12-2) (International Electrotechnical Commission, 2012) standards use this type of method. In these standards, all wind speeds are classed in 0.5 m/s bins. Power output is then modelled according to these discrete inputs. The general steps proposed by the IEC standard can be summarized as follow:

I. Installation of a meteorological mast with anemometer, wind vane, temperature and pressure sensors at hub height and at a distance between 2 and 4 rotor diameters of the tested wind turbine;

II. When the turbine to be tested is located in a complex terrain (see Annex B of IEC-12-1), a systematic difference in wind speed between the position of the meteorological mast and the centre of the turbine can be found. Prior to wind turbine installation, a site calibration will be required by means of a second (temporary) meteorological mast in order to establish flow correction factors for all wind measurement sectors;

III. Once the turbine installation has been completed (including installation of power measurement devices), the simultaneous collection of wind speed, power output, temperature, and pressure can begin. Data shall be collected continuously at a sampling rate of 1 Hz or higher. The mean (10-minute averages), standard deviation, maximum and minimum values for all measured parameters shall be stored in a database;

IV. Once the database is considered complete, data should be analyzed per the following steps:

A. Quality control of the recorded data (meteorological data, electrical data, turbine and data acquisition system availability),
B. Correction of wind speeds according to the flow correction factors obtained during the site calibration (for complex sites only),
C. Data normalization to account for air density impacts on power curve,
D. Power curve elaboration using the "bin method",
E. Calculation of the AEP by referencing the measured power curve with a reference wind speed frequency distribution, assuming 100% availability,
F. Evaluation of Type A and B uncertainties (As defined in GUM, 2008).

Figure 1-3 and Figure 1-4 schematically present the major steps required for the elaboration of a WTG power curve located in flat or complex terrain.

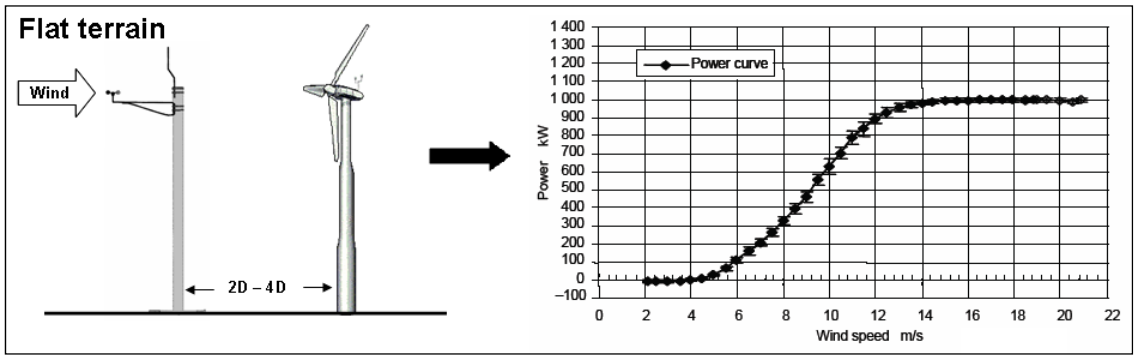

Figure 1-3 WTG power curve procedure in flat terrain
(Pelletier, 2007)

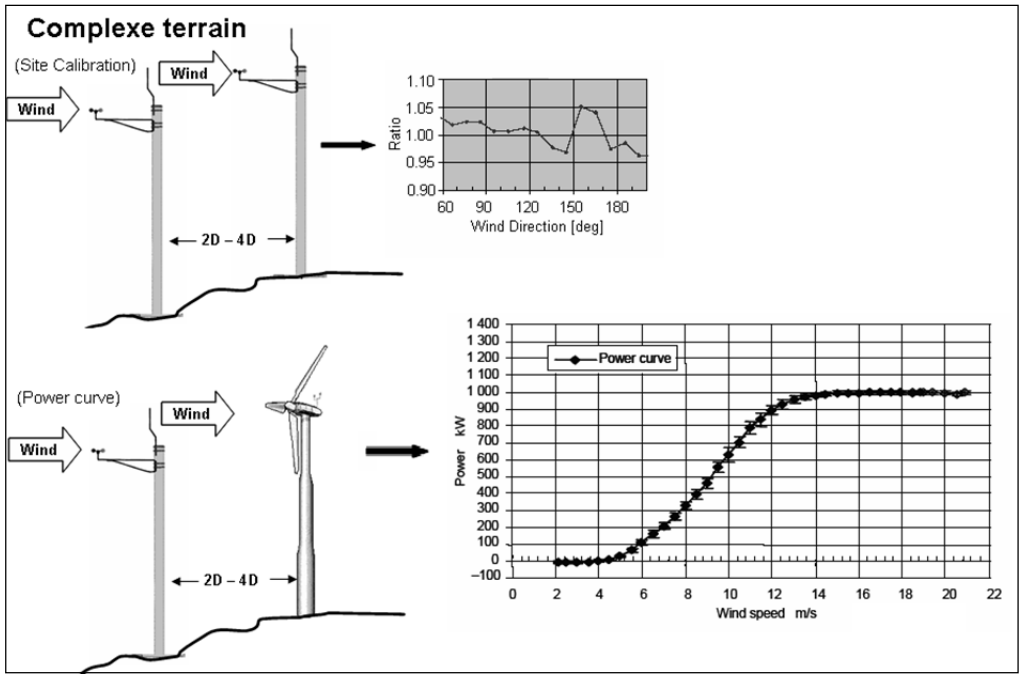

Figure 1-4 WTG power curve procedure in complex terrain
(Pelletier, 2007)

The IEC-12-2 (International Electrotechnical Commission, 2012) method is very similar to the standard IEC-12-1 with the difference being that instead of taking the wind speed data from a met mast, such data are collected using nacelle anemometry. As the nacelle, rotor and surrounding topography can affect the wind speed read by the nacelle anemometry; this standard requires a site calibration prior to turbine installation in order to establish a correlation between the wind speeds at the permanent met mast and the future location of the turbine.

In these PPE techniques, wind speed at hub height and air density are implicitly considered the only relevant input (independent) variables; power is the output (dependent) variable. Frandsen (Frandsen et al., 2000) and Albers (Albers et al., 2007), amongst others, mention that other parameters could significantly affect the power curve evaluation if not taken into account. According to the said authors, the secondary variables which affect the power curve evaluation are:

I. Turbulence intensity,
II. Vertical wind shear,
III. Atmospheric stability,
IV. Inclined wind speed.

Furthermore, IEC is aware of the limitations of its proposed methodology as mentioned in its introduction: "*Meanwhile, a user of the standard should be aware of differences that arise from large variations in wind shear and turbulence, and from the chosen criteria for data selection. Therefore, a user should consider the influence of these differences and the data selection criteria in relation to the purpose of the test before contracting the power performance measurements*."

Since Frandsen's report, several investigations have been completed related to the shortcomings of the IEC-12-1 (referred to as IEC61400-12 before 2005) standard. The following sections summarize the limitations of the IEC-12-1 standard as found in the literature.

1.1.2.1.1 Turbulence Intensity

Turbulence intensity (*TI*) depends on a number of site-specific conditions and has a wide range of variation. It is related to the standard deviation of the wind speed and can be expressed as follows:

$$TI = \frac{\sigma_{10min}}{v_{10min}} \tag{1.3}$$

where σ_{10min} is the standard deviation of the 10-min wind speed of a data sample
v_{10min} is mean wind speed in the 10-min data sample

According to theoretical studies and experiments (Albers et al., 2007; Frandsen et al., 2000), it can be concluded that i) a clear increase in power output with increasing turbulence intensity (approximately 1-2% increase in TI around the maximum C_p) in the transition from zone I and zone II and, ii) a decrease in power output with increasing turbulence intensity in the transition region to rated power (transition between zone II and III) were apparent. Similar results have been reported in previous studies conducted by (Honhoff, 2007; Kaiser et al., 2003; Radecke, 2004). Figure 1-5 shows the impact of turbulence intensity on the power curve.

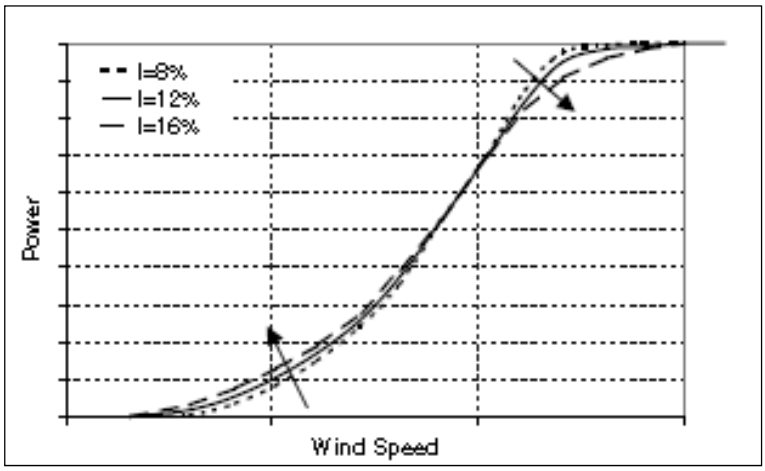

Figure 1-5 Typical effect of turbulence on power curve
(Kaiser et al., 2003)

With the objective of producing power curves that are both repeatable and independent of the turbulence intensity characteristic, several authors (Kaiser, Albers, etc.) have proposed different adjustment methodologies.

For example, Kaiser (Kaiser et al., 2003) used the Taylor series expansion in order to linearize the relationship between the power output of a turbine and the incident turbulence intensity at hub height. Albers (Albers et al., 2007) proposes a normal distribution model in order to correct for the 10-minute averaging impact on the power curves. More recently,

Albers (Albers, 2010) improved his method and has been able to obtain a complete turbulence normalization procedure. This procedure will probably be incorporated in the next issue of the IEC-12-1 standard. The method proposed by Albers mainly assumed the existence of a "zero turbulence" power curve. This zero turbulence power curve represents the power output of a given WTG type assuming no turbulence at all (i.e. no variation of wind speed with time). Once this equivalent power curve is obtained, all 10-minute data points can be recalculated for normalized turbulence intensity.

1.1.2.1.2 Vertical Wind Shear (vertical wind speed distribution)

Vertical wind shear can be defined as the distribution of the wind speed as a function of height above ground level. In general, wind shear is influenced by a combination of three main factors:

I. Surrounding topography and obstacles,

II. Surrounding surface roughness,

III. Atmospheric stability.

Figure 1-6 through Figure 1-8 present simplified examples of each of these three causes of wind speed gradient with height.

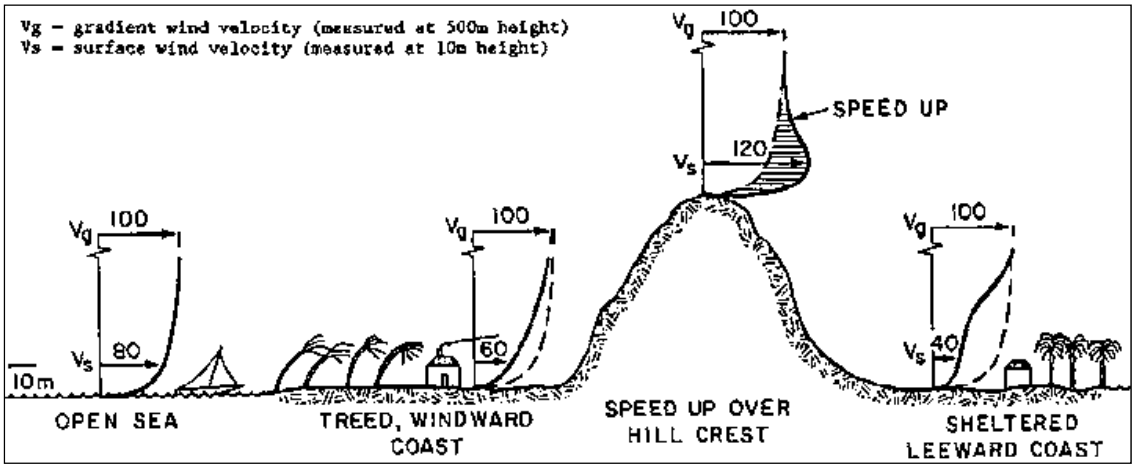

Figure 1-6 Influence of topography and obstacles on vertical wind speed distribution (Obtained from Bailey, 1997)

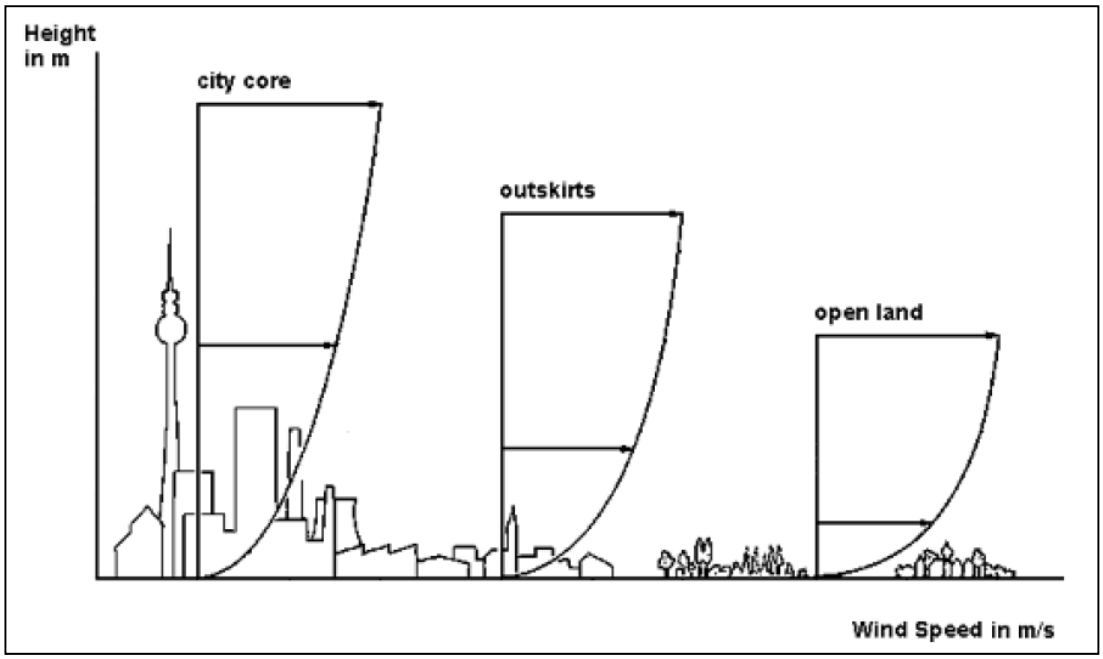

Figure 1-7 Influence of surface roughness on vertical wind speed distribution (Obtained from Berlin, 2007)

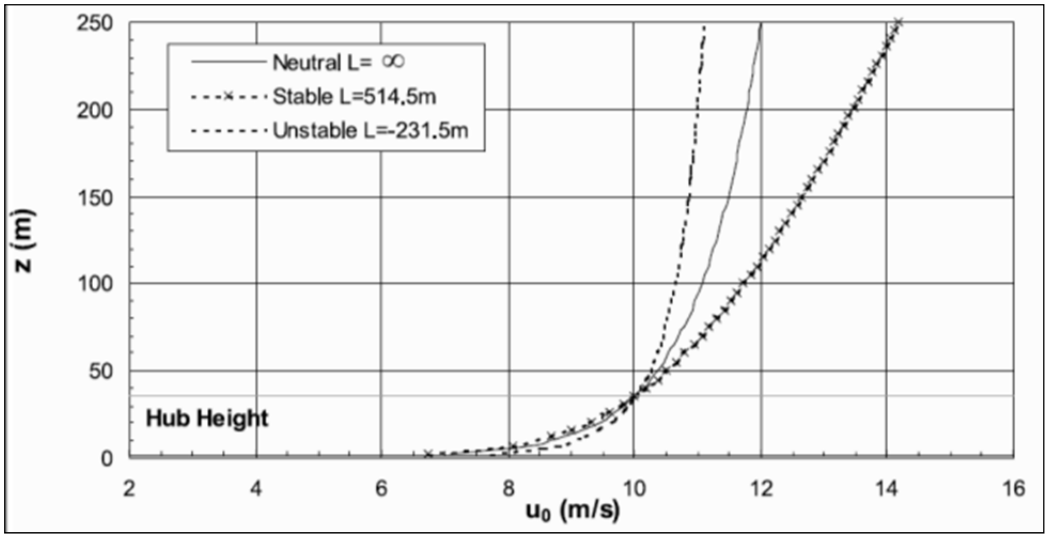

Figure 1-8 Influence of atmospheric stability on vertical wind speed distribution (Alinot et al., 2002)

In the IEC-12-1 standard, it is assumed that the hub height wind speed is representative of the wind over the entire rotor. While this assumption was adequate for wind turbines with small rotor diameters, in the case of newer turbines with large rotor diameters (up to 100 m), it is now assumed that wind speed variation within the rotor swept area will influence power production.

Theoretical models (Sumner et al., 2006) have been used to evaluate the impact of wind shear on the power performance of wind turbines. These models have systematically demonstrated that for similar hub height wind speeds, wind shear does influence the power output of wind turbines.

Experimental results (Albers et al., 2007; Antoniou et al., 2007; Bunse et al., 2008; Honhoff, 2007; Hunter et al., 2001) have also demonstrated the impact of wind shear on the power performance of wind turbines. Antoniou (Antoniou et al., 2007), using a 160 m tower, shows that using an increased number of wind speed measurement points significantly improves the correlation between wind input and power output. More recently, (Wagner et al., 2010a) has demonstrated the same, by using a LIDAR (Light Detection And Ranging) that is able to read the wind speed profiles higher than hub height.

1.1.2.1.3 Inclined Wind Speed

Inclined wind speed angle is evaluated by comparing the angle between the wind flow and the wind turbine shaft axis. Because there is a clear linear relationship between the angle of terrain slope and the flow inclination angle (Hannah, 1997), it is evident that wind turbines located in complex terrain will be exposed to inclined wind speed.

Pedersen (Pedersen, 2004; Pedersen et al., 2002) has demonstrated that vertical flow angle to the wind turbine rotor axis seems to influence power by a $\cos^2$ relationship.

1.1.2.1.4 Cup Anemometer Characteristics

Risø National Laboratory (Pedersen et al., 2002) has clearly demonstrated that different cup anemometers show different angular responses to inclined wind speed. Risø National Laboratory has also shown that dynamic over-speeding also varies with different anemometer brands under identical turbulence levels. This report concludes with suggestions for anemometer classification according to their turbulence response and angular characteristics.

Furthermore, ECN (Curvers et al., 2001) has found that average wind speeds measured with different types of cup anemometers may deviate by >7% relative to each other. This would have significant repercussions on the results when estimating the power curve of a wind turbine.

It is generally suggested that power curve comparison should be completed with the same type of anemometers in order to avoid any of these issues. The IEC standard clearly cautions users in this regard:

> "*A key element of power performance testing is the measurement of wind speed. This standard prescribes the use of cup anemometers to measure the wind speed. This instrument is robust and has long been regarded as suitable for this kind of test. Even though suitable wind tunnel calibration procedures are adhered to, the field flow conditions associated with the fluctuating wind vector, both in magnitude and direction will cause different instruments to potentially perform differently. Tools and procedures to classify cup anemometers are given in Annexes I and J. However, there will always be a possibility that the result of the test can be influenced by the selection of the wind speed instrument. Special care should therefore be taken in the selection of the instruments chosen to measure the wind speed.*"

1.1.2.1.5 Yaw Error

According to Beattie (Beattie, 2001), the general trend is for power curves to decrease in magnitude as wind direction variability increases. This is expected since it is generally

accepted that the power of a turbine changes with the $\cos^2$ of the angle between the wind direction and the turbine's orientation. Further details about yaw error will be provided in section 2.2.2.

1.1.2.1.6 Icing / Insects / Dust

Icing, insects and dust are all known to reduce the power performance of a wind turbine (Honhoff, 2007). Some studies have been conducted in order to evaluate the loss associated with each of these. Unfortunately, no clear relationship between these events and the impact on the power output has been properly established to date. For this reason, it is general practice to not take these events into consideration when analyzing the performance of wind turbines or WPP.

1.1.2.2 Parametric Methods

Parametric models are built from a set of mathematical equations that include parameters that must be adapted through a set of continuous data. Parametric methods generally use linear, non-linear, polynomial or differential equations, amongst others. The parameters present in these equations are generally determined through standard regression methods such as error minimization and maximum-likelihood, to name a few. Numerical methods can also be used to establish the parameter's value. The shape of the wind turbine power curve has inspired some authors in their choice of parametric models.

Table 1-3 provides a summary of techniques or functions that have been tested by several authors to evaluate the power curve of a WTG.

1.1.2.3 Non-parametric Methods

With the recent arrival of powerful database tools that can be used to archive tremendous amounts of data, new modelling methods have emerged. Instead of assuming a physical or analytical relationship between the input and output data, non-parametric methods establish a

correlation based only on the data provided. This is why these methods are referred to as "learning methods".

Table 1-4 presents the different types of non-parametric methods used in the past for elaborating the power output of a WTG.

Table 1-3 Parametric methods

Function type	**Description of proposed parametric method**	**Author and date**
Polynomial	Linear model with binned speed partition $P_i(V) = a_{0i} + a_{1i} \cdot V$	(Sainz et al., 2009) (Lydia et al., 2013)
	Adjustment of a "q" order polynomial function $P(V) = a_0 + a_1 V + \cdots + a_q V^q$	(Sainz et al., 2009)
	Partitioning the power curve by wind speed	(Llombart et al., 2005a)
	Partitioning by both wind speed and direction	(Llombart et al., 2005a)
Exponential	Double exponential $P(V) = \exp(\tau_1 \exp(V \cdot \tau_2))$	(Pinson et al., 2007)
	Improved exponential model $P(V) = \exp(-\exp(a - b \cdot V - c \cdot V^2 - d \cdot V^3)$	(Sainz et al., 2009)
Logistic	4-parameter logistic function $P(V) = a \frac{1 + me^{-V/\tau}}{1 + ne^{-V/\tau}}$	(Kusiak et al., 2009a)
	5-parameter logistic function $P(V) = d + (a - d) \Big/ \left(1 + \left(\frac{V}{c}\right)^b\right)^g$	(Lydia et al., 2013)

Table 1-4 Non-parametric methods

Method	**Description of proposed non-parametric method**	**Authors and date**
Learning	Learning method using data mining techniques such as MLP, M5P tree, random forest, boosting tree and k-NN to model power curves	(Kusiak et al., 2009a)
	Regression tree	(Clifton et al., 2013)
ANN	Wind speed only with MLP	(Kusiak et al., 2009a) (Marvuglia, 2011)
	Wind speed and wind direction with MLP	(Li et al., 2001a)
	Wind speed, relative humidity, generation hours with MLP	(Carolin, 2008)

As can been seen in Table 1-4, investigation has been limited in the area of non-parametric modelling where the inputs having the greatest impact such as air density, turbulence intensity and wind shear have not been considered, especially investigation where these parameters are considered simultaneously.

1.1.2.4 Stochastic Methods

Anahua (Anahua, 2007), Boettcher (Boettcher et al., 2007) and Gottschal (Gottschal et al., 2008) presented several papers related to the stochastic analysis of wind turbine power output and wind speed. They use the Markov chain theory to elaborate the power curve of wind turbines. The Markov chain analyzes the dynamic behaviour of a system (wind turbine) with respect to a stochastic signal or input (turbulent wind speed). This method resulted in power curves that are independent of the turbulence intensity level. While this method has the advantage of enabling a wind turbine power curve to be modelled within a few days, it has the disadvantage that no parameters other than wind speed and TI are taken into account.

This shortcoming makes these types of models inapplicable in the long-term operation context.

1.1.3 Shortfalls of Current Method

As previously mentioned, several shortfalls related to current PPE methods have been identified, the most relevant of which in the context of this work being:

I. To the author's knowledge, none of the methods has ever succeeded in modelling a power curve with more than three inputs simultaneously;

II. The level of uncertainty of these methods remains rather high, i.e. in the order of 5%;

III. Several articles contradict one another in identifying the method with the highest accuracy.

CHAPTER 2

POWER PERFORMANCE IMPROVEMENT – RESULTS FROM REVIEW OF LITTERATURE AND CONSULTATION

This section presents a synthesis of different techniques that could be used to improve the power output of existing WPP and that have been obtained by means of a review of literature and consultation through a steering committee and several other wind industry professionals with relevant experience.

2.1 Definition and Objectives of Power Performance Improvement (PPI)

The preceding section presented the review of literature with respect to the various techniques presently used to evaluate the power performance of operational WTGs. This chapter will focus on the current methods or techniques used to improve the power performance of operational WTGs or wind power plants.

PPI refers to any method, practice, or tool that can be used or implemented on a WTG in order to increase its annual energy output (AEP). It has been demonstrated by many authors that increasing the energy production of operational WTGs is possible. For example, GE with its WindBOOST application, Iberdrola with its WindCORE application, ECN with its changes in operational control and numerous other companies offering specific WTG performance optimization products and services are all claiming that they can improve the power performance of WTGs. Their biggest shortfall however is that few of them have ever properly demonstrated the true gain they argue they can achieve.

In this context, a review of literature has been conducted on this topic and several individuals and groups have been consulted to help identify possible avenues of power performance improvement. Parties involved in this context included the wind farm owner's technicians and management, consultants from renowned consulting firms, professionals from a major turbine manufacturer, and wind energy researchers. A steering committee was also formed in

this regard. During these consultations, the only limitations imposed to the aforementioned participants were the following:

I. The proposed changes had to be technically and financially feasible in the context and timeframe of a PhD;
II. Due to financial constraints, no physical components of any turbines (e.g. changing of a blade) could be considered;
III. Due to the high level of complexity involved, the control algorithm of the WTGs could not be changed; only the set points used by these control algorithms could be an area of investigation.

The results from this review and these consultations can be synthesized in two major types of improvement: i) improvement in availability and ii) improvement in performance while the turbines are operational.

Table 2-1 and Table 2-2 provide a summary of the proposed methods obtained through the review of literature or suggestions from consulted individuals.

Table 2-1 presents methodologies proposed to increase power performance by improving WTG availability while Table 2-2 presents recommendations for improving WTG output while the turbines are operational (available). Each of these tables indicates the source of these recommended methodologies, whether from the Steering Committee or from a referenced article.

Table 2-1 PPI methodologies based on availability improvement

Improvement Description	**Authors and year**
O&M team performance	Steering Committee
Maintenance plan (preventive, predictive and condition-based)	Steering Committee
Parts procurements and spare parts optimization	Steering Committee
Condition monitoring	(Wilkinson et al., 2013)
Advanced analysis of data and faults	(Kusiak et al., 2011)
Meteorology-based maintenance	(Pelletier et al., 2008)
Curtailment optimization	Steering Committee
Icing management	Steering Committee
In-service inspection and end-of-warranty hand-off strategy	Steering Committee
Preparation of wind farm service life extension	Steering Committee
Add wind turbines	Steering Committee
Relocate wind turbines	Steering Committee
Electrical network improvement (tree cutting, redesign, etc.)	Steering Committee

Table 2-2 PPI methodologies for WTGs during periods of availability

Improvement Description	**Authors and year**
De-icing system or improved operation during icing events	(Cattin, 2012)
Blade cleaning and repair (surface roughness)	(Dalili et al., 2007)
Wake management	(Mikkelsen et al., 2007)
Advanced control (LIDAR or changes in control algorithm)	(Angelou et al., 2010)
Improve forecasting accuracy (for better energy trading)	(Parkes et al., 2006)
Roughness adjustment (e.g. tree cutting)	Steering Committee
Underperformance detection tools (power curves, troubleshooting, etc.)	(Lindahl et al., 2012)
Yaw offset measurement – correction and optimization	see Section 2.2
Pitch and RPM optimization (stall and variable pitch turbines)	(Khalfallah, 2007) (Kusiak et al., 2009b)
Cut-in & cut-out optimization	Steering Committee
Parameter (set points) optimization	Steering Committee
Nominal power investigation or boost	Steering Committee

While all these propositions represented plausible improvement techniques and most of them were theoretically achievable in the context of this project, it was not realistically possible to elaborate a test for all of these methods given temporal and financial limitations. Choices had to be made in order to achieve concrete results in the timeframe of a PhD. The following section will present the selected method for testing in the context of this project: the yaw offset optimization.

2.2 Yaw Offset Optimization

After multiple investigations, discussions and negotiations, it was decided by the wind farm owner, the turbine manufacturer and the author that a power performance optimization could be tested on two operating wind turbines. Specifically, it was agreed that testing related to yaw offset optimization could prove valuable in light of the technical and commercial interest of this aspect and also due to the fact that such an undertaking respected the three previously-mentioned constraints. This section of the document will present the context and the key findings from a review of literature specifically related to yaw error and yaw offset optimization.

2.2.1 Context and Definitions

The yaw system of a wind turbine is the component responsible for orienting the rotor into the wind. Multi-megawatt turbines are mainly equipped with active yaw systems which primarily comprise two components: i) a wind vane (to detect wind direction) and ii) a yaw system (to orient the nacelle into the wind), as illustrated in Figure 2.1.

As wind direction is stochastic by nature, and due to the inertia of a multi-megawatt turbine, the rotor plane cannot always be perfectly perpendicular to the wind direction (i.e. misalignment of the rotor axis (wind turbine centre line) and the wind direction in the horizontal plane of the nacelle); this is known as yaw error. Two main types of misalignments are possible: static and dynamic. Figure 2-2 through Figure 2-4 briefly present the difference between these types of misalignment.

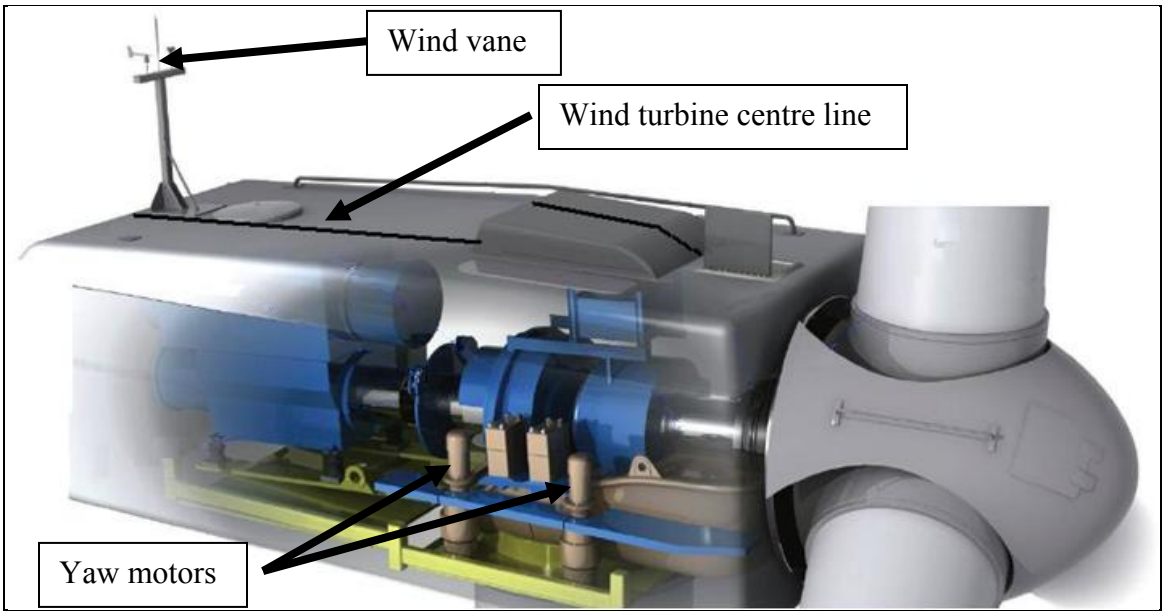

(Ref.:http://farm4.static.flickr.com/3555/3376591869_2b664406a6_o.png)

Figure 2-1 Wind Turbine nacelle and yawing system

Figure 2.2 presents a wind turbine with no yaw error, i.e. the rotor's axis is perfectly aligned with the wind direction. As can been seen from this figure, the rotor axis (referred to as the centre line of the wind turbine) is parallel to the wind flow and also to the zero reference degree of the wind vane.

In reality, however, the rotational speed of the nacelle is not sufficient to ensure that the nacelle is always perfectly oriented in the axis of the wind direction. Figure 2-3 illustrates the yaw error of a wind turbine. The yaw error therefore corresponds to the angle between the rotor's axis (the center line of the nacelle) and the wind direction. When the wind vane on the nacelle is perfectly aligned with the center line of the wind turbine, then the wind direction deviation is equivalent to the yaw error. Since yaw error is related to the wind direction, it is also referred as a dynamic error.

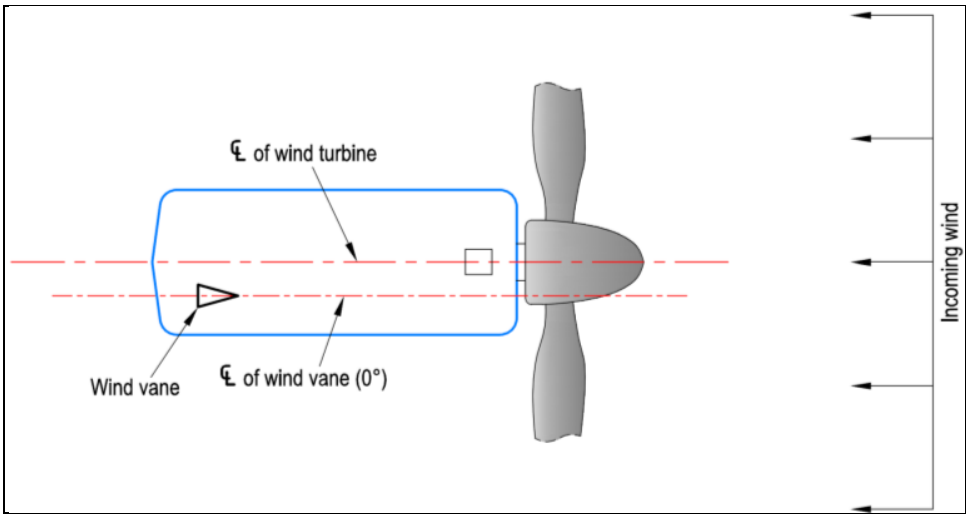

Figure 2-2 Perfect alignment of wind vane with nacelle centre line

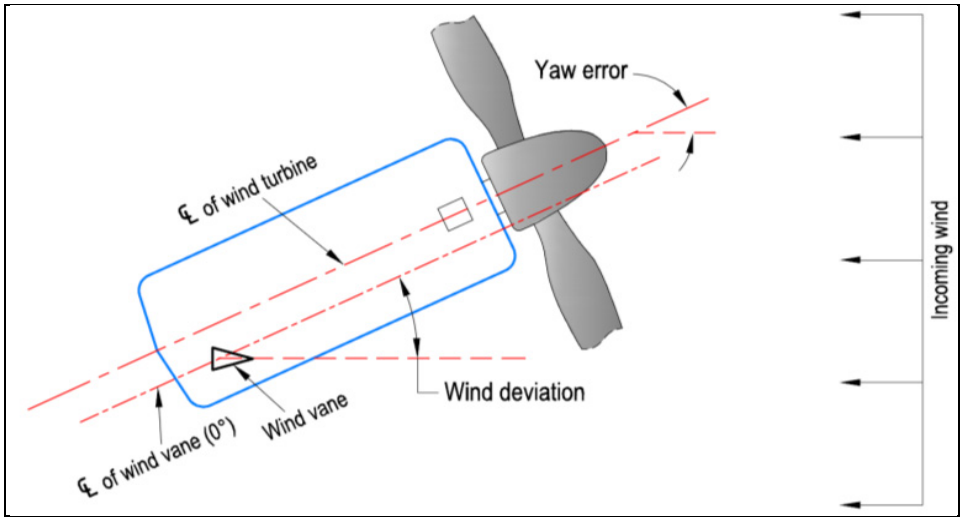

Figure 2-3 Yaw error (dynamic)

Figure 2-4 illustrates a yaw offset. Yaw offset arises when the wind vane center line is not properly aligned with the center line of the nacelle. As the yaw offset is not related to the wind direction but rather due to the improper installation (orientation misalignment) of the wind vane, it is sometimes referred to as a static error. In cases where the wind vane is not aligned with the nacelle centre line, the wind deviation is then not equivalent to the yaw error.

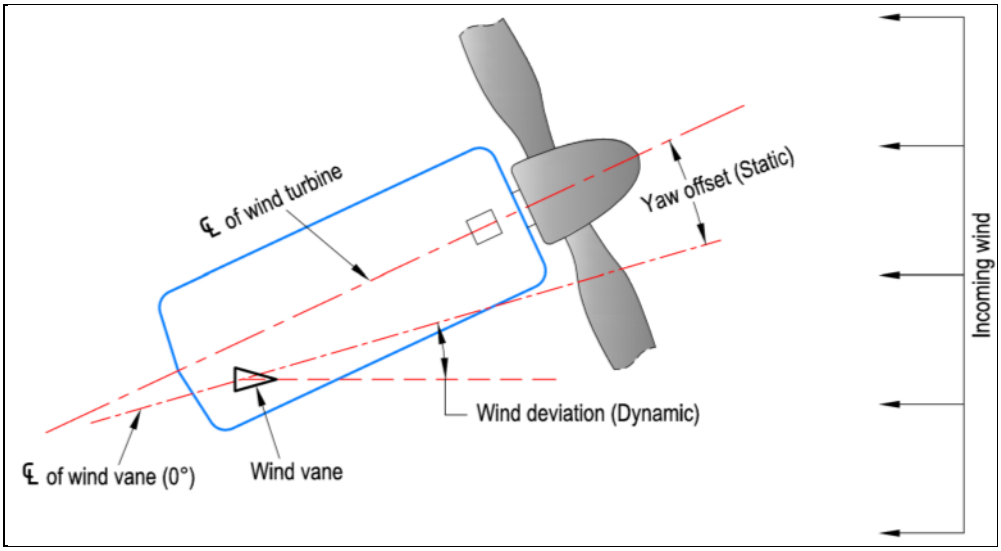

Figure 2-4 Yaw offset (static)

Clarifications with regard to yaw error (dynamic) and yaw offset (static) is important since the current project is primarily focused on correcting only the latter.

2.2.2 Literature Review

As previously demonstrated, yaw error can originate from one or a combination of two distinct causes: i) a dynamic error caused by a change in wind direction and ii) a static error due to poor installation of the nacelle wind vane. The following sections will present a review of literature on i) the impact of yaw error on production ii) the estimated value of the yaw offset in modern multi-megawatt and iii) a summary of the attempt to improve energy production through yaw error management.

2.2.2.1 Energy Loss Due to Yaw Error

While some authors (Perovic et al., 2010) assume a $\cos^3$ relationship between the yaw error and lost production, the vast majority of articles reviewed demonstrated or assumed a $\cos^2$ relationship. For example, (Pedersen, 2004) interpreted the results of the study conducted by Madsen (Madsen, 2000) and presented Figure 2-5 where the relative production is provided

according to the yaw error angle. Pedersen also compared the relative production with the cos and $\cos^2$ relationship with the yaw error angle. He concluded that the energy lost is proportional to the $\cos^2$ of the yaw error, as shown in Figure 2-5.

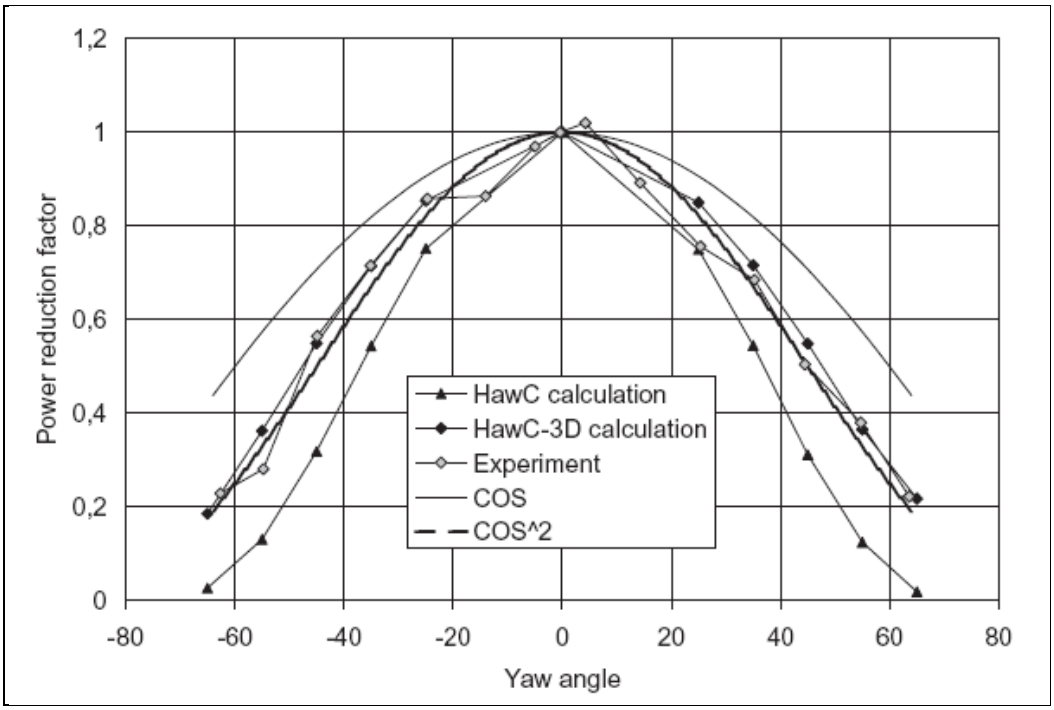

Figure 2-5 Power vs. yaw error: measured and calculated relative power

2.2.2.2 Experiences with Yaw Offset

Experience suggests that, until recently, little effort has been made to ensure proper alignment of the wind vane with the wind turbine centre line. While some turbine manufacturers have internal protocols to ensure the proper alignment of the wind vane with the rotor axis, many (if not most) align the instrument in an approximate manner (by eye) or lack a standard procedure altogether. Table 2-3 presents the expected yaw offset values obtained by various authors. The angle values presented represent the value at 1σ for a normal distribution.

Moreover, yaw offset measurements have been taken on two wind turbines by the author with a wind vane calibration tool (see Annex I for further details on this tool for which a

patent is pending). Results of these measurements have shown yaw offset of +3° and +4° for the two tested wind turbines.

Table 2-3 Estimated yaw offset distribution (1σ)

Estimated yaw offset [°]	Authors and year
Approx. +/-7	(Gaumond et al., 2013)
+/-10	(Dakin, 2009)
+/- 10	(Perovic et al., 2010)
+/- 5 [a]	(Auld et al., 2003)
+/- 5 to 10 [a]	(Roeth, 2010)

a) For wind vane installation on met mast

Based on these results and the author's experience in met mast installation, it is reasonable to assume that the average precision of wind vane installations on the owners fleet is probably in the order of +/-5° (with a coverage factor k = 1σ). This is likely due to the fact that multi-megawatt wind turbines have begun to be widely deployed only recently, and prior to their arrival, it simply was not cost-effective to invest time and resources in accurate wind vane alignment for the sake of a potential 1-2% gain in efficiency.

2.2.2.3 Performance Improvement Attempt through Correction of Yaw Error and Yaw Offset

With the multi-megawatt turbines in operation today, a gain of just 1% represents a financial interest, which is likely why research is beginning to be conducted on yaw error and yaw offset. The following two sections will present the results of a review of literature on efforts to minimize the energy losses due to i) yaw error and ii) yaw offset.

I. Yaw Error (Dynamic)

Catch the Wind (now rebranded as BlueScout Technologies) has published several commercial papers (Dakin, 2009; Dakin et al., 2010; Mamidipudi et al., 2011) related to the use of a nacelle LIDAR that enables the reading of wind speed and wind direction a few

hundred metres in front of the wind turbine. In its papers, the company states that reading the wind speed before it reaches the wind turbine enables a better control (mainly blade pitching and rotor orientation) and therefore results in higher production. The company indicated that it was able to increase power output by >10% on some of the wind turbines it had tested.

Kusiak (Kusiak et al., 2009b) attempted to optimize the yaw algorithm of a wind turbine through data mining analysis. The resulting increase in energy output was rather low, however.

Perovic (Perovic et al., 2010) have proposed a blade load sensing system; the authors suggest that by accurately processing the amplitude, phase, and other related signal characteristics of the blade bending loads, it is possible to measure the yaw error.

Wind technology and service company ROMO Wind (ROMO, 2013) is also proposing a yaw control system to position the rotor plane perpendicular to the wind direction. This system mainly consists of a spinner anemometer, which is a sonic anemometer, installed on the nose of a wind turbine. ROMO claims that this system, by being "in front of" the wind turbine, is less affected by the wind deviation caused by the nacelle and blades and therefore better positioned to accurately determine wind direction.

Figure 2-6 Romo's spinner anemometer

Kragh (Kragh, 2013), has recently published his PhD thesis in which he tempted to enhance the performance of multi-megawatt wind turbine though wind speed reading from a nacelle-

mounted LIDAR. His conclusion in regard of the potential energy gain through optimisation of the dynamic of the yawing of a wind turbine is: "*In summary, it appears that the potential of improving the power output by improved yaw alignment is only significant for badly calibrated turbines, and that more detailed in wind measurements will not enable significant power increases for well calibrated turbines*."

Lastly, in the course of this project, it should be mentioned that the turbine manufacturer presented a report that claimed that the current settings implemented in its turbines are likely optimal. This statement is mainly explained by the fact that although a turbine not properly aligned with the wind is under-producing energy, attempting to achieve optimal alignment at all times would result in increased energy consumption of the yaw motors. An optimal control algorithm therefore is required that strikes a compromise between following the wind and the energy consumption of the yaw motors.

II. Yaw Offset (Static)

Avent Lidar Technology [www.aventlidartechnology.com] is currently evaluating the feasibility of yaw offset correction by means of LIDAR technology. Avent contends that by comparing the LIDAR wind direction reading to that of the wind direction sensor, it is possible to detect a potential misalignment (yaw offset). The company states that in a recent study of more than 12 wind turbines, it measured an average Yaw offset (misalignment) of 6.2°, which in its opinion is equivalent to a 2% loss in annual energy production. Unfortunately, no details are provided on how the LIDAR itself is aligned with the wind turbines' rotor axis.

CHAPTER 3

DATABASE DESCRIPTION AND IMPLEMENTATION

An essential part of this project has been dedicated to the elaboration and implementation of an important database that enables the gathering of real data from operational WTGs. Therefore, several months of discussions have proven necessary in order to obtain all the commercial and technical approvals from the wind farm owners, the turbine manufacturer, the provider of the database and ÉTS. Ultimately, a database of high quality was implemented. The present section will present in some details the architecture of the database installed in the context of this PhD. The difficulties encountered in the course of this process might explain why so little research has been completed to date on operational WTGs by other researchers.

The second part of this section summarizes the data obtained and archived within this database.

3.1 Database Architecture

Three large-scale wind farms have been connected to this database. Figure 3-1 presents a simplified representation of the architecture of this system.

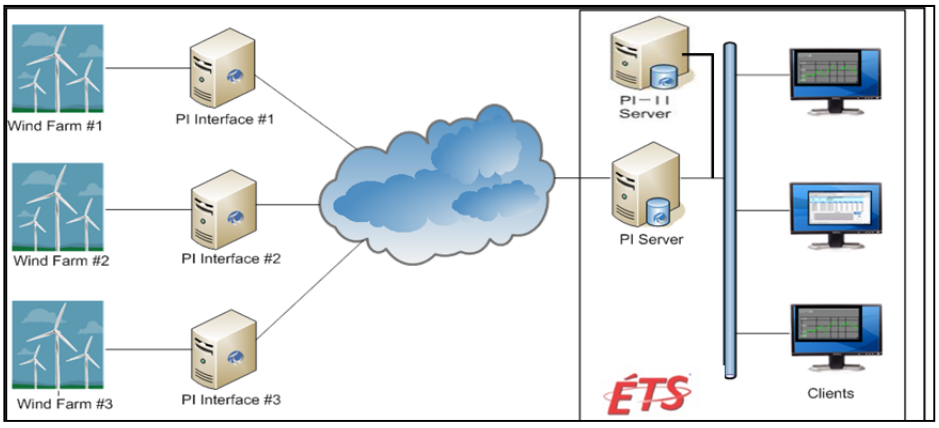

Figure 3-1 Architecture of database

As can be seen from this system, hardware (PI interfaces) had to be installed directly on site. These interfaces were connected directly onto the wind turbine manufacturer's interface, hence giving access to more than 100 inputs for each wind turbine. Data from meteorological masts as well as from the substation and collector grid were connected to these sites' interfaces. More than 30,000 tags (points) were connected through this method and were transferred to the server at ÉTS where all these data are archived.

Throughout the elaboration of this project, a second server was installed in order to enable this system to perform more advanced analyses.

Figure 3-2 and Figure 3-3 present the general layout of the two experimental wind turbines used in this study. Green circles represent the locations of the meteorological towers.

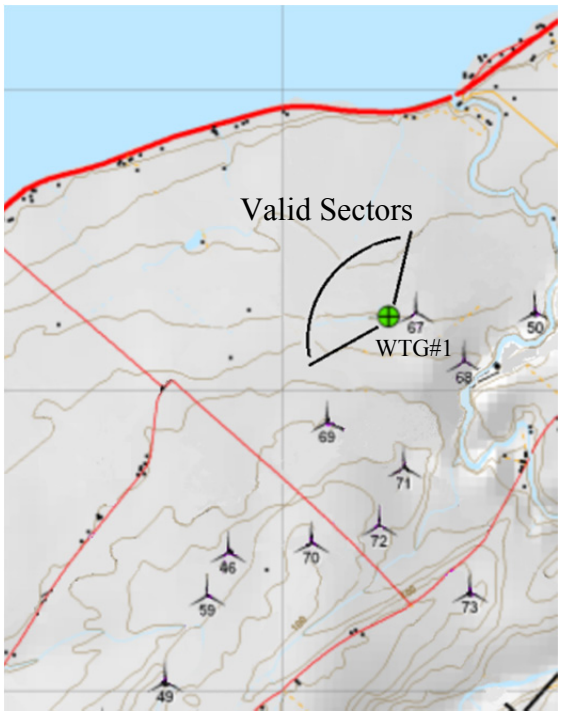

Figure 3-2 Layout – Site no. 1

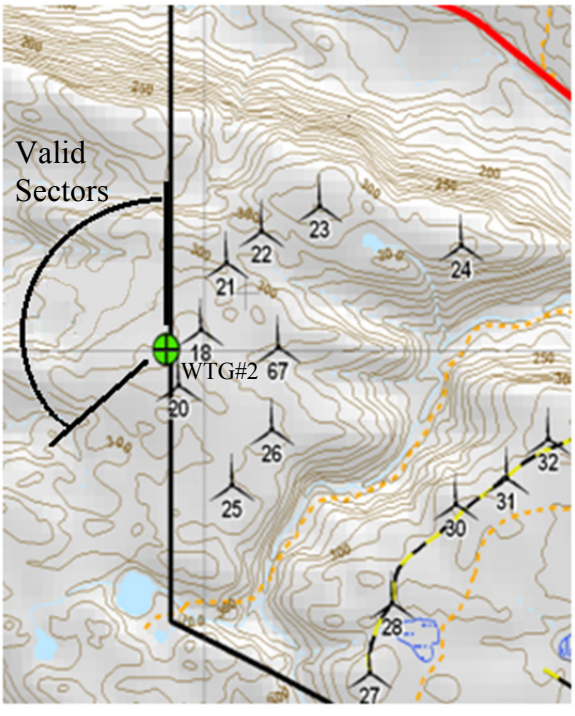

Figure 3-3 Layout – Site no. 2

3.2 Archived Data

For each turbine, over 100 parameters were archived, including power, meteorological data, operational data, vibration, temperature of components, and turbine status. For the met masts, meteorological parameters at different measurement levels (40 m, 50 m, 60 m, 70 m and 80 m) were acquired. Though the data were recorded and logged at a high sampling frequency (1 Hz), the standard 10-min averages were calculated and used in this work.

While all connected tags can be viewed live, it is imperative that the collected data be archived. Several methods of compression are available for data archiving in order to minimize the disk space and the bandwidth of the communication link through internet. In order to ensure the maximum representativeness of the acquired data, no data compression was used and all data acquired at a frequency of 1 Hz were archived. The archiving of high-frequency data has several advantages (Pelletier et al., 2010) not only for the current project but also for future projects. For example, in the context of this project, one-second data allow for the testing of the potential impact of the third and fourth moment (kurtosis and skewness) of the wind speed on the elaboration of models which would not have been possible with lower-frequency data.

The amount of data archived per year is approximately 0.6 terabytes. This system became fully operational in January 2009 and has been continuously archiving data since then, thus representing nearly five years of archived data.

CHAPTER 4

MODELLING OF POWER PERFORMANCE THROUGH ARTIFICIAL NEURAL NETWORKS

Artificial Neural Network (ANN) is an adaptive statistical model based on an analogy with the structure of the brain. According to Dr. Robert Hetcht-Nielsen (1989), ANN can be seen as "*...a computing system made up of a number of simple, highly interconnected processing elements, which process information by their dynamic state response to external inputs*." Several works have been conducted on ANN and a number of applications have been found. ANN is generally used for the following purposes, amongst others:

I. Pattern recognition,
II. Classification & Clustering,
III. Function approximation,
IV. Prediction/forecasting,
V. Optimization,
VI. Control.

According to Dreyfus (Dreyfus et al., 2004), ANN should be chosen as a modelling procedure only under specific conditions, namely:

I. Availability of a sufficient amount of data. Since ANN is "learning" from data, the amount of data needs to be sufficient and must be representative of all the input data involved.
II. Before modelling with ANN, it should always be verified that non-linear models are necessary. Linearization of a process is always preferable since it is much less time consuming for the computer, more stable to outliers, and the results are better validated with this type of model.
III. If it is determined that linear models are not precise enough to model a process, a parametric function (e.g. polynomial or other types of defined functions) should be investigated.

IV. ANN should be considered only after determining that the process follows a non-linear process that cannot be estimated with a known function like a polynome.

In summary, ANN should only be considered in the modelling of a process when sufficient data are available for an efficiency training of the ANN, no linearization of the process is possible (as shown from many results in the literature) and that the relationship between the inputs and outputs of a process is unknown. These conditions have been met in the context of elaborating WTG power curves.

The following section will briefly explain the concept of ANN, its strengths and weaknesses, and a justification for its use in PPE of WTGs. Comparison of the results obtained through ANN with other standard methods for two tested WTGs will also be presented.

4.1 Description of ANN

Basically, neural networks are built from simple units called neurons or cells by analogy with the real neurons of the human brain. The general form of an artificial neuron can be described in two stages, as shown in Figure 4-1.

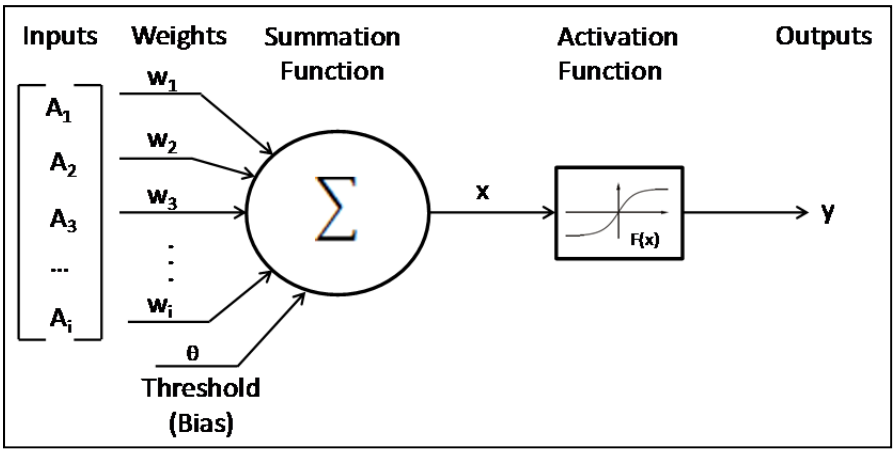

Figure 4-1 General neuron model

In the first stage, a linear combination of the inputs is calculated according to the following equation:

$$x = \sum_{i=1}^{N} A_i W_i + \theta \tag{4.1}$$

Each value of the array of inputs is associated with a weight value (W_i), generally between 0 and 1). The θ value represents the threshold or the bias of the neuron. This threshold enables the activation or deactivation of the neuron.

The sum of the product is calculated and then passed to the second stage of the neuron to perform the activation function which generates the output from the neuron. The activation function can be of multiple forms (linear, quadratic, logsig, tansig, exponential, etc.), but in the vast majority of the cases, it is either linear or sigmoid. In the case of a sigmoid function (Figure 4-2), the output of the neuron would be evaluated using the following equation:

$$y = \frac{1}{1 + exp^{(-x)}} \tag{4.2}$$

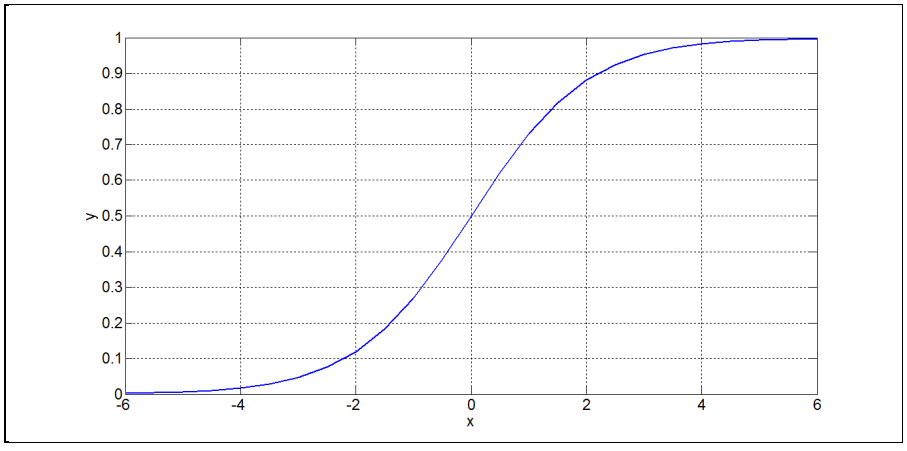

Figure 4-2 Sigmoid function

As can be seen in Figure 4-2, the results of the activation function (the output of the neuron) are limited to the range [0, 1]. As x approaches $-\infty$, the sigmoid function approaches 0, and when x approaches $+\infty$, the sigmoid function approaches 1.

An artificial neural network is obtained by connecting multiple neurons. The most common structure of connecting neurons into a network is by layers. The simplest form of layered network is the single-layer network. This type of network is also referred to as a feed-forward network (see Figure 4-3) because the connections between the units are not recurrent, meaning that the outputs are not recycled into the input layer as opposed to recurrent neural network where they are (see Figure 4-4).

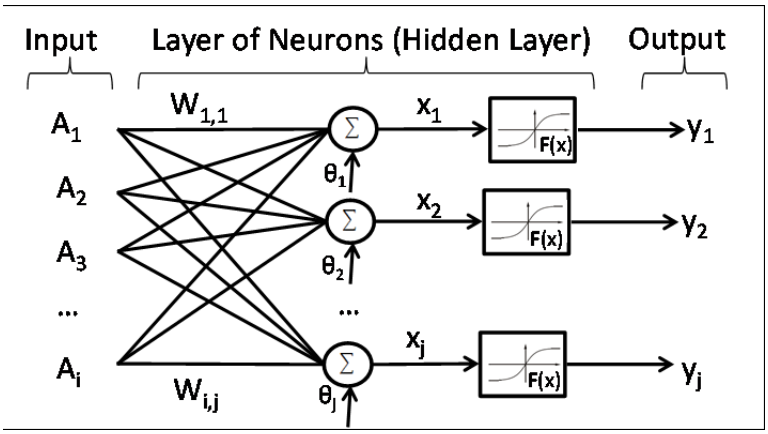

Figure 4-3 Feed-forward single-layer network

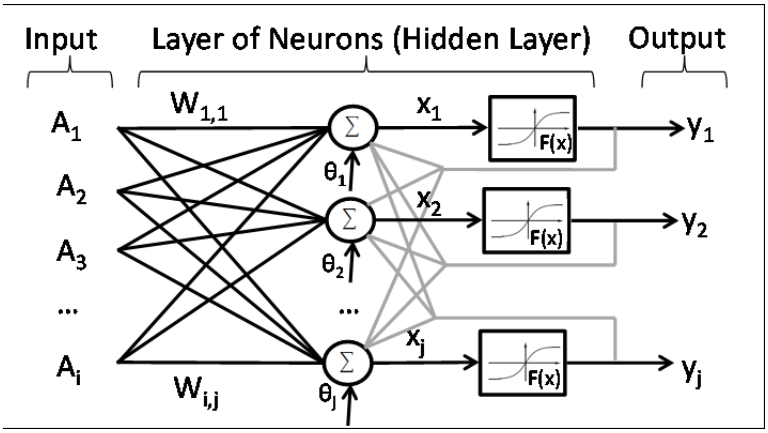

Figure 4-4 Recurrent single-layer network

As shown in Figure 4-5, multilayer ANN can be obtained by connecting the output of the first layer of neurons to the second layer of neurons. Multiple layers of neurons are possible, hence the name multi-layer neural network.

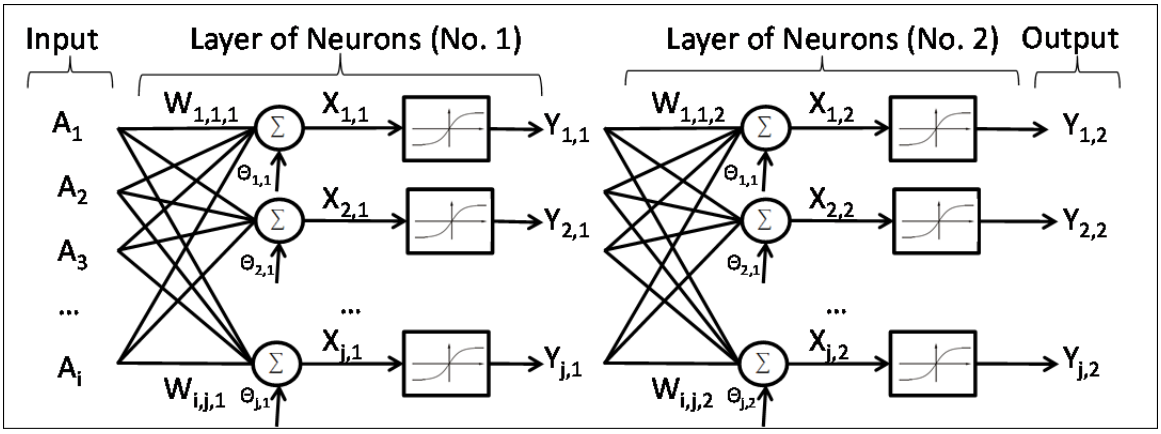

Figure 4-5 Feed-forward multilayer neural network (multilayer perceptron (MLP))

Therefore, the first challenge in elaborating an ANN is to define its structure – also called its topology – which consists of defining the number of layers, the number of neurons in each layer, the activation functions and determining if the ANN is of the feed-forward or recurring type.

The choice of topology depends on the application analyzed. Dynamic systems are better modelled through recurring networks while static processes are better modelled with feed-forward topology. It has been found however that ANNs with more than two hidden layers do not contribute to a significant increase in modelling capabilities. ANN is therefore generally limited to two layers. The choice of activation function is again dependent on the application for which the ANN is used. Once all these items are identified, the only parameter that remains to define in the topology of the ANN used is the number of neurons in each layer.

4.2 Learning Process and its Challenges

Once the topology of an ANN has been established, each connection value of the ANN (weights (W_i) and threshold (θ)) must be evaluated. The process of optimizing these connections is known as "training" or "learning". Two types of learning processes are possible for ANN: i) supervised or ii) unsupervised. In supervised training, both the inputs and the outputs are provided. The network then processes the inputs and compares its resulting outputs against the desired outputs. Errors are subsequently calculated, causing the system to adjust the weights (and threshold) which control the network. This process occurs repeatedly until the established stopping criteria have been obtained. In unsupervised training, the network is provided with inputs but not with desired outputs. The system itself must then decide what features it will use to group the input data. This is often referred to as self-organization.

The greatest challenge in training an ANN is to ensure that the network is not "overfitting" the input data. Overfitting occurs when a statistical model describes random error or noise instead of the underlying relationship, hence losing its generalization capability. In the context of data learning, the best model is not the one on which the parameters (weight and threshold) are providing the smallest error (residual) with the sample data, but rather the model that enables the best capability of generalization. Figure 4-6 shows the results of a model with an overfitting problem (black line).

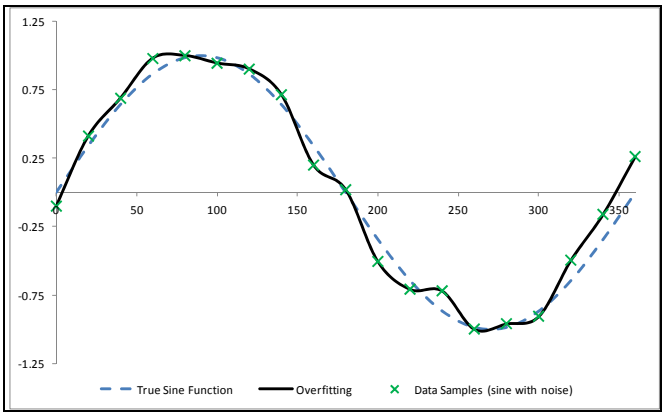

Figure 4-6 Example of a modelling function with overfitting

Figure 4-6 shows the response of an ANN that has been trained to approximate a noisy sine function. The underlying sine function is shown by the dotted line, the noisy measurements are given by the 'X' symbols, and the neural network response is represented by the solid line. Clearly, this network has overfitted the data and will not generalize well.

Another known limitation of ANNs (Maier et al., 2000) is that they cannot extrapolate beyond the range of the training data. This should be borne in mind when interpreting the output results of an ANN.

Several avenues to limit the risk of overfitting while training an ANN exist. One method for improving network generalization is to use a network that is just large enough to provide an adequate fit. The larger the network (i.e. the higher number of neurons), the more complex the functions this network can create (see Figure 4-7); however, with a higher number of neurons, the ANN begin to be prone to overfit the data. Figure 4-7 provides an example of this issue. The figure on the left provides the results for an ANN that was trained from a sinusoid function (blue line). The blue dots represent the noisy data obtained from this sinusoid function and used to train the different ANN. The red symbols (O) represent the output of the ANN once training of the latter has been completed. As can been seen from this figure, the low number of neurons does not allow this ANN to properly model the sinusoid function, as the ANN lacks the necessary flexibility. The figure in the middle represents the results obtained through an ANN with four neurons and shows a good generalization of the sinusoid function. The figure on the right is the result of an ANN with 50 neurons and clearly shows a lack in generalization capacity. Therefore, the number of neurons in a network should be as low as possible in order to reduce the overfitting risk but not so low that it lacks the flexibility to estimate the true complexity of the behaviour of the process.

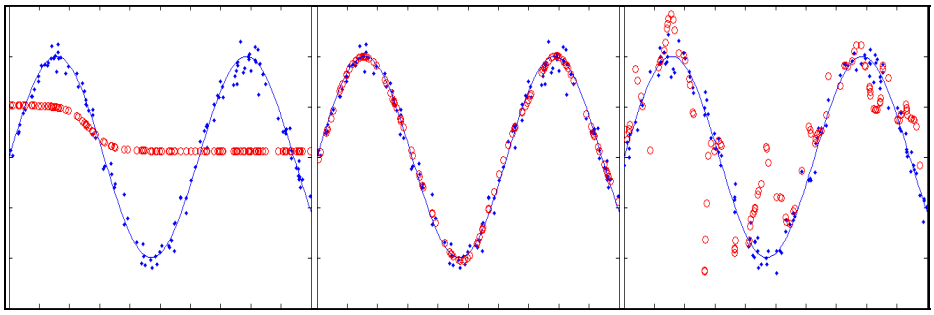

Figure 4-7 Function approximation (in red) with 1, 4, and 50 neurons

Another element to consider in order to minimize the risk of overfitting is to ensure that a sufficient quantity of data is used for the training. As shown in Figure 4-8, it would be nearly impossible to overfit the data with this quantity of data (assuming the data provided for the training are randomly distributed around the average).

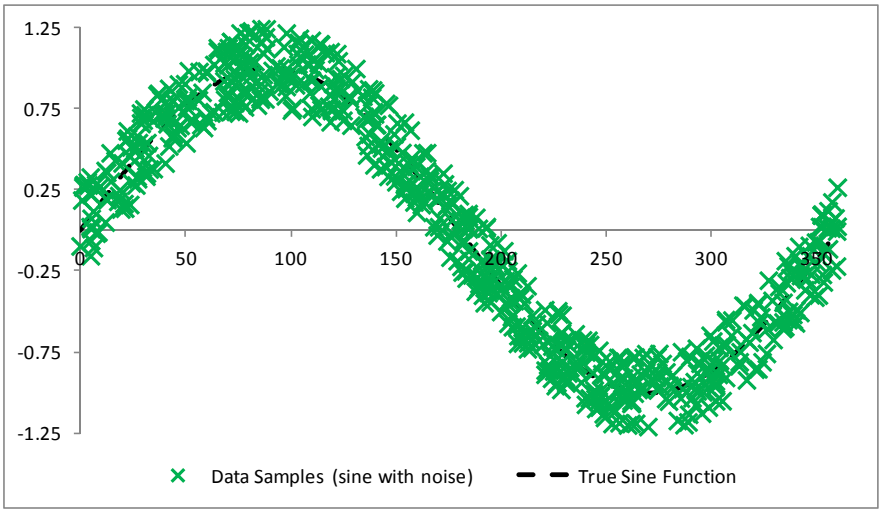

Figure 4-8 Impact of the quantity of data sampling on overfitting

A third technique, known as “early stopping”, is used in the training process in order to lower again the chances of overfitting. In this technique, the available data are divided into three subsets. The first subset is the training set, which is used for computing the gradient necessary to update the weights and biases of the network. The second subset is the validation set. The errors in the training and validation set are monitored during the training

process. The validation error normally decreases during the initial phase of training, as does the training set error. However, when the network begins to overfit the data, the error in the validation set typically begins to increase. When the validation error begins to increase for a specified number of iterations, the training is stopped, and the weights and biases at the point of the lowest validation error are returned. Figure 4-9 depicts an example of an early stopping procedure.

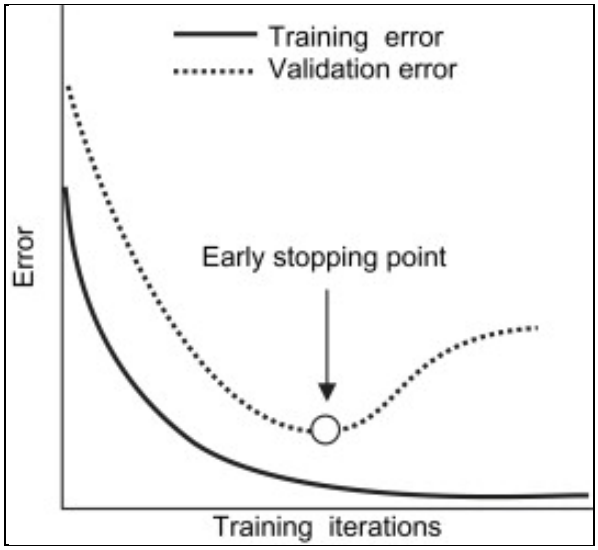

Figure 4-9 Early stopping
(Asension-Cuesta et al., 2010)

The third subset is the test set. The test set error is not used during training. If the error in the test set reaches a minimum at a significantly different iteration number than the validation set error, this might indicate a poor division of the data set. The test set can also be used to compare different models. Generally a 70%-15%-15% division between the training, validation, and test sets is used to ensure a proper division of the data.

Lastly, a supplementary measure has been used in this project in order to further limit the risk of overfitting. Instead of using the result of a single ANN, 30 networks have been built and the median of the 30 ANN has been used as the equivalent answer. While this method seems

to greatly improve the robustness of the results, however it has the disadvantage of being very time consuming for the computer(s).

4.3 WTG Power Curve Modelling Using Artificial Neural Network

Because i) a sufficient quantity of data has been acquired, ii) the interaction between the inputs and the outputs of a wind turbine model (power curve) is non-linear, and iii) analytical solutions to the impact of many parameters could not be found, ANN seemed to be a logical technique for modelling the power curve of a wind turbine.

Data from two operational wind turbines located in Nordic and complex environments were used for the elaboration of wind turbine power curves using ANN. (see Figure 3-2 and Figure 3-3). Data from 80 m meteorological masts (met masts) compliant with IEC 61400-12-1 and installed in proximity to the tested turbines on each of the two sites have also been used.

For each turbine, over 100 parameters were archived, including power, meteorological data, operational data, vibration, temperature of components, and turbine status. For the met masts, meteorological parameters at different measurement levels (40 m, 50 m, 60 m, 70 m, and 80 m) were acquired. Though the data were recorded and logged at a high sampling frequency (1 Hz), standard 10-min averages were calculated and used in this work.

The following sections describe the different steps used for modelling a wind turbine power curve through ANN and compare the results with other standard modelling methods through error analysis. While modelling of wind turbine power curves through ANN (Fugon et al., 2008; Li, 2003; Li et al., 1998; Li et al., 2001b) has been done in the past, none of them has ever modelled the power curve of a wind turbine with more than 3 inputs.

4.3.1 Data Pre-processing

As the volume of collected data is substantial, errors caused by sensors or the data acquisition system are possible. For example, out-of-range values, missing data due to turbine availability and/or electrical shut-down or corrupted data due to icing events are possible

incidents that would require the removal of recordings from the data set. Multiple quality control algorithms were used (Bailey et al., 1997). Additionally, a filtering technique similar to the one used by Kusiak (Kusiak et al., 2009a) was used to remove remaining outliers. Site-specific adaptations of the statistic Tukey criteria (Tukey, 1977) were implemented.

Furthermore, data corresponding to directional sectors prone to wake effects on the tested turbines were not retained for analysis. Figure 3-2 and Figure 3-3 illustrate the valid wind direction sectors in order to avoid wake effect. These sectors were widened compared to the IEC-12-1 standard. Table 4-1 provides the results obtained through the quality control process.

Table 4-1 Data set description for WTG#1 and WTG#2

	Start time stamp:	**End time stamp:**	**Complete data set: [# 10-min data]**	**Quality Control data set: [# 10-min data]**	**% complete**
WTG#1	2009/03/24 13:30:00	2010/01/31 23:48:00	225 796	12 832	5.6
WTG#2	2009/05/01 14:20:00	2010/02/19 01:28:00	218 880	77 131	35.2

The low recovery rates (5.6% and 35.2%) are mainly due to the removal of data that lay outside the valid wind direction sectors.

4.3.2 Modelling Inputs and Derived Parameters

In order to properly model the power output of a wind turbine, over 50 independent variables (directly observed or derived) from the met mast, neighbouring wind turbines or directly from the reference wind turbine were considered and tested (see Annex II). A stepwise forward selection method (Dreyfus et al., 2004) was used for the proper selection of the input parameters. For the available data set, it has been found that the 6 input parameters ensuring

the highest accuracy of the wind turbine power curves were: nacelle wind speed (V), air density (ρ), turbulence intensity (TI), wind shear (WS8040), wind direction (WD), and yaw error (Φ_y). These inputs are known to have an impact on the power curve (International Electrotechnical Commission, 2005).

Since multiple metrics for the wind shear parameter are possible (e.g. thermal stability values, roughness length based on logarithmic profile, shear exponent based on the power law, numerous definitions of equivalent wind speeds or vertical gradient, etc.) (Wagner, 2010), investigations were conducted to identify the most relevant metric for this parameter in the context of this work. Following these investigations, it appeared that the most appropriate metric to define wind shear (WS) in the context of this research is the wind speed ratio (WS8040) evaluated from the wind speeds at 80 m and 40 m levels.

4.3.3 Database Re-sampling

Because 1 Hz data were archived in the database used in this work, it was possible to generate numerous 10-min averaged sets separated by a time delay (Pelletier et al., 2010). A 2-min delay was chosen since the time constant of the wind turbines is in the order of 45 seconds (as expressed by the turbine manufacturer). This 2-min delay thus ensures that all 10-min data are seen as mutually independent by the turbine controller. A static model (as opposed to a dynamic model) can then be assumed. Because ANNs are prone to overfitting, this 2-min delay, which enables a five-fold increase in the database, is considered an appropriate method to lower this risk.

4.3.4 Cross-correlation Analysis

As it is generally agreed that thermal stability has simultaneous effects on both TI and wind shear values, a correlation between these two parameters is usually assumed (Albers et al., 2007; G.P., 2008; Sumner et al., 2006; Wagner, 2010; Wagner et al., 2010b). Since a significant correlation between parameters has an impact on the modelling quality of a process, a cross-correlation investigation on several parameters was completed. Analysis was

conducted for several 1 m/s wind speed bins. Figure 4-10 illustrates an example of the cross-correlation results for the 3-4 m/s bin at Site no.1.

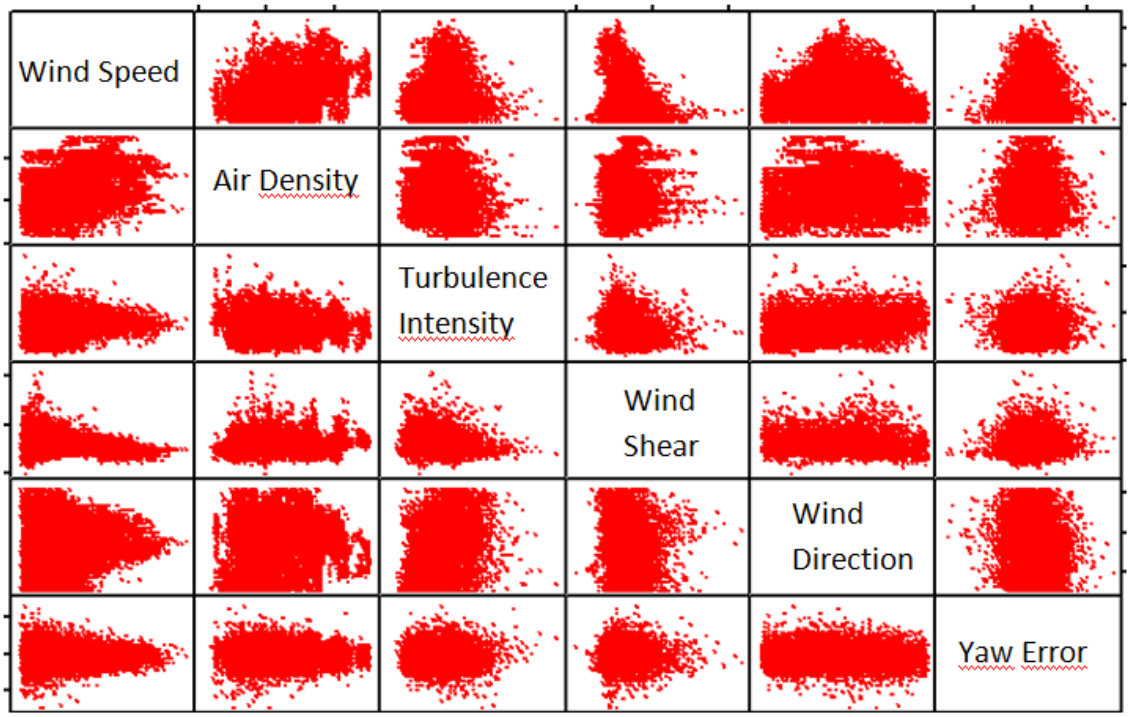

Figure 4-10 Typical example of cross-correlation graphics for 3-4 m/s bin (Site 1)

As can be seen in Figure 4-10, no significant correlation was statistically identified, which indicates a poor relationship between the investigated parameters. The same conclusion was drawn for the other wind speed bins as well as for the other turbine.

This absence of a significant correlation between TI and wind shear is potentially attributable to the sites' topographical complexities and surface roughness. The two sites' wind regimes are probably more driven by synoptic patterns than by thermal effects. This finding enables the separate modelling of TI and wind shear and all other parameters without the risk of inappropriately considering their mutual dependence. Such an approach greatly facilitates the modelling process and enhances its repeatability.

4.3.5 ANN Modelling Elaboration

A feed-forward neural network (also known as a multilayer perceptron (MLP)) with back propagation algorithm was implemented in order to model the wind turbine power curves from 10-minute data sets. Two-layer MLPs with sigmoig and linear activation functions have been used. Figure 4-11 shows the topology used for the MLPs employed for power curve modelling.

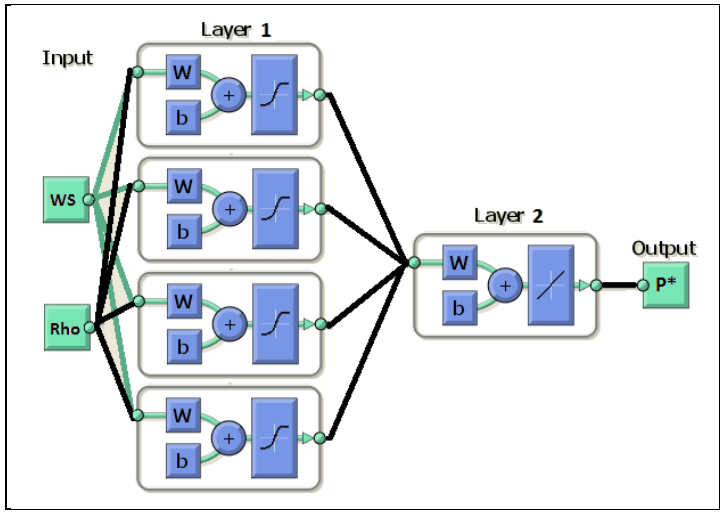

Figure 4-11 MLP Topology

This type of topology is known as a *universal approximator* (Dreyfus et al., 2004). Therefore, the topology elaboration only requires the number of nodes in the first layer to be established. The quantity of nodes in the first layer up to 100 nodes was tested and showed that 4 nodes in the first layer provides the best compromise between the model's precision and the risk of overfitting.

Multilayer perceptrons can generally incorporate the number of inputs desired. However, the greater the number of inputs, the greater the number of data necessary to avoid overlearning; moreover, the validation methods used to ensure that there is no overlearning become more complex. For this reason, and due to the fact that no interaction between independent variables has been found, modelling by means of successive steps, i.e. multi-stage modelling,

was developed. For example, for the first step, the power output is modelled with the wind speed and air density. Once the converged solution of the first ANN has been obtained, the power is normalized for the average density of the experimental data. A second neural network is then trained with the normalized power data (normalized for air density), wind speed data, as well as the subsequent input (i.e. turbulence intensity in this case). Subsequently, the power is re-normalized and this is continued for all variables deemed to have a significant impact on the wind turbine power modelling. These steps can be repeated as long as relevant variables are available. For example, if in the future the wind field above hub height is characterized (using LIDAR for example), this parameter could be modelled without having to repeat the entire process. Figure 4-12 illustrates the first two stages of the ANN training process.

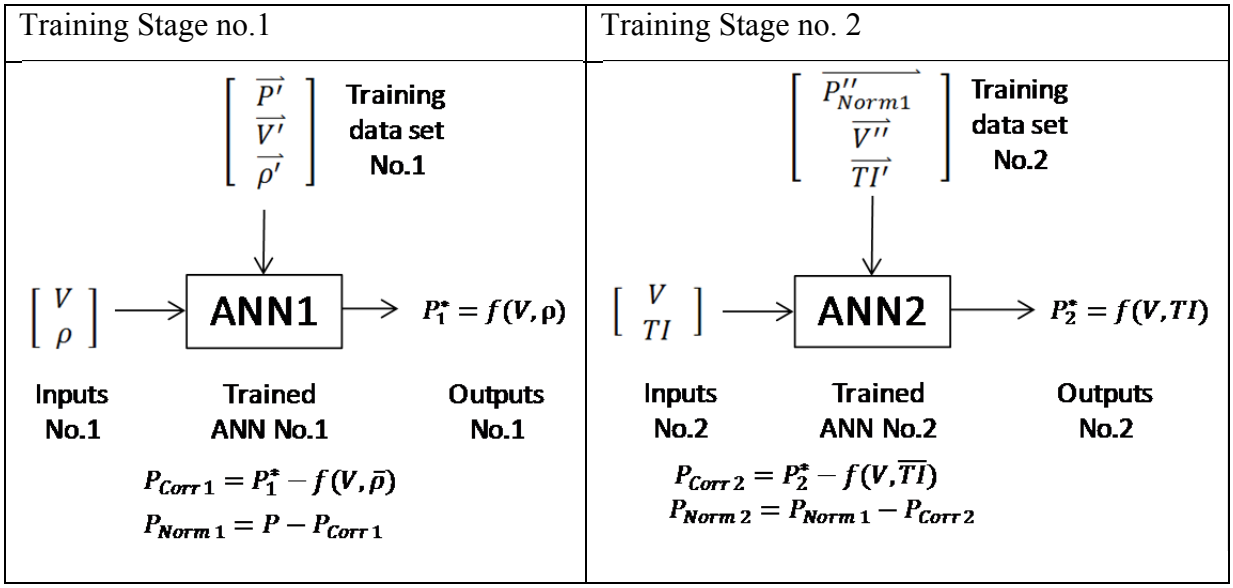

Figure 4-12 ANN training stages methodology

4.3.6 Training of the ANN

Because non-parametrical models are data-driven, they are more prone to "learn" from the data, thereby representing a risk of overfitting. In order to control overfitting, a 70%-15%-15% random distribution was performed to attribute the data to training, validation, and test

databases, respectively. MLP utilizes a supervised learning technique called back-propagation for training the network. Table 4-2 shows the training algorithm and stopping criteria used.

Table 4-2 Training algorithm and stopping criteria

Training algorithm	Levenberg-Marquardt
# of max iterations	1000
Gradient min	1E-10
Mu min	1E-10
Cross-validation	20 successive iterations

4.3.7 ANN Model Validation

Once all stages of the ANN training were completed, the output results also had to undergo a multi-stage process for the evaluation of the estimated output. Figure 4-13 depicts this process.

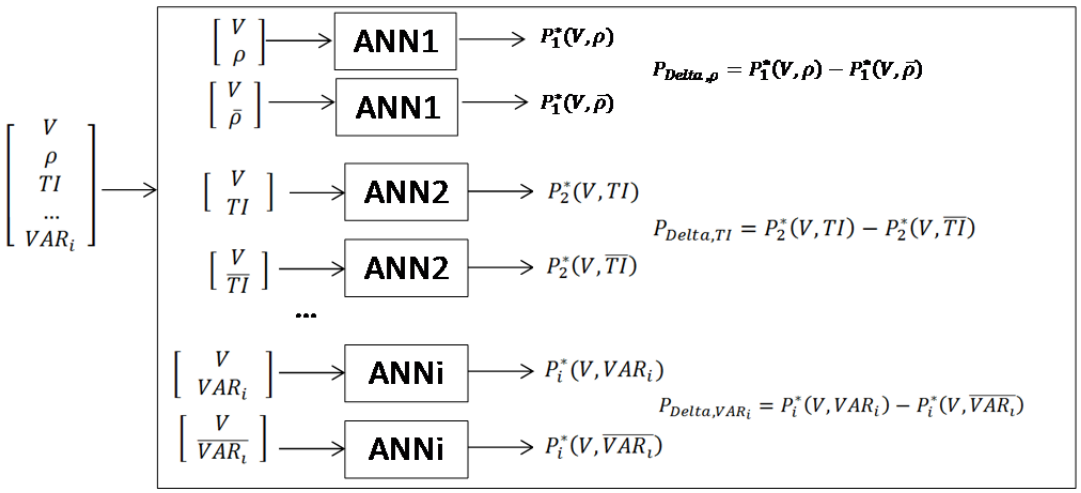

Figure 4-13 Multi-stage evaluation process

Lastly, the estimated power output (P) is evaluated through the following formula:

$$\hat{P}(V, TI, \dots, VAR_i) = P_{Delta,\rho} + P_{Delta,TI} + \cdots + P_{Delta,VAR_{i-1}} + P_i^*(V, VAR_i) \quad (4.3)$$

Once the results were obtained, a validation process could be completed. The model validation consisted of a qualitative comparison of the ANN power outputs and power coefficient (C_p) against the expected results from the literature. Figure 4-14 illustrates the overall behaviour of the ANN's power curve and C_p as a function of air density, turbulence intensity, and wind shear. The red lines represent the behaviour of the power curve and the C_p for the averaged value of the investigated parameter (air density, TI, or wind shear). The green lines represent the behaviour of the power curve and C_p for a lower value than the average of the investigated parameter, while the black lines represent the behaviour for a higher-than-average value. Black arrows indicate the direction of the evolution of the power curves with increasing values of the investigated parameter (with all other parameters being kept equal). Blue dots represent the 10-min data.

As can be seen in Figure 4-14, all power curves obtained using the ANN have a standard (sigmoid) shape and are properly located inside the scatter of 10-min data. No power curves have been found to follow outlier data, giving qualitative indication that the quantities of data and the training method were able to properly control the overfitting. C_p curves also exhibit typical behaviour. Furthermore, the power curve behaviour as a function of a change in air density as shown in Figure 4-14a exhibits a similar evolution as that specified in the IEC-61400-12-1 standard. As air density increases, the power curve shifts to the left, meaning that the Annual Energy Production (AEP) will increase with increasing average air density. Figure 4-14b also illustrates the impact of turbulence intensity on the power curve. Again, as demonstrated by several authors (Albers, 2010; Pedersen et al., 2002), the same impact on the power curve is observed in the model results. The 10-min average power output tends to increase with increasing turbulence intensity near the cut-in wind speed and decrease with increasing turbulence intensity in the transition region to rated power. Lastly, some authors present theoretical (Sumner et al., 2006; Wagner et al., 2010b) and experimental (Montes et al., 2009) results of the impact of the wind shear on the power curve. Again, ANN results, as shown in Figure 4-14c, show similar results to what has been found in the literature, i.e. that

higher AEP values are obtained when wind shear is low. These qualitative results provide further indication that overfitting was properly controlled during the modelling process.

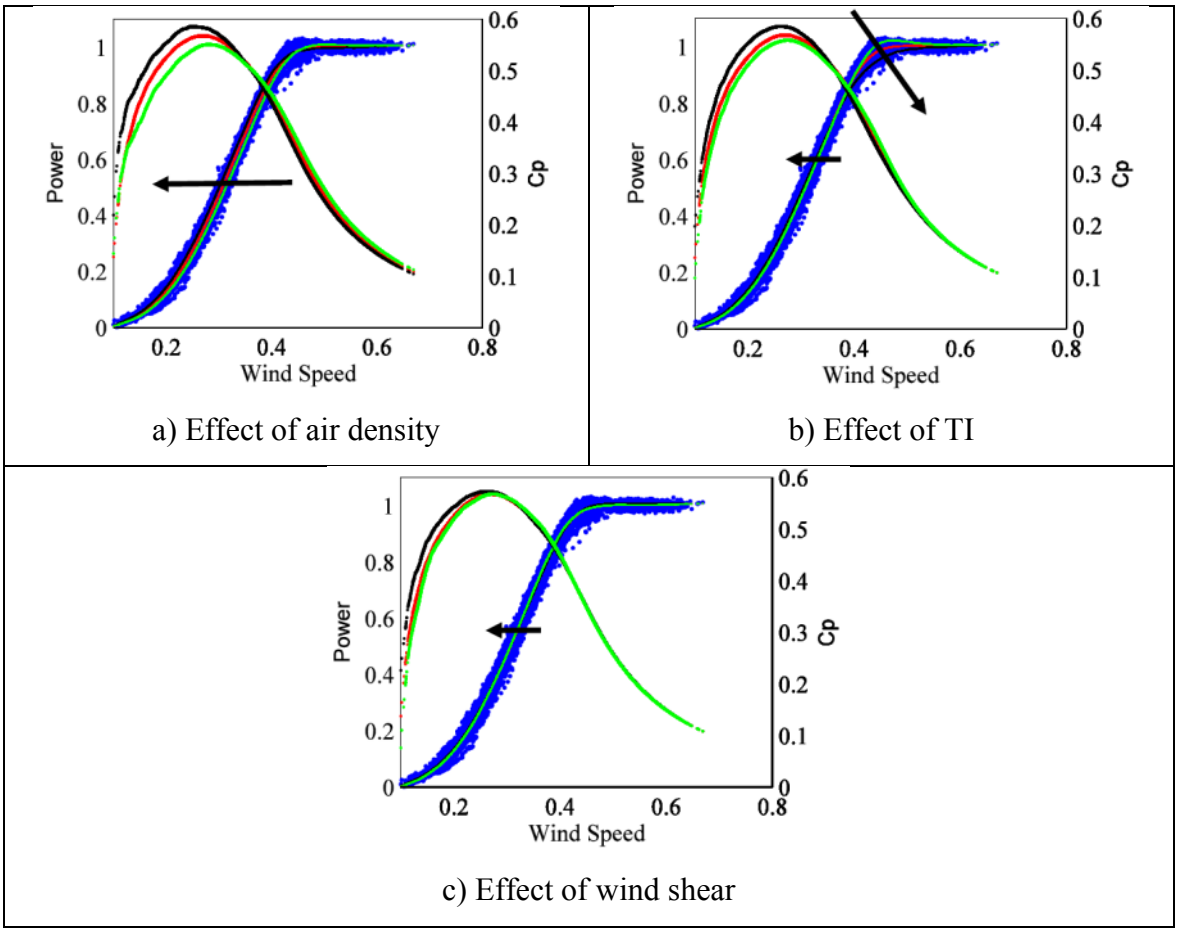

Figure 4-14 Impact on power curve and power coefficient (C_p)

4.3.8 Results on Power Curve Comparison

Results obtained using the ANN model with six inputs were compared with those generated by parametric (5^{th} and 9^{th} order polynomial functions, double exponential, logistic), non-parametric (k-NN), and discrete (IEC61400-12-1, IEC61400-12-2, Albers' turbulence normalization) models. All models used the same two data sets and each comprised approximately one year of data. The modelling comparison was largely performed using three different methods: power curve visualization, error calculations for each wind speed

bin, and global weighted errors according to a representative Weibull wind speed distribution of the sites.

Figure 4-15 shows the power curves obtained with all models for WTG#1. Similar results were obtained for WTG#2. The blue dots represent the 10-min data used to model the power curves. Power curves obtained from each model are illustrated as green dots. In order to compare a unique power curve from each model, air density normalization (for the site average air density) was performed prior to running the models.

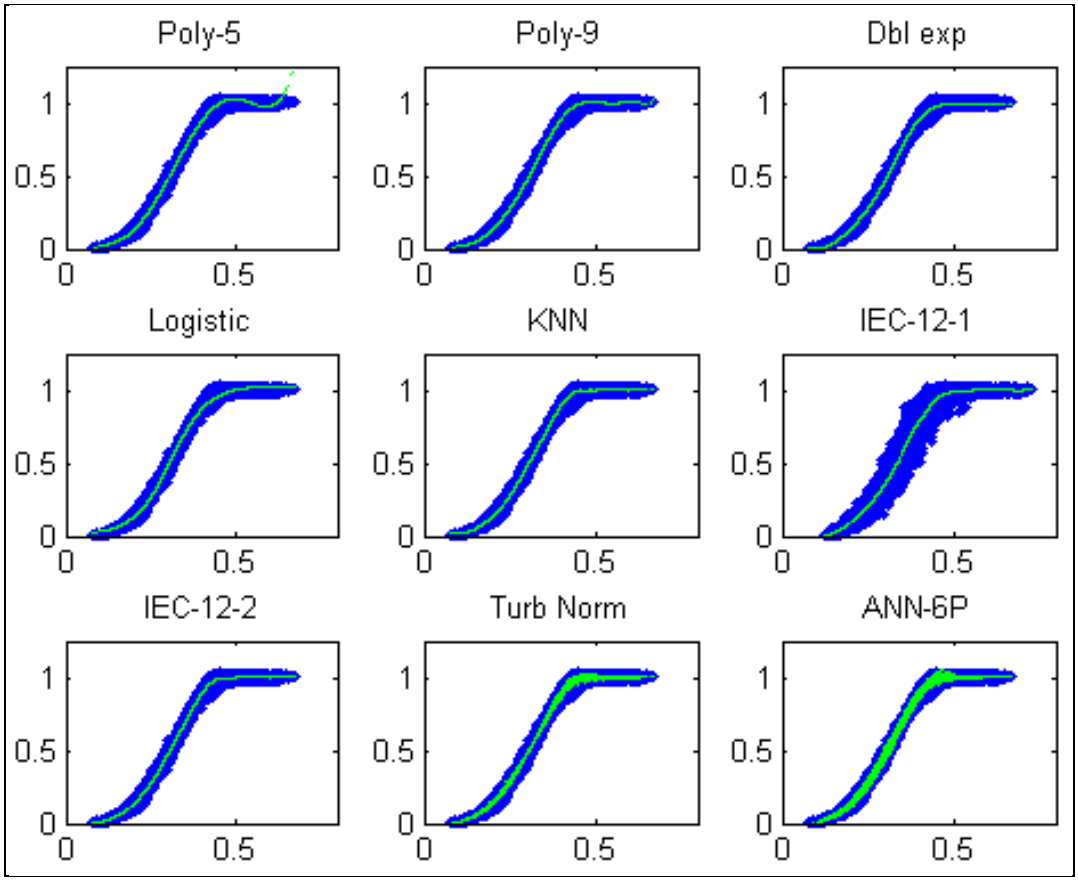

Figure 4-15 Wind turbine power curve modelling

In this case and as can been seen in Figure 4-15, parametric models (Poly-5, Poly-9, Dbl exp, logistic) have difficulty modelling the power curve over the entire wind speed range (this will

be further demonstrated in the following section). The k-NN model and the IEC61400-12-2 present very similar results. The IEC61400-12-1 generally exhibits lower repeatability since the dependent variable (wind speed) is taken from the measurements at the met mast which is at a greater distance of the wind turbine compared to all other methods (which are using wind speeds from nacelle anemometry located significantly closer to the turbine). Lastly, Alber's turbulence normalization (Albers et al., 2007) and the proposed ANN models predict a range of power values (rather than a unique power value) for a given wind speed since these two models consider not only wind speed and air density as independent variables, but also include supplementary inputs, namely turbulence level for the turbulence normalization model and four other parameters (turbulence level, wind shear, wind direction, and yaw error) for the proposed ANN model.

4.3.9 Error Calculations for Each Wind Speed Bin

In order to compare the performance of the ANN model with the other modelling techniques, error calculations were performed. Two metrics were used: mean error (ME) and mean absolute error (MAE); these have been evaluated according to Equations (4.4) through (4.6).

$$\varepsilon_i = P_i^* - P_i \tag{4.4}$$

$$ME = \frac{1}{N}\sum_{i=1}^{N} \varepsilon_i \tag{4.5}$$

$$MAE = \frac{1}{N}\sum_{i=1}^{N} |\varepsilon_i| \tag{4.6}$$

where:

P_i^* is the predicted wind turbine power output;

P_i is the observed (measured) wind turbine power output;

ε_i is the residual between the predicted and observed values; and

N is the number of 10-min data used for these statistical calculations.

The mean error ME is not an absolute measurement of precision, as it does not provide information on the prediction errors. For example, a perfect score, ME≈0, does not exclude

that the model is imprecise; rather, it could mean that errors of opposite signs are merely compensating each other. With a significant amount of data, ME will provide indications of biases in the model (systematic error). For example, ME can indicate if the model is over- or underestimating the phenomena.

The mean absolute error (MAE) is a quantity used to measure how close predictions are to the expected value. The MAE measures the average magnitude of the errors in a set of predictions, without considering their direction. Therefore, MAE provides an indication of modelling accuracy.

Because different anomalies may manifest themselves at different sections of the power curve, and because it is critical that power curve modelling be not only sound on the whole but also throughout the entire power curve, calculations were first completed for all wind speed bins of the power curve. Figure 4-16 and Figure 4-17 illustrate the results obtained for Site no. 1.

As demonstrated in Figure 4-16, the proposed ANN model has a minimum ME for almost all wind speed bins. It can also clearly be seen that parametric models have important biases for some wind speed bins, especially at higher velocities (at nominal power output). Figure 4-17 shows that, for almost all wind speed bins, the proposed ANN provides the results with the lowest MAE (highest accuracy). Parametric models generally exhibit poor accuracy. The model with the lowest accuracy is the IEC61400-12-1 model. This can be explained by the fact that this is the only model where the wind speed is measured at a different location (met mast) as opposed to the other methods which use wind speeds recorded close to the nacelle.

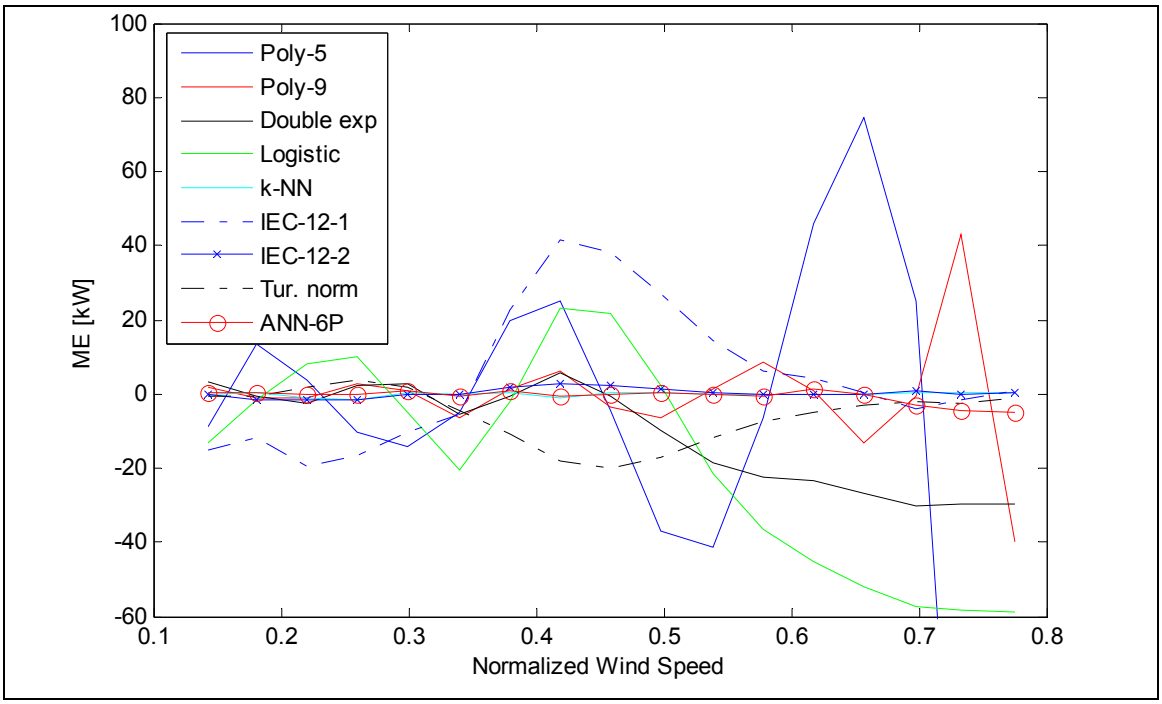

Figure 4-16 Mean Error (ME) for each normalized wind speed bin (Site 1)

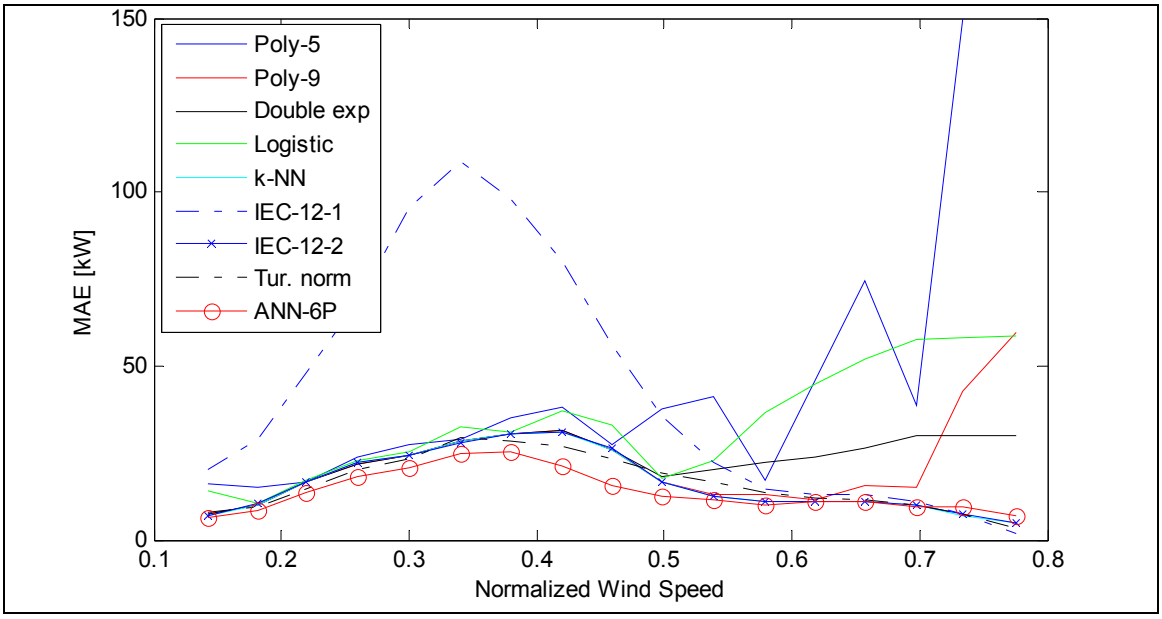

Figure 4-17 Mean Absolute Error (MAE) for each normalized wind speed bin (Site 1)

4.3.10 Weighted Error Calculations

Once calculated for all wind speed bins, the ME and the MAE were weighted averaged according to site-specific Weibull wind speed distributions. Site-specific results are presented in Figure 4-18 and Figure 4-19.

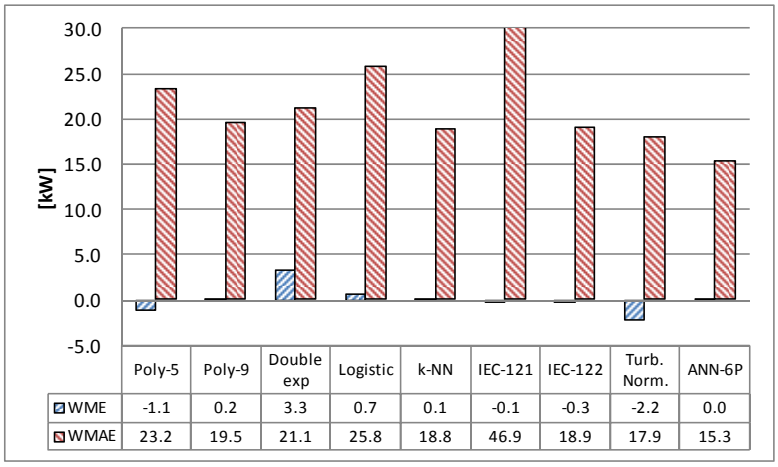

	Poly-5	Poly-9	Double exp	Logistic	k-NN	IEC-121	IEC-122	Turb. Norm.	ANN-6P
WME	-1.1	0.2	3.3	0.7	0.1	-0.1	-0.3	-2.2	0.0
WMAE	23.2	19.5	21.1	25.8	18.8	46.9	18.9	17.9	15.3

Figure 4-18 Modelling error calculations for WTG#1

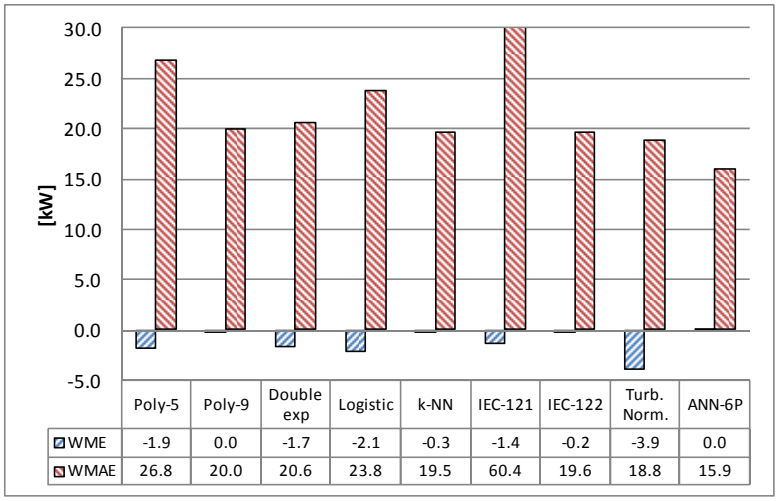

	Poly-5	Poly-9	Double exp	Logistic	k-NN	IEC-121	IEC-122	Turb. Norm.	ANN-6P
WME	-1.9	0.0	-1.7	-2.1	-0.3	-1.4	-0.2	-3.9	0.0
WMAE	26.8	20.0	20.6	23.8	19.5	60.4	19.6	18.8	15.9

Figure 4-19 Modelling error calculations for WTG#2

As can be seen in Figure 4-18 and Figure 4-19, the proposed ANN model shows the best modelling performance, having the ME and MAE consistently the lowest value for both sites. Furthermore, the proposed ANN is the only model that is able to incorporate additional inputs (e.g. wind speeds above hub height), which could potentially further improve the model's performance, as demonstrated recently by Wagner (G.P., 2008).

The results obtained from these error analyses demonstrated that the incorporation of six inputs in a multi-stage ANN modelling technique showed the highest accuracy for the two wind turbines studied. If further data had been available (e.g. wind speeds above hub height, wind veer, etc.) more inputs could have easily been added into the model and improvement of accuracy could potentially have been obtained. This is rendered possible due to the facts that low interactions between inputs have been found at the two sites considered and that power normalization between each modelling step was performed. These results demonstrate the potential of the two-layer MLP neural network to properly model the power performance of wind turbines.

4.4 Investigation on Air Density Impact

It is generally accepted that the relationship provided in the IEC 61400-12-1 standard is appropriate to account for the impact of air density on the power curve of a wind turbine. This standard assumes that Equation (4.7) allows for the correction of the wind speed for an active control wind turbine:

$$V_n = V_{10min}\left(\frac{\rho_{10min}}{\rho_0}\right)^{1/3} \tag{4.7}$$

However, the impact of air density derived from the results of the ANN training for a given wind turbine has been compared with the correction stipulated in the IEC61400-12-1. While the overall impact of the air density on the power curve is similar between the IEC standard and the ANN model, the (1/3) exponent of Equation (4.7) has been further refined with the ANN model via a minimization of the error.

Figure 4-20 illustrates the exponent value obtained by means of the aforementioned error minimization process for different values of air density. Air density values were selected so as to ensure the ANN had a sufficient quantity of data for these values, thereby ensuring proper behaviour of the ANN.

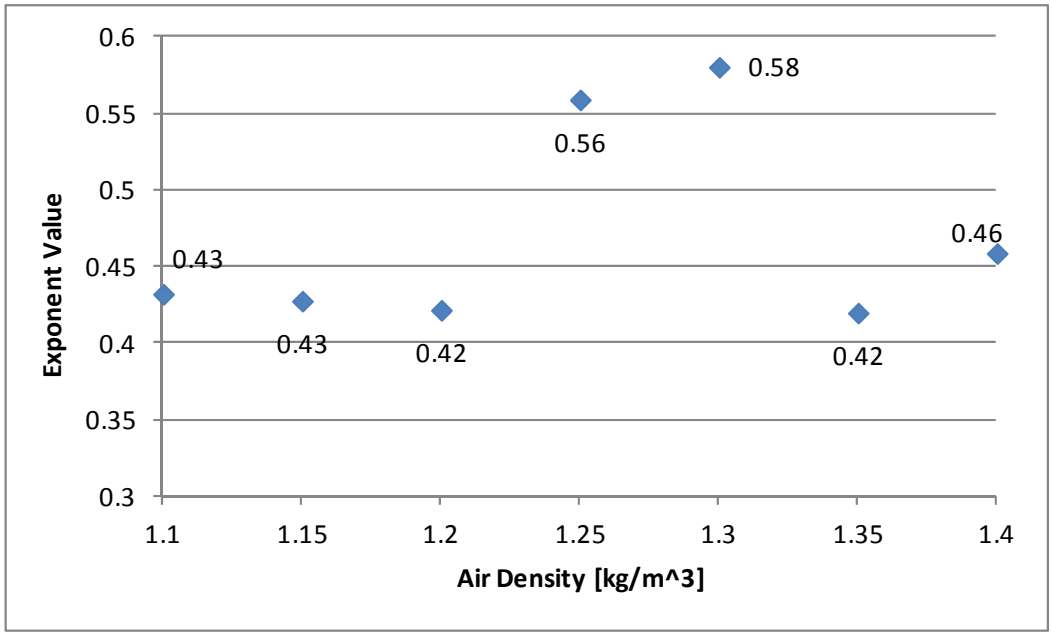

Figure 4-20 Air density correction

As can been seen in Figure 4-20, the optimized exponents are in the order of 0.42 to 0.58, depending on air density values. Values above 0.5 were obtained for air densities in the range of the average air density of the site (1.3 kg/m^3). The small adjustment in power curve for these cases could potentially render these results unstable. Further investigation is warranted.

Correcting Equation (4.7) to account for the impact of air density by using an exponent of 0.4 instead of 1/3 results in a difference in AEP of +1% for an air density of 1.4 kg/m^3 compared to the reference air density of 1.225 kg/m^3 (i.e. the reference value of the warranted power curve provided by the turbine manufacturer). The impact of air density should be investigated on additional wind turbines and the potential cause of such impact should also be more

thoroughly examined. If clearly demonstrated and properly understood, this finding could impose a significant amendment to the IEC 61400-12-1 standard, with consequences for power performance testing warranties and AEP expectations.

CHAPTER 5

POWER PERFORMANCE IMPROVEMENT – TEST NO.1: YAW OFFSET OPTIMISATION

Now that an improved wind turbine power curve modelling technique has been obtained through ANN, it is expected that smaller changes in performance can be detected. In order to validate this hypothesis, and because even small potential energy gain could represents substantial financial benefits, it was decided to use the previously developed ANN modelling technique to validate the impact of yaw offset angle and potentially determine the optimal yaw offset value. In this context and after lengthy negotiations with the turbine owner and manufacture, yaw offset testing was conducted on two operational multi-megawatt wind turbines.

This section of the document will present the testing process as follows:

I. Context,
II. Definitions,
III. Testing protocol,
IV. Testing Implementation
V. Data analysis,
VI. Results and recommendations.

5.1 Context

As demonstrated in Chapter 2, the review of literature has demonstrated that yaw offset of wind turbines is not uncommon and that significant energy losses are associated therewith. Despite this, very few experimental studies have been found in order to evaluate experimentally the energy losses at various levels of yaw error, in particular on multi-megawatt wind turbines.

Conducting testing on operating utility-scale wind turbines brought with it a number of commercial and technical challenges. After several discussions and validations, it was agreed

by both the turbine manufacturer and the wind farm owner that changes in both the control algorithm and the nacelle instrumentation could be made on the two operating wind turbines in order to complete the investigation on the yaw offset optimization.

The main premises of this testing is to impose a known yaw offset error value (hereafter referred to as the imposed yaw offset (IYO)) on the wind turbine. Random values have been provided through a testing protocol (see Section 5.3) in order to randomly impose a known yaw offset from -18° to + 18° (Limitation to +/- 18° was imposed by the turbine manufacturer for structural reasons). Figure 5-1 illustrates the definitions of a negative and positive yaw error for a clockwise-rotating wind turbine.

It is worth noting the level of innovation of the testing currently being conducted compared to the results of the review of literature presented, in particular those presented by Pedersen (Pedersen et al., 2002) on an investigation related to yaw completed in 1999 (Madsen, 2000). Table 5-1 demonstrates the degree of innovation of the current tests compared to what has been done previously.

Table 5-1 Comparison of current testing and Madsen test (1999)

Current methodology	**Madsen testing methodology**
Applied on multi-megawatt turbines with variable pitch and variable RPM	Applied on 75 kW wind turbine with constant pitch and constant RPM
Testing on two multi-megawatt turbines	Testing on one wind turbine
Results will be presented from a broad region of the power curve (from 400 kW to 1200 kW)	Results presented for wind speeds between 8-9 m/s only
Focus on small yaw error (+/-18°)	Focused on large yaw error (+/-70°)
Results based on 10-minute averages	Results based on <10-minute averages
Yaw error is imposed randomly and it was ensured that the yaw error was constant in the 10-minute intervals	Yaw error continuously changing (the turbine was turned at a constant wind angle speed of 0.5^{o}/sec) and the yaw angle represents the average of the interval

Current methodology	Madsen testing methodology
Evaluated the nacelle wind speed transfer function as a function of yaw error	Assumed no significant transfer function differences for different yaw error values
2 x 125 days of testing	Equivalent of 20 minutes (1200 s) of testing
Consideration to V, ρ, TI, WS	No consideration of inputs other than wind speed

5.2 Definitions

This section presents the definitions of key terms in order to allow for a better understanding of the testing protocol and the results obtained.

Figure 5-1 illustrates the references for the wind direction, nacelle orientation, and yaw error. The yaw error angles are attributed a positive or negative (+ or -) sign. For example, a (+) yaw error occurs when the wind direction is from the right of the centre line of the nacelle while a (-) angle corresponds to a wind direction from the left of the nacelle (as viewed from atop the nacelle).

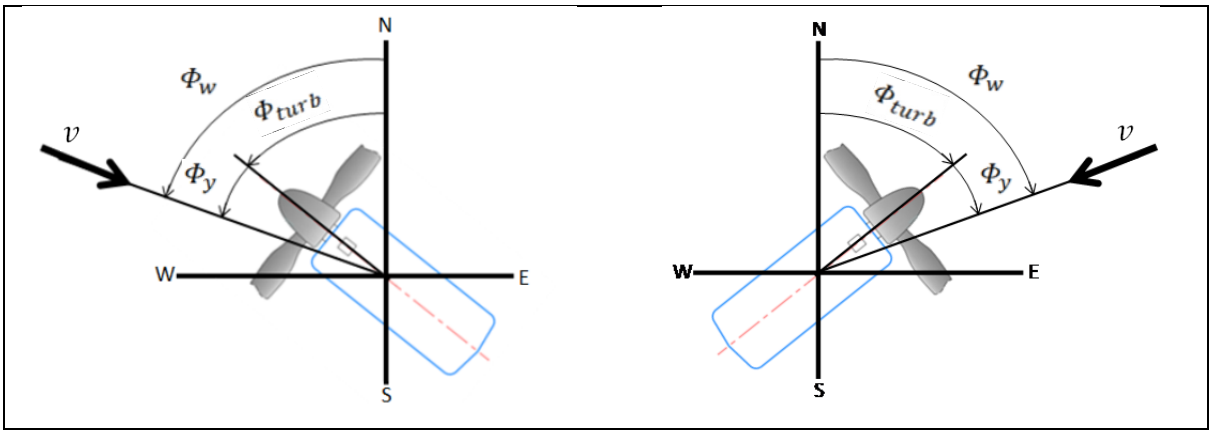

Figure 5-1 Top view of a clockwise-rotating turbine with negative (left) and positive (right) yaw error Φ_y

Φ_y is the instantaneous (1 s) yaw error angle. This value is positive when the wind is coming from the right of the central axis of the turbine and negative when it comes from the left. Yaw error is also known as the wind direction deviation relative to 0° of the wind turbine nacelle. Yaw error can also be obtained by comparing the wind direction and the nacelle orientation.

$$\Phi_y = \Phi_w - \Phi_{turb} \tag{5.1}$$

Φ_w is the wind direction instantaneous angle. This angle should always be measured relative to true north and not magnetic north.

Φ_{turb} is the nacelle orientation instantaneous angle. Again, this angle should always be measured relative to true north and not magnetic north.

The average yaw error $\overline{\Phi_y}$ is defined as the average of 1 s yaw error readings over a given period (i.e. 10 minutes):

$$\overline{\Phi_{y,10min}} = \frac{1}{600}\sum_{i=1}^{600} \Phi_{y,i} \tag{5.2}$$

Because the nacelle wind vane is not always perfectly aligned with the wind turbine centre line (rotor axis), it is necessary to introduce another variable: the yaw offset angle. Figure 5-2 illustrates the differences between a wind direction deviation, a yaw offset and a yaw error.

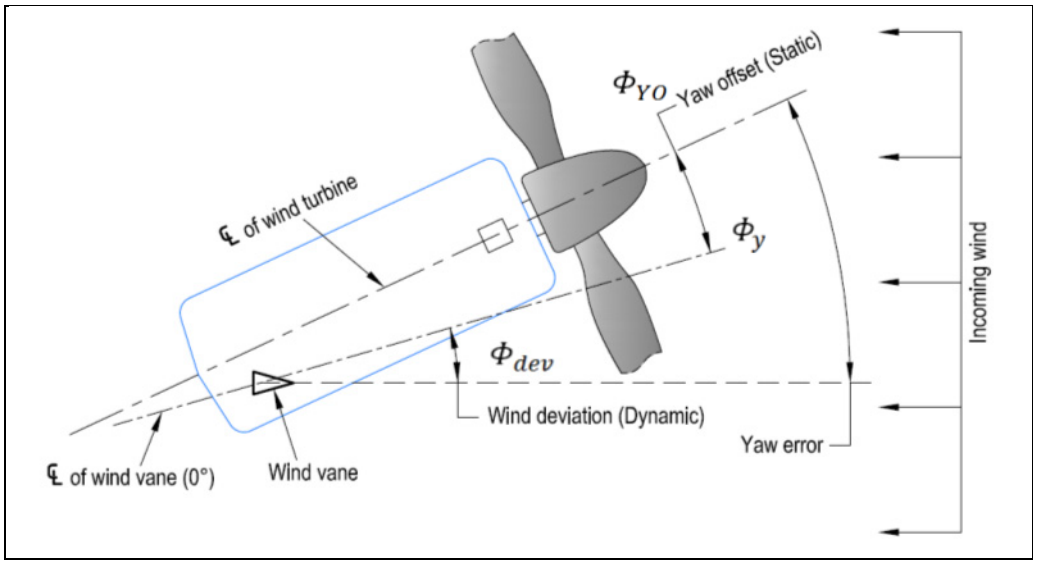

Figure 5-2 Angle nomenclature

Looking at Figure 5-2, the yaw error can be obtained through the following formula:

$$\Phi_y = \Phi_{dev} + \Phi_{YO} \tag{5.3}$$

where:

Φ_y is the yaw error

Φ_{dev} is the wind vane direction deviation (also referred to as dynamic error). Φ_{dev} is positive if the wind direction is from the right of the centre line of the wind vane (0°) and negative if the wind is coming from the left of 0°.

Φ_{YO} is the yaw offset (static error or misalignment of the wind vane) and corresponds to the angle between the centre line and the 0° of the nacelle wind vane. This angle is mainly due to misalignment of the wind vane on the turbine nacelle. Φ_{YO} is positive if the misalignment of the wind vane is on the right of the centre line of the nacelle and negative if the misalignment is on the left.

Figure 5-3 illustrates the 10 minute-average distribution of the wind vane direction deviation Φ_{dev} for WTG no. 1 for a period of approximately 9 months. The x-axis represents the 10-minute average wind direction deviation and the y-axis represents the occurrences.

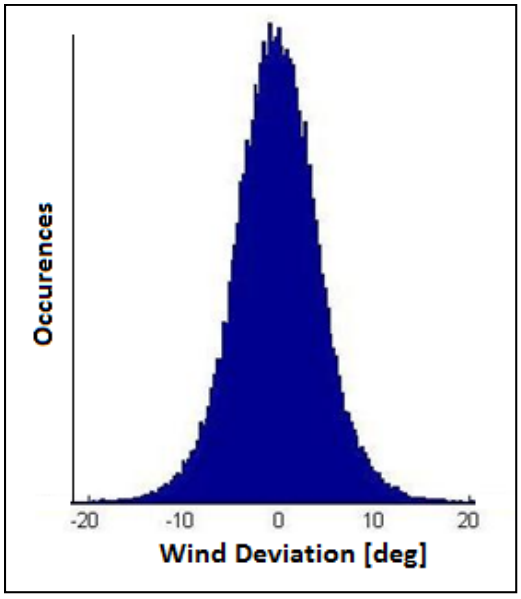

Figure 5-3 10-minute average wind deviation (Φ_{dev}) distribution for WTG#1

As can been seen in the preceding figure, the distribution of the 10 minute-average wind deviation seems to be normally distributed with an average of μ = -0.1° and a standard deviation of σ = 4.6°. Unfortunately, the average (μ = -0.1°) cannot be considered to reflect the true yaw offset, because it may not be representative of the true average of the wind direction relative to the nacelle center line of this wind turbine. For example, an error in the wind vane orientation (i.e. misalignment during installation) could yield an average Φ_{dev} close to zero, whereas in reality the wind turbine nacelle orientation may still be offset from the wind by several degrees. The standard deviation as shown in Figure 5-3 could give an indication of the performance of the yawing algorithm (a larger value for σ means less adjustment in direction). It is important to note that the optimization of the yaw control algorithm (reducing the σ) is not the main objective of this testing.

5.3 Testing Protocol

A testing protocol is a tool that describes an experiment. It defines the objectives, hypothesis and the structure of an experimental test in order to ensure good results are obtained upon conclusion of the testing. A testing protocol entails the following six steps:

I. Definition of test objectives,
II. Selection of process variables and data scaling,
III. Selection of experimental design,
IV. Execution of experimental design,
V. Verification that data are consistent with the experimental assumptions,
VI. Analysis and interpretation of results.

5.3.1 Define Objectives of the Test

The determination of the optimal imposed yaw offset (IYO) for a given wind turbine represents the main objective of this experimental protocol. Optimal IYO represents the angle at which the wind turbine's power performance is optimal (i.e. the highest efficiency to extract the energy from the wind). The optimal IYO is not necessarily obtained at IYO=0 degree, since the wind vane sensor may have been misaligned during installation or may have shifted under influence of the rotor.

5.3.2 Select Process Variables

An important part of any testing protocol is to choose the proper inputs for modelling. In Chapter 4, the most influential independent inputs have been investigated (see Annex II for a list of all tested inputs) and identified.

The dependent inputs identified are the following:

I. V,

II. ρ,

III. TI,

IV. WS.

Contrary to Chapter 4, wind direction and yaw error have not been considered in the actual modelling process. The wind direction sensors were found to be defective for the period of investigation, rendering them unusable. Further, the yaw error has been removed because of its relationship with the IYO. In the context of this testing there is only one dependant output, which is the active power output of the turbine, while the controllable variable is the IYO. Figure 5-4 illustrates the variables investigated in the context of this testing.

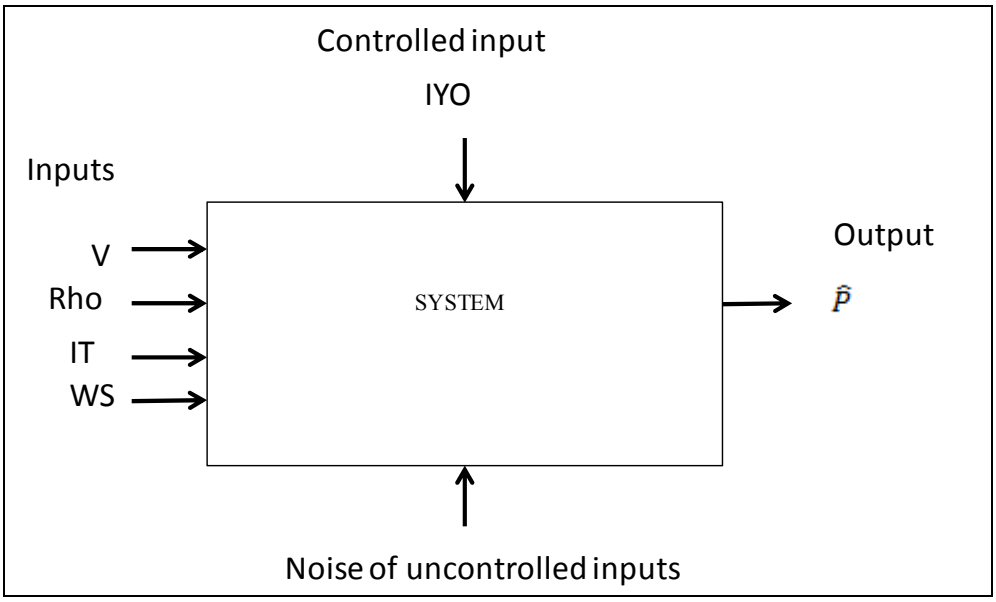

Figure 5-4 Variables used in model

5.3.3 Data distribution

The distribution of each variable is important to analyse in order to i) visualize the domain of the experimental space and ii) qualify the completeness of the archived database during this experiment.

Ideally, the future experiment will have to be based on the same variable distribution (space) as the one used for modelling. WTG#1 and WTG#2 have been modelled separately. For this reason, the variable distribution will not be the same for both sites as presented in Table 5-2.

Table 5-2 Data distribution

Description	Variable	Units	Min	Max
Active power output	P	kW	400	1200
Imposed Yaw Offset	IYO	°	-18	+18
Nacelle wind speed	V	m/s	3.5	25
Air density	ρ	kg/m^3	1.15	1.34 (WTG1) 1.30 (WTG2)
Turbulence intensity	TI	%	0.04	0.31
Wind shear (80/40)	WS		0.75 (WTG1) 0.70 (WTG2)	1.7

While the nacelle minimum wind speed value has been imposed in order to avoid modelling the power curve at very low power where the energy increase is minimal but represents a significant modelling challenge, data distribution of the active power output, air density, turbulence intensity, and wind shear variables have been identified by examining the spreading of each of these variables used for the modeling. For example, Figure 5-5 illustrates the spreading of the air density used for modelling the power output of WTG#1. The black line shows the data distribution used for modeling. Data outside of the black square where not considered during this investigation.

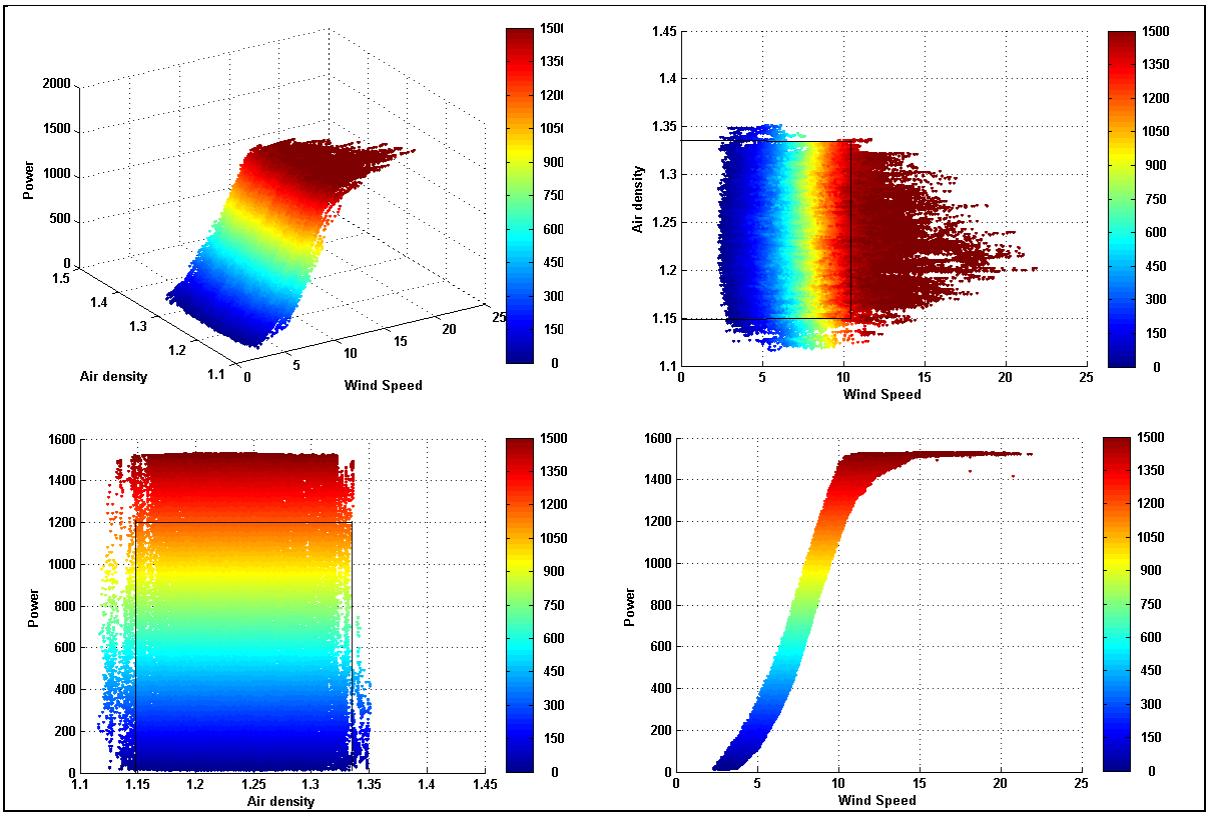

Figure 5-5 Air density scaling value ($1.15 \geq \rho \leq 1.34$)

Figures for the other inputs used for the ANN training (air density, turbulence intensity and wind shear) can be found in Annex IV for both Turbines 1 and 2.

5.3.4 Data Recoding

According to Baléo (Baléo et al., 2003), data recoding is often necessary in order to lower the disparity of the analyzed data and thereby lower the potential undesirable impact on the statistical analysis performed on these data. Data recoding is generally done for three main reasons:

I. To correct the hypothesis of the normality of data distribution. Some mathematical transformations can help improve the normality of the data,

II. To improve the linearity of the relationship between variables,

III. To improve the homogeneity of the amplitude of the data. A better homogeneity is important in order to ensure that the weight factors used in any modelling are interpreted in a consistent manner.

In the present case, only the third reason justified the recoding of certain data. Therefore, the active power output has been normalized by the nominal power output of the turbines, while the wind speed has been divided by 25. Thus, all investigated variables are of the same order of magnitude, i.e. around 0 and 1.

5.3.5 Select an Experimental Design

The choice of an experimental design depends on the objectives of the experiment and the number of factors to be investigated. In the present case, the only factor investigated was the Imposed Yaw Offset. Furthermore, the author has been allowed by the turbine manufacturer structural engineer to test yaw offset between -18° to +18° only. This limitation was mainly imposed for structural reasons.

Because it is a good assumption that the optimal IYO is probably close to zero, and also because the difference in power output in this region is probably low, a randomization of the IYO value according to the following probability density function has been developed manually for the first part of the testing. The blue line of Figure 5-6 illustrates the chosen probability level, while the red line shows the obtained distribution of the tested IYO. This first testing was conducted between 1 May 2012 and 6 September 2012 for both turbines.

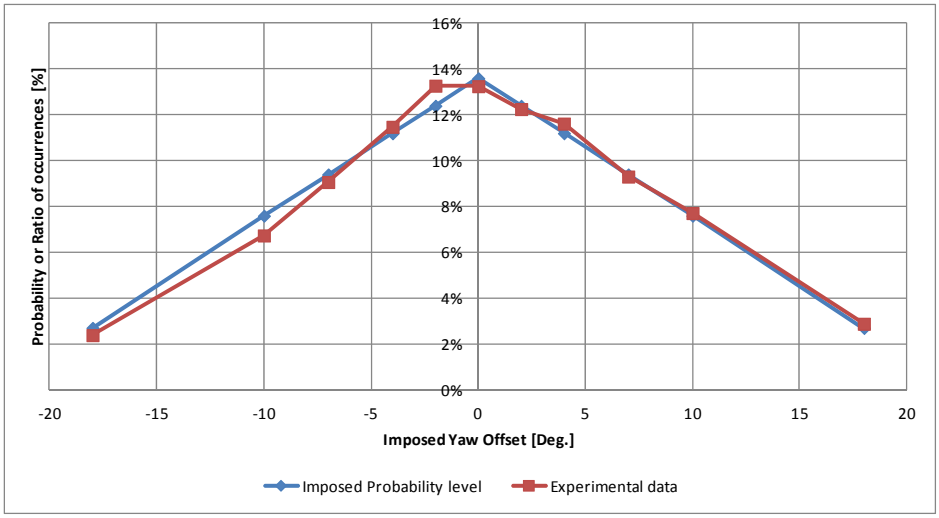

Figure 5-6 Probability of occurrences for the first testing period

A second IYO testing phase has been developed. At the time of its elaboration, it was decided to focus the analysis on a value of approximately +3°. The reason for this decision was the fact that measurement of the initial wind vane orientation indicated a deviation around + 3°. The intention was to install the second wind vane (sonic anemometer) with the same yaw offset. However, for technical reasons, it was not possible to confirm that the orientation of the second wind vane was at this angle. This second testing was conducted between 26 November 2012 and 20 March 2013.

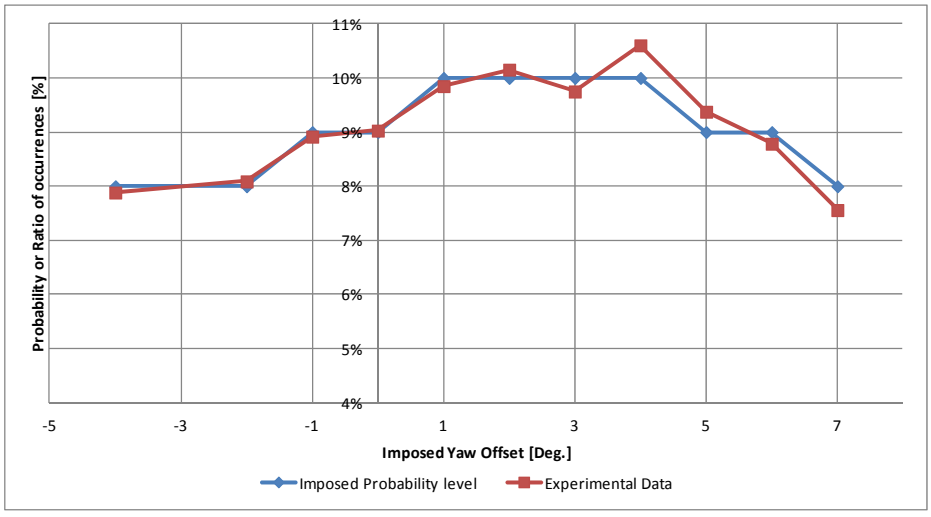

Figure 5-7 Probability of occurrences for the second testing period

Figure 5-8 illustrates the combined distribution of IYO for the entire testing period.

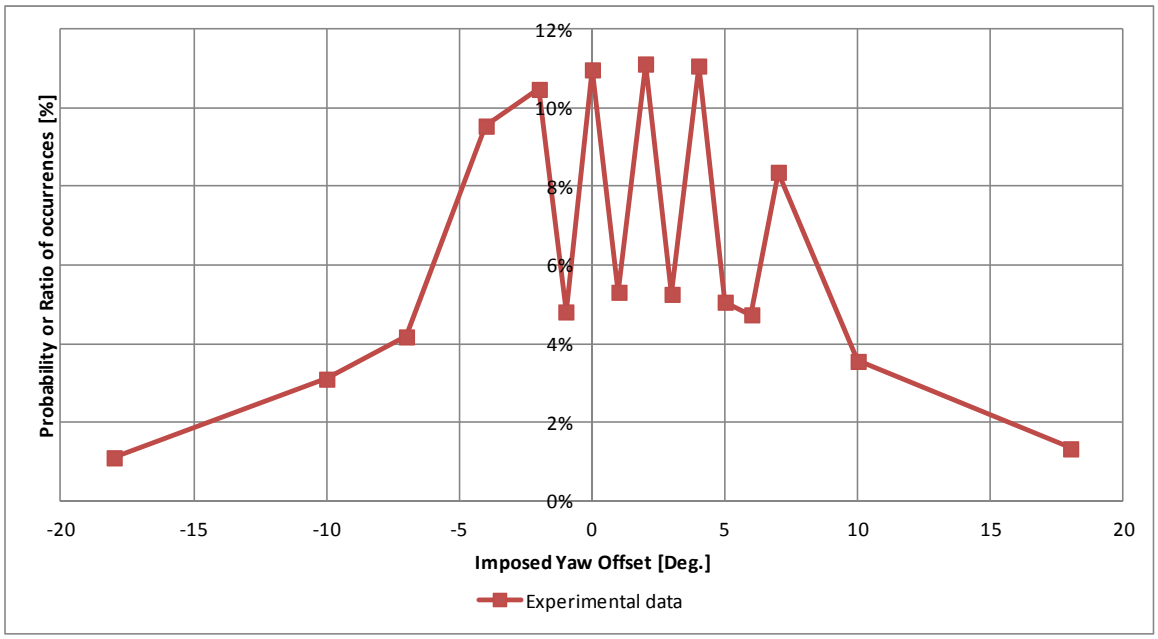

Figure 5-8 Probability of occurrences for the two testing period

In order to minimize the impact of meteorological conditions on the investigated power output, the IYO was randomly changed every 40 minutes. Alternating between two or more values is referred to as a toggle test. The interval of 40 minutes was chosen in consideration of the nacelle yawing speed (which is in the order of 1 deg/sec) but also due to the fact that the control algorithm for the definition of a yaw offset value is unknown, as the turbine manufacturer wished to keep this parameter confidential. Therefore, 40 minutes was estimated to be a sufficient time lapse to ensure that the turbine had enough time to adjust to its new setting (IYO) while being short enough to ensure that all influential meteorological inputs are properly distributed in all IYO conditions. In general this is one of the advantages of toggle testing in the wind industry context, as it allows for a reduction of the impact of meteorological influences on the testing being conducted.

Lastly, it is worth mentioning that a resampling procedure (Pelletier et al., 2010) has been completed in order to multiply five-fold the number of available data for investigation.

5.4 Testing Implementation

Several modifications had to be made to the two test turbines in order to be able to complete the proposed Imposed Yaw Offset testing. The data acquisitioning system (PI system) began to acquire data in early 2009 and has collected data continuously until present at a high frequency sampling rate (1 Hz) for Site 1 and Site 2. Unfortunately, at the beginning of 2011 for Site 1 and 2012 for Site 2, a significant change in the control algorithm of the turbines had a major consequence on the behaviour of these two turbines (see red dots vs blue dots in Figure 5-9). This change in performance significantly diminished the available data for the elaboration of a reference model through ANN; with this change, 2-3 years of data were lost.

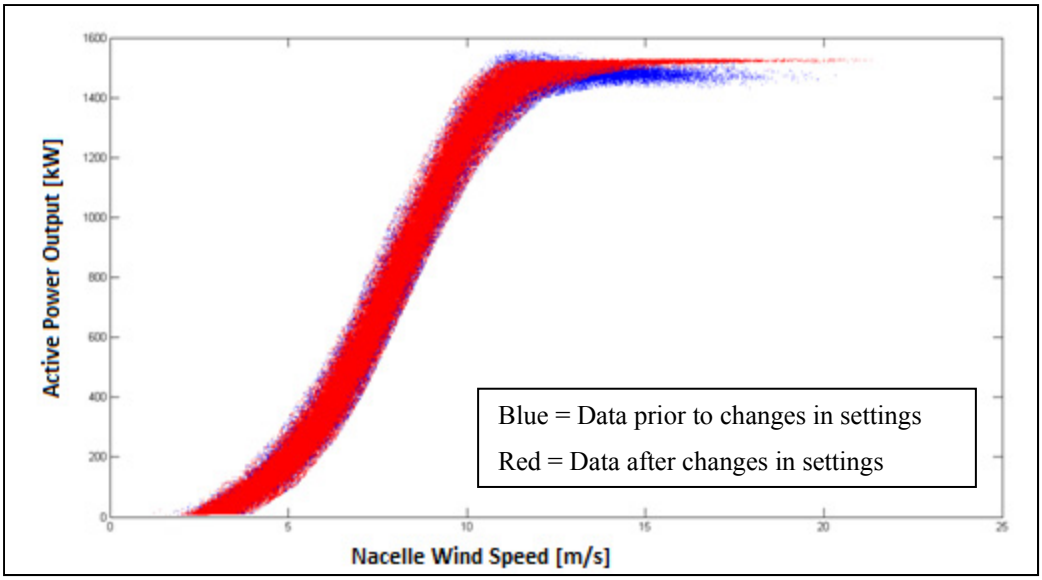

Figure 5-9 WTG#1 scatter plot before (blue) and after (red) 2011

In March 2011, the wind vanes on both turbines were changed. This was necessary since the old wind vanes were specifically designed for the turbine yaw control and therefore gave only 4 directional readings (right or left at 0° or 180°). This limitation in direction resolution rendered their use for the completion of the IYO testing impossible. It was decided to install

sonic anemometers that can measure simultaneously wind speed and direction with a high wind direction resolution. Figure 5-10 presents the former and new installation.

Figure 5-10 Nacelle instrumentation pre- (left) and post- (right) installation of sonic anemometer

As can been seen, the old heated NRG anemometer (the instrument on the right in both photos) has been retained, allowing for the monitoring of the nacelle wind speed (a crucial metric in this research) to remain unchanged.

The second major change that had to be completed for this testing was the elaboration of a special control algorithm. The main objective of this special control algorithm - developed and installed by the turbine manufacturer – was to allow random IYOs to be imposed at constant intervals. This control algorithm was implemented on 4 May 2012, marking the start of the first testing period. This testing lasted approximately 3 months, ending on 6 September 2012. The second IYO testing began 26 November 2012 and lasted 4 months, ending 30 March 2013. Figure 5-11 and Figure 5-12 provide the beginning and end dates of both the reference periods used for the ANN modeling and the IYO testing periods.

Figure 5-11 WTG no.1 – Project Schedule

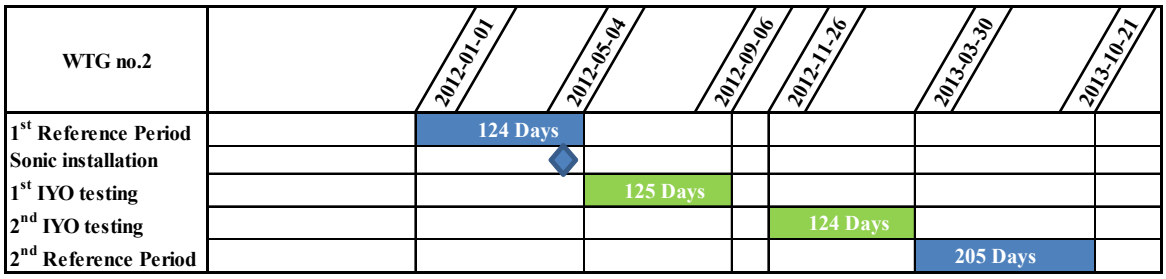

Figure 5-12 WTG no.2 – Project Schedule

The 1st and 2nd reference period combined yield a total of more than 600 days for WTG no.1 and 329 days for WTG no.2 of available data for the ANN models for both tested wind turbines. The two IYO testing periods total nearly 250 days of data available for both turbines to complete the analysis.

5.5 Results of IYO Testing

In order to evaluate the potential impact on performance for different IYO values, the energy output at a given IYO was compared with the results of the ANN modelling under the following meteorological conditions: V, ρ, TI, and WS. Equation (5.4) gives the power factor (PF) which is related to the turbine performance increase (if PF >1) or decrease (if PF <1) for any given IYO:

$$PF_{IYO} = \frac{P}{\hat{P}} \tag{5.4}$$

PF_{IYO} is therefore the ratio between a given IYO of the real power output and the expected energy output obtained from the multi-stage ANN at a given V, ρ , TI, or WS. PF_{IYO} have been corrected (PF_n) in order to ensure that PF_n is equivalent to 1 at IYO = 0. This normalization facilitates the evaluation of the true potential energy gain or loss when compared to a given change in the orientation of the currently installed wind vane (IYO = 0°).

Because the air flow around the nacelle anemometry could be altered by the IYO, a validation of the nacelle wind speed transfer function was completed. If a bias of the measured nacelle wind speed is found after imposition of an IYO when compared to the baseline (IYO = 0°), then a correction factor was applied. The potential correction factors have been established by comparing the nacelle wind speed with an external reference (i.e. meteorological mast) for each value of IYO. Figure 5-13 provides the transfer function for two IYO values (+18° and 0°).

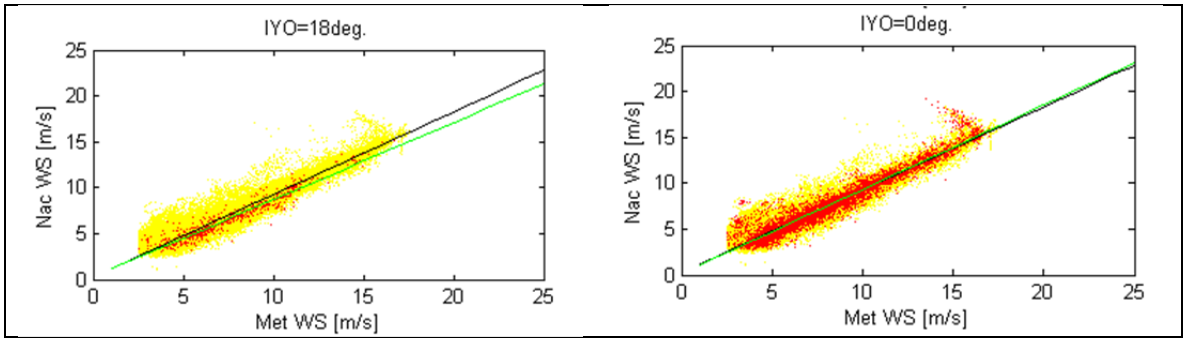

Figure 5-13 Nacelle wind speed transfer function

In Figure 5-13, the black line represents the transfer function for the reference period (without IYO). This first transfer function is obtained by comparing the nacelle wind speed and the wind speed from the proximate mast wind speed (yellow points).

The 2nd transfer function (green line) was obtained by once again comparing the nacelle wind speed against the met mast wind speed but this time at a given IYO value. The red points are

therefore the data used for this. It can therefore be seen in the left part of Figure 5-13 that there is a significant difference between the transfer function for the reference period and the transfer function when IYO is +18°, while this difference is non-significant (the two lines are superposed) when IYO = 0°. The entire set of transfer function evaluations for all IYO values from -18° to +18° is presented in Annex III.

Lastly, after transfer function correction, ANN modelling of each 10-minute input and data normalization to IYO = 0, the results of the impact of the IYOs were obtained for the two wind turbines. Figure 5-14 and Figure 5-15 present the normalized Power Factor (PF_n) as a function of the IYO. These results are representative of the power output between 400 kW and 1200 kW. The lower value (400 kW) has been chosen in order to avoid any intermittent phenomena due to cut-in wind speed, while the higher value (1200 kW) has been chosen to avoid any impact related to power regulation that occurs at nominal power (1500 kW).

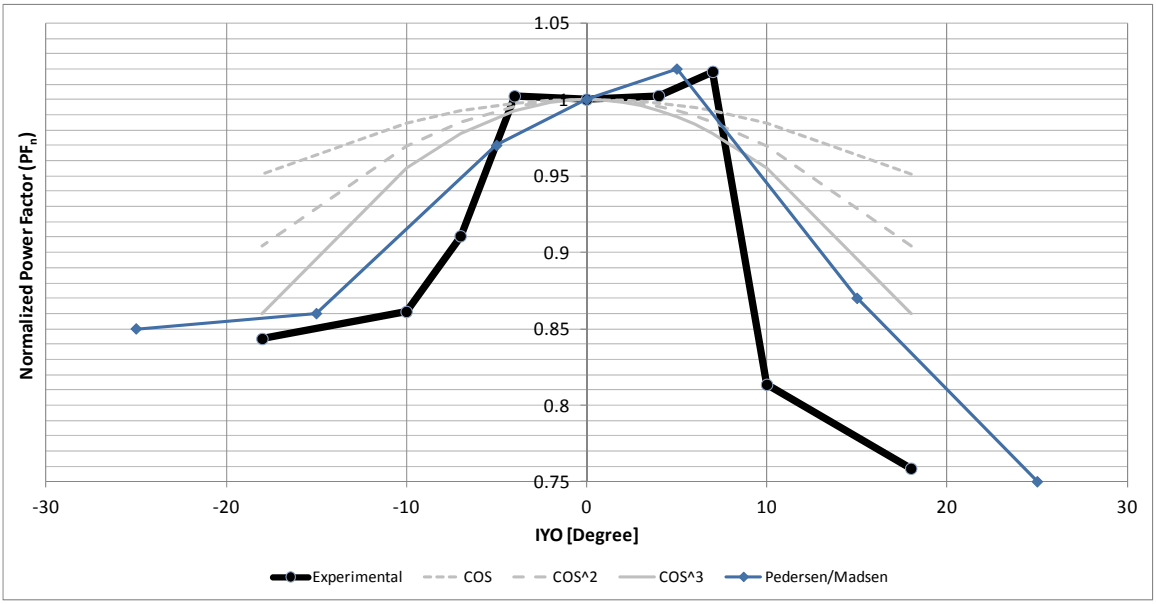

Figure 5-14 WTG#1 – PF_n vs. IYO

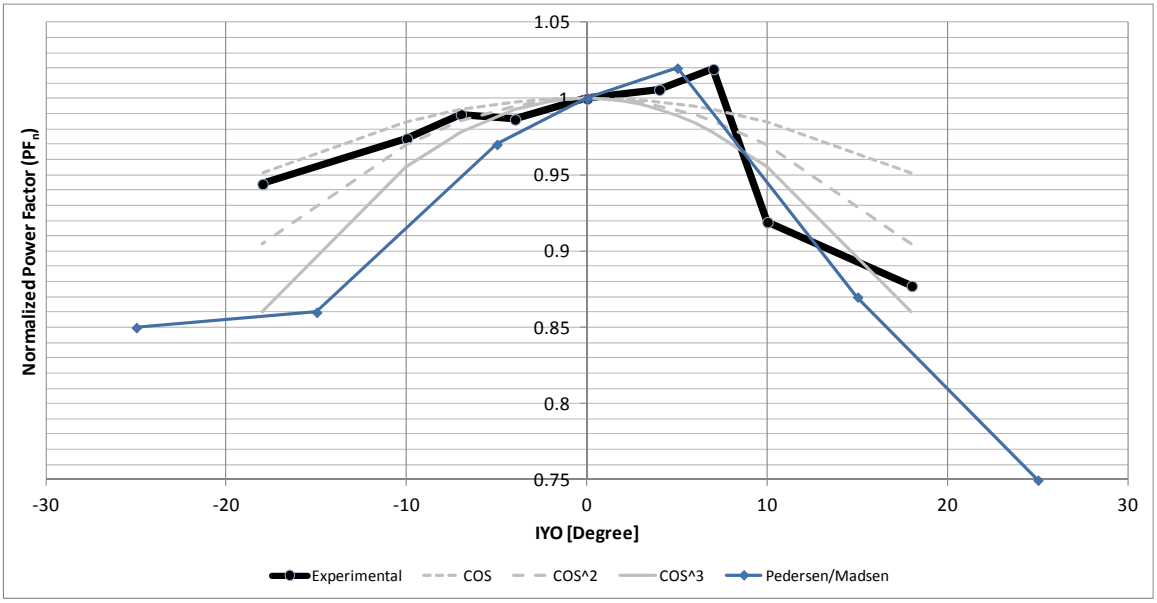

Figure 5-15 WTG#2 – PF_n vs. IYO

5.6 Analysis and Interpretation of Results

Analysis of Figure 5-14 and Figure 5-15 reveals similarities and differences between both tested turbines and the test results presented by Pedersen/Madsen. These observations are described in the following sections.

5.6.1 Similarities

I. As shown by the PF_n curves of the two test turbines as well as the Pedersen/Madsen curve, the decrease in PF_n is faster with positive IYO than with negative values.

II. With the exception of WTG#2 (for negative IYO), and as proposed by Pedersen, the impact of the yaw error at low IYO (less than +/-20°) seems to be higher than a $\cos^2$ relationship.

III. At approximately +5 to +7° performance for all three tested turbines seems to be optimal.

IV. The potential increase in performance shown by all three turbines (including Pedersen/Madsen) is in the order of 2%.

This increase in performance at low (+5° to +7°) angles may potentially be attributable to two factors:

I. Aerodynamic – for clockwise-rotating turbines with a positive yaw error, it implies that when a rotor blade is above hub height, it "sees" an increased wind speed compared with no yaw error, while the blade is below the hub, it sees less wind speed. The gain (when the blade is above) is potentially greater than the loss (when the blade is below) due to wind shear.

II. Transfer function – rotating rotor blades affect the wind regime around the nacelle. Fluctuation in direction can therefore affect the wind vane reading. A transfer function should then be imposed in order to correct the wind direction. The manufacturer in this study is not imposing any transfer function to correct for the wind vane direction.

Further investigations should be completed in order to validate these two hypotheses.

5.6.2 Discrepancies Observed

Observations of the results suggest that certain turbines or site-specific conditions might influence the results of the testing. Specifically, the following discrepancies have been found when comparing the results of the two tested turbines and those of Pedersen/Madsen.

I. Even though WTG#2 is showing a faster decrease with positive IYO and an optimal performance at approximately +7°, the performance losses are much less significant than the other two turbines.

II. While the optimal performance for the Pedersen/Madsen power curve seems to occur at approximately +5°, it seems to occur at +7° for WTG#1 and WTG#2. This difference may be due to an offset error on the wind vanes. It may be interesting to measure the yaw offset of these two turbines.

III. While the PF_n are similar for WTG#1 and Pedersen/Madsen results, they are not entirely identical.

Reasons that might potentially explain these site- (or turbine-) specific results could be:

I. Anemometers on the nacelle and the met mast can be affected by the vertical component of the wind. This vertical component can be induced both by

topographical effects and improper installation (leveling) of the anemometers. Improper instrument installation can affect the wind speed readings and thereby the results of the ANN model or the transfer functions between met mast readings and nacelle wind speed readings;

II. Site 1 is located in terrain of low complexity, while Site 2 is located in what is considered to be complex topography. In light of this, the wind direction distribution could be significantly different for the two tested turbines;

III. As it was not measured on either tested turbine, nor published in the Pedersen or Madsen articles, the yaw offset at each wind turbines may be different.

IV. For Site 2, the lower decrease in performance could be due to the fact that the database size was significantly lower than for Site 1.

V. Wind veer (difference in wind direction with height) has not been measured in the context of this project and may have been different for the two tested turbines.

5.7 Conclusion

In this chapter, definitions of yaw error and offset have been provided. The inputs used for the ANN modelling of the power output of two operational turbines have been presented. A testing protocol has been defined and the results of the testing have been presented.

While Figure 5-14 and Figure 5-15 show a potential energy improvement at a small, positive IYO, these results should be interpreted with caution. Given that this finding is based on a mere three turbines (including the results from Pedersen/Madsen), further investigation should be conducted in order to ensure the repeatability of these results.

Furthermore, it is important to note that if one were inclined to voluntarily impose a yaw error of +7°, the risk that the turbine's power performance would decline rather than improve might be substantial. As previously mentioned, for a positive yaw error greater than +7° there is a rapid decrease in performance (more so than for negative angles). Therefore, if a party were to impose a yaw error while lacking an accurate installation procedure for wind vane

alignment, this could severely affect the power performance. In order to assess more realistically the potential energy gains (or losses), a Monte Carlo simulation assuming different levels of accuracy in wind vane alignment procedure has been completed. Three levels of misalignment distribution (+/-5°, +/-1° and +/-0.5°) have been simulated for different IYO angles for both tested turbines. Figure 5-16 illustrates the dispersion of wind vane alignment (at IYO = 0°) for these three level of precision. Each of the three samples were composed of 10 000 random trials.

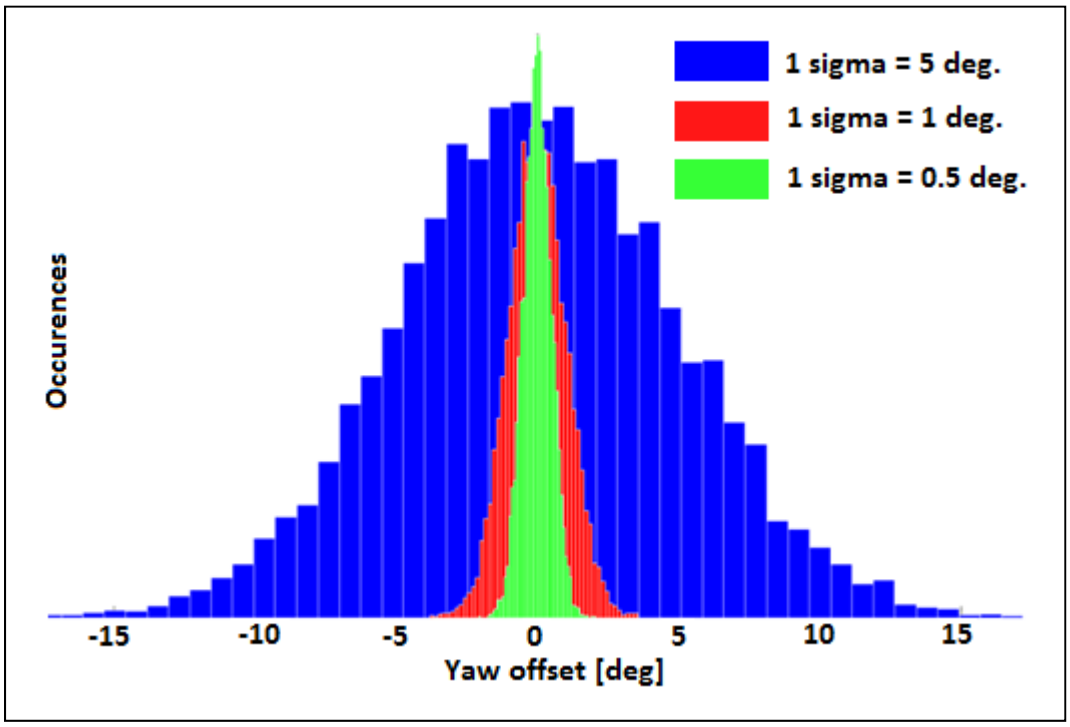

Figure 5-16 Monte Carlo results for the distribution of three levels of accuracy in wind vane alignment

Using these three distributions and calculating the energy gain (or loss) attributed to each alignment from Figure 5-14 and Figure 5-15, it is possible to evaluate the mean energy gain or loss at each level of accuracy. This process has been repeated for average angles of alignment (from -7° to +10°) and for both tested turbines. Figure 5-17 and Figure 5-18 show the obtained results.

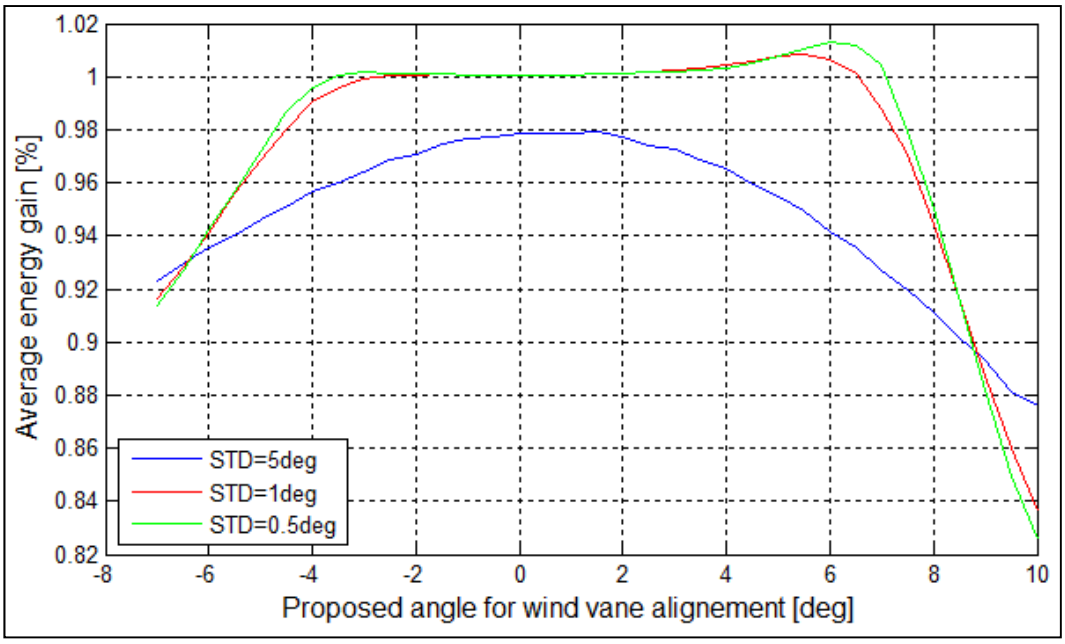

Figure 5-17 WTG#1 – energy gain at different IYO values and levels of accuracy

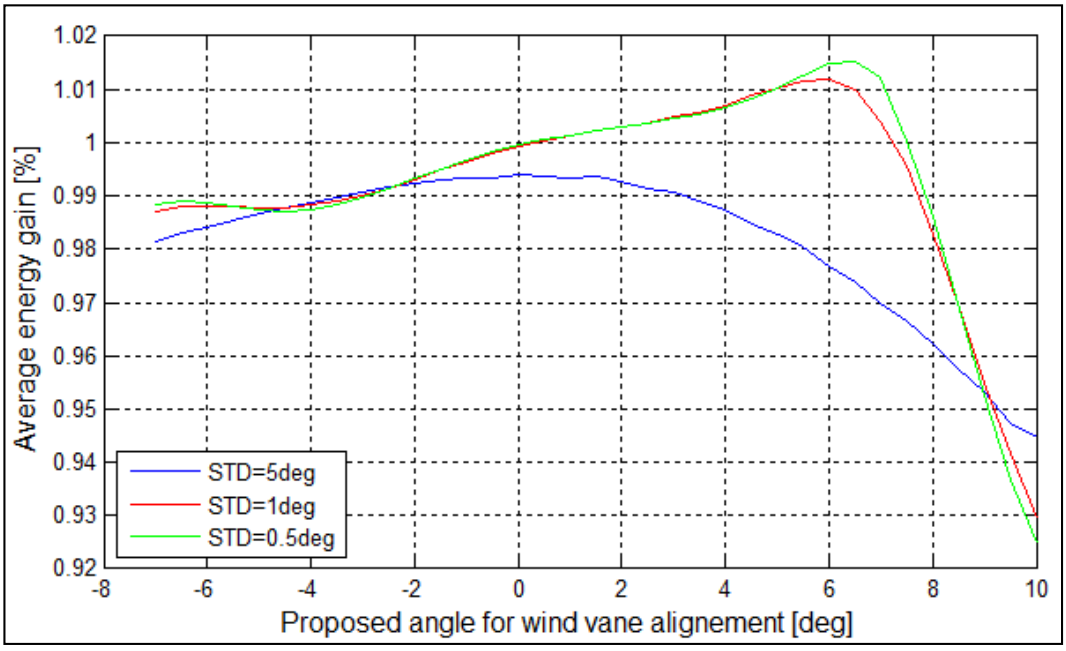

Figure 5-18 WTG#2 – energy gain at different IYO values and levels of accuracy

Assuming the results of this research are representative of the owner's entire fleet, it is interesting to note that a poor alignment method (+/- 5° or more) could represent energy losses of between 1% (WTG#2) and 2% (WTG#1). Therefore, simply by realigning the wind vane with a more precise methodology (+/- 1°), the aforementioned levels of gain could be achieved. A further increase in energy output might be obtained if the wind vanes were realigned at small positive angles. The level of IYO depends on the level of precision of the calibration method. For example, using a method with a precision of +/-1°, the optimal IYO for both turbines would be +5.5°, while it would be +6.5° if an even more precise method were used (+/-0.5°). Of course, validation with the turbine manufacturer for structural impact should be completed prior to proceeding with such a change. It should be noted however that no adjustment should be made to the wind vane alignment before a proper measurement of the 0° of the wind vane is taken on the future investigated turbines.

Lastly, further investigation is warranted at angles close to +5 to +10° in order to improve the results of this investigation since linear interpolations have been assumed between the values obtained from this test.

5.8 Recommendations

The following recommendations are made to the wind farm owner in order that it might attempt to achieve a potential energy increase of the two tested turbines and potentially its entire fleet.

I. If alignment methods are of poor precision (> +/-5°), do not attempt to align the wind vane at angles other than 0°. Otherwise, potential energy losses can be expected;

II. Accurately measure the current wind vane offset of the two tested turbines. This measurement will enable the assessment of the true offset value related to the optimal IYO (+5.5°) found in this project;

III. After imposing on both turbines a constant IYO of +5.5°, complete a side-by-side testing (see Chapter 6) on these two turbines for a period of 6 months in order to assess precisely the potential energy gain;

IV. Accurately measure the current wind vane offset of its entire fleet of wind turbine using a high precision method. Correct turbines misalignment where relevant;

V. If results prove conclusive, gradually set the yaw error to +5° on the entire fleet. This should be done gradually in order to properly validate that there is a real increase in turbine performance every time a turbine wind vane has been implemented with an offset.

CHAPTER 6

POWER PERFORMANCE IMPROVEMENT – TEST NO. 2

A number of findings from this project have been applied to various industrial projects in different contexts. Specifically, one wind farm owner has requested the services of the author to analyze the energy gain achieved pursuant to the installation of an improvement package on some of its wind turbines. Accurately quantifying the energy gain was important since it had repercussions on contractual bonuses or penalties.

The improvement package mainly consisted of aerodynamic devices and a new control algorithm. Since permanent components were installed on the blades, toggle testing (switching between two settings as in Test no. 1) could not be conducted. Rather, a side-by-side methodology with the use of statistical tests has been developed in order to properly assess the energy gain.

The following sections of this report will present the test site, the methodology used and the results obtained. The steps used for this analysis are as follows:

I. Section 6.1: Description of test site,
II. Section 6.2: Description of side-by-side methodology,
III. Section 6.3: Testing results for turbines WTG#3 and WTG#5,
IV. Section 6.4: Comparison with other performance testing methods,
V. Section 6.5: Conclusion.

6.1 Description of Test Site

The investigated turbines are located in a wind farm that comprises several multi-megawatt wind turbine generators. The wind farm site is characterized primarily by flat terrain, with some trees. Figure 6-1 presents a zoom of the layout around the two tested wind turbines (WTG#3 and WTG#5). The proximate reference turbines WTG#4 and WTG#6 are also

identified in this map. Also shown in Figure 6-1 is a meteorological mast, erected in conformance with the IEC61400-12-1 standard in close proximity of these turbines.

Figure 6-1 Zoom of wind farm layout showing turbines relevant to analysis

6.2 Description of the Side-by-Side Methodology

The side-by-side comparison method represents an alternative to the IEC 61400-12-1 method when the task is to quantify an AEP improvement for an operational turbine. This method is also expected to be readily applicable on turbines located in simple or moderately complex terrain. It is emphasized that the method can only be used for evaluating the relative change in the AEP, not for quantifying the AEP itself.

This method involves as a minimum the use of two proximate turbines (a test turbine and a reference turbine) and is based on the assumption that the wind fields (i.e. average wind speed, TI, wind shear, distribution, etc.) in front of these two turbines are statistically identical.

In brief, the side-by-side methodology comprises the following steps:

I. Step 1: Selection of test (WT_{test}) and reference (WT_{ref}) turbines;

II. Step 2: Establishment of the power output difference (P_{test}-P_{ref}) as a function of the power output of the reference turbine (P_{ref}) for the reference period (Period 1);
III. Step 3: Upgrade of the tested turbine;
IV. Step 4: Re-establishment of the power output difference (P_{test}-P_{ref}) as a function of the power output of the reference turbine (P_{ref}) for the test period (Period 2);
V. Step 5: Energy gain calculation through comparison of (P_{test}-P_{ref}) between Period 1 and Period 2.

The primary advantages of this method are:

I. Assessments of changes in performance for turbine modifications that do not enable the use of toggle tests (changes between two different states at very short intervals (e.g. every 40 minutes)) are highly sensitive to certain meteorological parameters such as air density, TI, wind shear, thermal stability, etc. (IEC61400-12-1 (E.4.2) and IEC61400-12-2 (F.2)). In such cases, including the present analysis (i.e. where it is not possible to remove and re-install the package every 40 minutes), an appropriate method to lower the potential impact of these phenomena would be to ensure that the reference period and the testing period take place under similar meteorological conditions (for example by conducting such tests during the same season). While such an approach will lower the potential impact of meteorological conditions on the results, some impact is still present and is difficult to quantify with the major disadvantage being that the period needed to complete the testing would need to be greatly increased. The manner in which the side-by-side method is applied removes the potential impact of these meteorological impacts, thereby representing a clear increase in precision, in addition to a shorter period required for completion of testing.
II. The side-by-side method is independent of wind speed measurements and the installation of a met mast.

III. No normalization of power for air density, TI, wind shear, or any other meteorological parameter is necessary since wind speed is not a factor in this type of calculation.

IV. Existing wind farm SCADA can be used for the verification of results.

V. Since the side-by-side method consists of a *relative* measurement of power output, the uncertainty in the results will be lower than the IEC 61400-12-1. This decreased uncertainty is mainly attributable to the fact that Type B uncertainties (e.g. instrumentation biases) are mostly cancelled out. For a typical IEC evaluation (where the focus is on *absolute* power performance), the AEP uncertainty is in the order of 5%, whereas the uncertainty values in the *relative* AEP improvement as calculated per the side-by-side method often fall in the range of 0.5% to 1.5%, depending on the locations of the tested turbines.

6.3 Testing Results for Turbines WTG#3 and WTG#5

Side-by-side testing has been completed to assess the AEP gain for the two turbines equipped with the package: WTG#3 and WTG#5. The present section presents the steps taken to estimate the gains in AEP.

6.3.1 Reference Period

The reference period has been defined in order to be as long as possible but also to be representative of the normal behaviour of both reference and test turbines. It is the author's opinion that a minimum period of one year should be used for the reference period in order to include any potential seasonal effects but also to ensure a sufficient amount of data in each power bin. Longer periods are more desirable, however. Periods that exhibit unrepresentative performance due to changes in settings, curtailment, or any other factor should not be considered as part of the reference period. In the present case, a reference period of 30 months has been used, as shown in Table 6-1.

Table 6-1 Reference period start and end dates

Start of reference period	End of reference period
January 1, 2010	August 31, 2012

6.3.2 Testing Period

According to information transmitted by the Owner, the installation of the package was completed on several wind turbines of the Wind Farm site in mid-September 2012. As a precautionary measure, however, it was decided to commence the testing period on October 1, 2012. The testing period lasted until March 20, 2013, thereby representing nearly six (6) months of data, as shown in Table 6-2.

Table 6-2 Testing period start and end dates

Start of testing period	End of testing period
October 1, 2012	March 20, 2013

6.3.3 Data Quality Control

As the volume of collected data is substantial, errors caused by sensors or the data acquisition system are possible. For example, out-of-range values, missing data due to turbine availability and/or electrical shut-down, or corrupted data due to icing events are possible incidents that would require the removal of data from the data set. Multiple quality control algorithms were used to validate the representativeness of the data for both the reference and testing periods.

6.3.3.1 Obstruction Analysis (adapted from IEC61400-12-1 Annex A)

In addition to the quality control tests, an obstruction analysis was conducted on both the reference and test turbines to define the directional sectors prone to wake effects. Wind direction data were collected from the meteorological mast installed at the Wind Farm in

close proximity to the tested turbines (see Figure 6-1). This analysis assumes that the wind vanes are properly calibrated and that their directional data is sufficiently accurate. Data corresponding to sectors subject to wake were not retained for analysis. The sectors shaded white in Figure 6-2 and Figure 6-3 below therefore represent the sectors deemed to be wake-free for *both* reference and test turbines. This is an important nuance in the context of a side-by-side analysis, as data subject to wake from either turbine will significantly affect the measured difference in output (P_{test}-P_{ref}). As a conservative measure, the wake-prone sectors (gray) were slightly widened compared to the IEC-61400-12-1 standard in an effort to increase the level of confidence in the results by mitigating the phenomenon of wake meandering which otherwise could impact the evaluation of the energy gain.

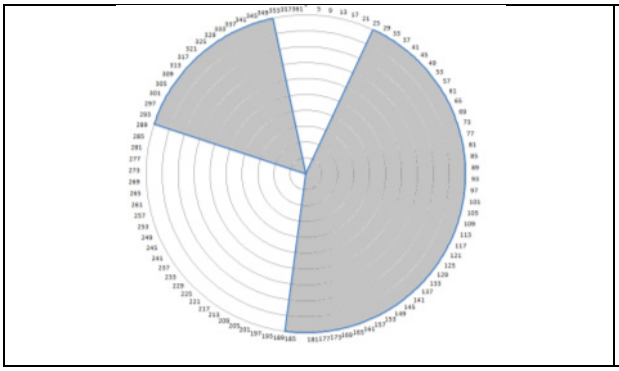

Figure 6-2 Valid wind direction sectors (white) – WTG#3 and WTG#4

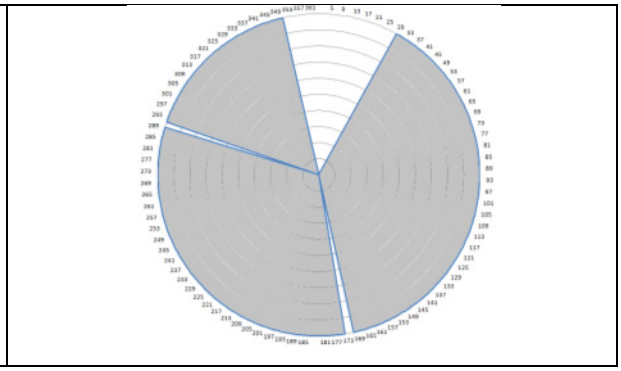

Figure 6-3 Valid wind direction sectors (white) – WTG#5 and WTG#6

As can be seen in Figure 6-2 and Figure 6-3, WTG#3 and WTG#4 offer a much wider wind direction sector available in the predominant wind sector (WSW). Conversely, WTG#5 and WTG#6 exhibit only a narrow wake-free sector in the north direction, hence representing a very low amount of available data for the completion of the side-by-side validation testing. This will have a major impact on the convergence of the statistical tests, which will be discussed in greater detail in the following sections.

6.3.3.2 Power Output Comparison

After receiving all data (reference and test periods) from the owner and completing quality control of the data including the removal of waked sectors, the power output difference between the reference turbines and the tested turbines was evaluated. Figure 6-4 and Figure 6-5 present the results of the difference in power (P_{test}-P_{ref}) as a function of the power output of the reference turbine (P_{ref}) for both the reference and test periods. Ten-minute averaged differences in power output (P_{test}-P_{ref}) are represented by blue dots for the reference period and red dots for the testing period. Average power difference (P_{test}-P_{ref}) for each power bin (P_{ref}) is depicted using a black line for the reference period and a green line for the testing period.

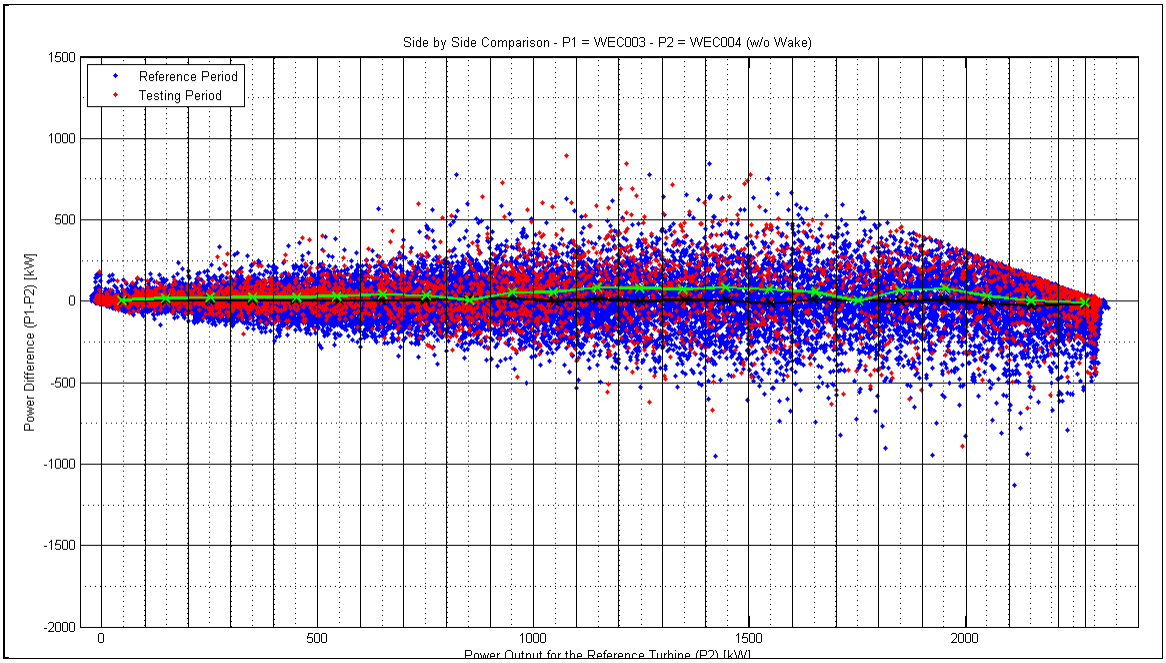

Figure 6-4 WTG#3 vs. WTG#4

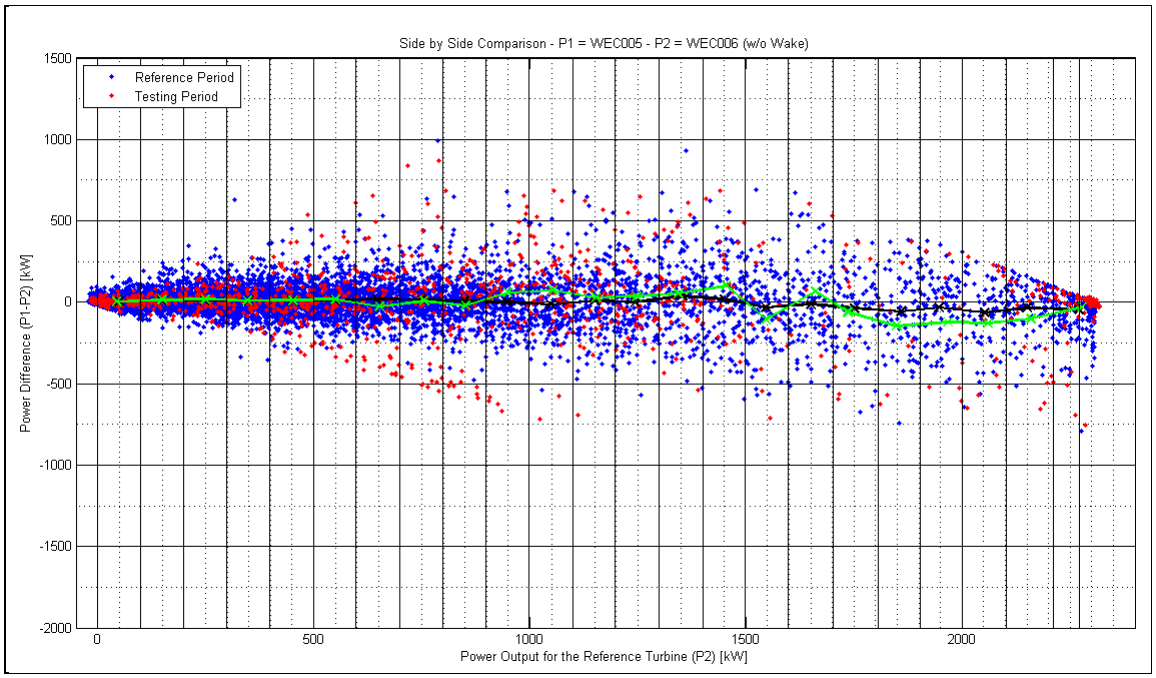

Figure 6-5 WTG#5 vs. WTG#6

As can be seen from the comparison of the green and black lines in the preceding figures, no major improvement in power output is apparent for power under approximately 1000 kW. However, at power outputs above 1000 kW, a tangible increase in power output (green line higher than black line) is observed for the testing period. This increase is less pronounced for WTG#5 vs. WTG#6, mainly due to the low amount of data available in some power bins.

6.3.3.3 Statistical Hypothesis Testing

When calculating the difference of averages between two samples, it is important to ensure that the calculated difference is not attributable mostly to randomness. Statistical test hypotheses are used to assess the level of confidence of an obtained result. Generally, a level of confidence of 95% is recommended for such tests.

In the present analysis, several statistical tests have been applied to each power bin in order to assess whether the differences in mean (or in median) were statistically significant. For each power bin, the applicable tests had to be properly chosen as a function of whether or not

the sampling distribution was determined to be normally distributed or not. Results of these tests are presented in Annex V. Figure 6-6 presents, via gray shading, the power bins where these statistical tests have shown the differences in power output bin obtained between the reference period (Period 1) and the test period (Period 2) to be non-significant. Non-shaded regions represent power bins that exhibited a significant difference in power (with a level of confidence of ≥95% and therefore assumed not to be due to randomness). The power bins with significant differences were then considered appropriate for consideration in the evaluation of the AEP gain.

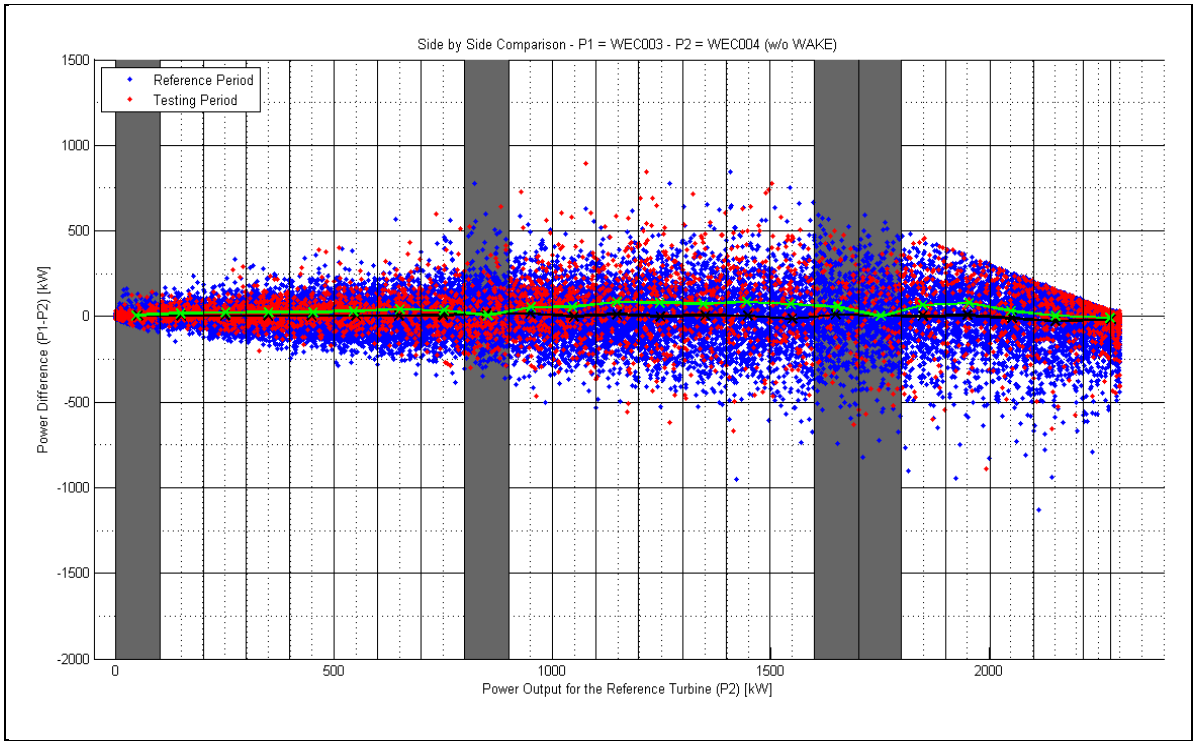

Figure 6-6 Results of side-by-side comparison including statistical testing of each power bin – WTG#3 & WTG#4

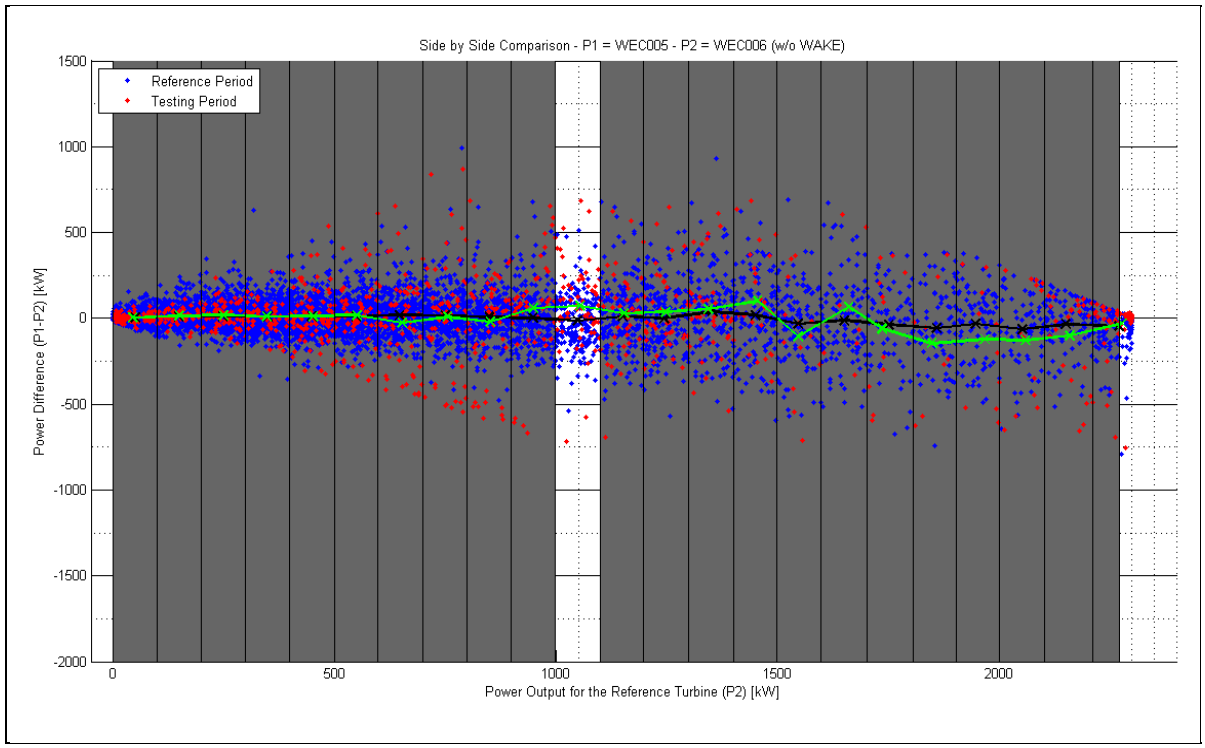

Figure 6-7 Results of side-by-side comparison including statistical testing of each power bin – WTG#5 & WTG#6

As can be seen in Figure 6-6 and Figure 6-7, WTG#3 has a limited number of power bins exhibiting insignificant differences (shaded gray) between the reference period and the testing period, while nearly all of WTG#5's power bins were rejected by the statistical tests. This suggests that the amount of data available for the side-by-side analysis is insufficient for WTG#5. Although nearly 6 months of data have been gathered, the paucity of wake-free directional sectors is the main reason for the low amount of bins with statistical convergence. It is the author's opinion that it would be inappropriate to assess the energy gain of this turbine based on the results of only one power bin and therefore, results for WTG#5 should not be considered representative of the true AEP gain achieved with the package.

6.3.3.4 Calculation and Evaluation of AEP Gains

In order to evaluate the energy gain attributable to the package, only bins with a statistically demonstrated difference in power output have been combined with the number of hours

associated with each of these bins. The number of hours has been deducted from a representative Weibull distribution for which the shape and scale parameters have been provided by the wind farm owner as follows:

I. Shape factor (K): 2,

II. Scale factor (c): 8.46.

Therefore, bins showing no statistical difference have been assumed to represent a power increase of zero, i.e. no contribution to the AEP increase. Bins exhibiting a statistical decrease in power have also been considered in the AEP evaluation. Therefore, if the package increases the power in some portions of the power curve, but reduces it in other portions, this has been taken into account.

Table 6-3 presents the AEP gain when calculated using this methodology.

Table 6-3 AEP gain evaluation

Description	WTG#3	WTG#5
AEP (w/o package) [MWh/yr]	8,369	8,352
AEP (w/ package) [MWh/yr]	8,564	8,368
AEP Gain [MWh/yr]	194.6	16.0
AEP Gain [%]	2.3	0.2

6.3.3.5 Uncertainty Analysis

Uncertainty in a power curve is a function of the statistical uncertainty due to scatter in the data (Category A uncertainty) and measurement uncertainty due to biases or uncertainty in the measurements (Category B uncertainty).

Unlike the standard IEC61400-12-1, which has the objective of evaluating the AEP with reference to wind speed distribution, the side-by-side method is independent of wind speed readings. When conducting an uncertainty evaluation of a power curve (such as per

IEC61400-12-1), the level of uncertainty will typically be in the order of 5% of AEP, while uncertainty values calculated per the side-by-side method often fall in the range of 0.5% to 1.5% depending on the selected turbines (e.g. the separation distance between the reference and test turbines, and the complexity of the surrounding terrain).

Uncertainty level results for each power bin are provided in Annexe V, while details on the uncertainty calculations are presented in Annex VI.

Once uncertainty levels for each power bin have been calculated (as per standard combination of Type A and B uncertainties as specified by the (GUM, 2008), the total AEP uncertainty is calculated using the following formula:

$$u_{AEP} = \sqrt{\sum_{i=1}^{n} (F_i . S_i)^2 \cdot 8760} \qquad (6.1)$$

where:

u_{AEP} is the total uncertainty in the annual energy gain related to the package option

F_i is the frequency of each power bin, representing the relative number of hours in a year for each power bin (i). The number of hours is obtained through the representative Weibull distribution for the specific site.

S_i is the combined uncertainty (Type A and B) for each power bin (i)

n is the number of power bins

Lastly, it should be emphasized that with respect to the data provided by the Owner, potential (i) uncertainty in data accuracy or (ii) degradation of data (caused by compression of the data or improper data downloading technique) have not been considered in the context of this mandate. Notwithstanding the foregoing, it is the author's opinion that the provided data were appropriate for the present analysis.

Table 6-3 presents the gains in Annual Energy Production (AEP) and the associated levels of uncertainty for WTG#3 and WTG#5.

Table 6-4 AEP gains and associated uncertainty levels

Description	WTG#3	WTG#5
AEP Gain [MWh/yr]	194.6	16.0
AEP Gain [%]	2.3	0.2
AEP uncertainty [MWh/yr]	91.3	16.2
AEP uncertainty [%]	1.1	0.2

6.4 Comparison with Other Performance Testing Methods

In order to gain confidence in the results obtained through the side-by-side method, power performance evaluations have been investigated using a number of methods. The results of each of these methods have been compared in an effort to assess the impacts of various factors on power performance analyses, namely:

I. Type of methodology used,

II. Wake effects,

III. Application (or not) of statistical tests.

Results of these investigations are presented in the following tables along with relevant observations and commentaries.

Table 6-5 Nacelle power curve (without statistical tests, wake included)

	WTG#3	WTG#4	WTG#5	WTG#6
Production – ref. period [MWh]	8427.4	8588.1	8617.3	8481.8
Production – test period [MWh]	8896	8776.7	8965.7	8606.4
Absolute gain [MWh]	468.7	188.6	348.5	124.55
Absolute gain [%]	5.6	**2.2**	4.0	**1.5**
Real absolute gain [MWh]	283.6		221.9	
Real relative gain [%]	**3.4**		**2.6**	

Table 6-6 Nacelle power curve (without statistical tests, wake excluded)

	Sectors affected by wake excluded			
	WTG#3	**WTG#4**	**WTG#5**	**WTG#6**
Production – ref. period [MWh]	8369.8	8543.4	8351.9	8131.8
Production – test period [MWh]	8850	8774.6	8910	8527
Absolute gain [MWh]	480.2	231.2	558.1	395.6
Absolute gain [%]	5.7	**2.7**	6.7	**4.9**
Real absolute gain [MWh]	253.7		151.7	
Real relative gain [%]	**3.0**		**1.8**	

Table 6-7 Nacelle power curve (with statistical tests (alfa=0.5), wake included)

	Sectors affected by wake included			
	WTG#3	**WTG#4**	**WTG#5**	**WTG#6**
Production – ref. period [MWh]	8427.4	8588.1	8617.3	8481.8
Production – test period [MWh]	8897.5	8777.8	8964.9	8614.1
Absolute gain [MWh]	470.1	189.7	347.6	132.3
Absolute uncertainty [MWh]	34.5	13.9	41.2	19.9
Absolute gain [%]	5.6	2.2	4.0	1.6
Absolute uncertainty [MWh]	0.4	0.2	0.5	0.2
Absolute gain expression [%]	5.6 +/- 0.4	**2.2 +/- 0.2**	4.0 +/- 0.5	**1.6 +/- 0.2**
Relative gain [MWh]	280.4	N/A	215.3	N/A
Relative gain [%]	3.3	N/A	2.5	N/A
Relative gain uncertainty [%]	0.4	N/A	0.5	N/A
Relative gain expression [%]	**3.3 +/- 0.4**	N/A	**2.5 +/- 0.5**	N/A

Table 6-8 Nacelle power curve (with statistical tests (alfa=0.5), wake excluded)

	Sectors affected by wake excluded			
	WTG#3	**WTG#4**	**WTG#5**	**WTG#6**
Production – ref. period [MWh]	8369.8	8543.4	8351.9	8131.8
Production – test period [MWh]	8856.5	8788.4	8709.2	8238.7
Absolute gain [MWh]	486.7	245.0	357.3	106.9
Absolute uncertainty [MWh]	65.5	29.0	171.2	89.7
Absolute gain [%]	5.8	2.87	4.3	1.3
Absolute uncertainty [MWh]	0.8	0.3	2.0	1.1
Absolute gain expression [%]	5.8 +/- 0.8	**2.9 +/- 0.3**	4.3 +/- 2.05	**1.3 +/- 1.1**
Relative gain [MWh]	241.7	N/A	250.4	N/A
Relative gain [%]	2.9	N/A	3.0	N/A
Relative gain uncertainty [%]	0.9	N/A	2.3	N/A
Relative gain expression [%]	**2.9 +/- 0.9**	N/A	**3.0 +/- 2.3**	N/A

Table 6-9 Side-by-side (without statistical tests, wake included)

	Sectors affected by wake included			
	WTG#3	**WTG#4**	**WTG#5**	**WTG#6**
Production – reference period [MWh]	8369.8	N/A	8351.9	N/A
Production – test period [MWh]	8411.4	N/A	8552.8	N/A
Absolute gain [MWh]	41.6	N/A	200.9	N/A
Relative gain [%]	**0.5**	N/A	**2.4**	N/A

Table 6-10 Side-by-side (without statistical tests, wake excluded)

	Sectors affected by wake excluded			
	WTG#3	**WTG#4**	**WTG#5**	**WTG#6**
Production – reference period [MWh]	8369.8	N/A	8351.9	N/A
Production – test period [MWh]	8575.1	N/A	8341.1	N/A
Absolute gain [MWh]	205.3	N/A	-10.8	N/A
Relative gain [%]	**2.5**	N/A	**-0.1**	N/A

Table 6-11 Side-by-side (with statistical tests (alfa=0.5), wake included)

	Sectors affected by wake included			
	WTG#3	**WTG#4**	**WTG#5**	**WTG#6**
Production – reference period [MWh]	8369.8	N/A	8351.9	N/A
Production – test period [MWh]	8413.8	N/A	8542.9	N/A
Absolute gain [MWh]	44	N/A	191	N/A
Absolute uncertainty [MWh]	24	N/A	57	N/A
Absolute gain [%]	0.53	N/A	2.3	N/A
Absolute uncertainty [%]	0.3	N/A	0.7%	N/A
Absolute gain expression [%]	**0.5 +/- 0.3**	N/A	**2.3 +/- 0.7**	N/A

Table 6-12 Side-by-side (with statistical tests (alfa=0.5), wake excluded)

	Sectors affected by wake excluded			
	WTG#3	**WTG#4**	**WTG#5**	**WTG#6**
Production – reference period [MWh]	8369.8	N/A	8351.9	N/A
Production – test period [MWh]	8564.4	N/A	8367.9	N/A
Absolute gain [MWh]	194.6	N/A	16	N/A
Absolute uncertainty [MWh]	89	N/A	16.2	N/A
Absolute gain [%]	2.3	N/A	0.2	N/A
Absolute uncertainty [%]	1.1%	N/A	0.2	N/A
Absolute gain expression [%]	**2.3 +/- 1.1**	N/A	**0.2 +/- 0.2**	N/A

The following observations can be made from the preceding tables:

I. Analysis of the nacelle power curve comparison method (Table 6-5 to Table 6-8) shows that WTG#4 and WTG#6 are exhibiting increases in performance between 1.1 and 4.9%, even though no changes were made to these turbines. This is a clear indication of the limitation of the power curve comparison at different periods of time. Even though the power curves have been corrected for air density, the difference in meteorological conditions might be the main cause for these results.

II. Again, analysis of the power curve comparison method in Table 6-6 shows that the absolute energy gains for WTG#3 (5.7%) and WTG#5 (6.7%) are abnormally high, likely due once again to meteorological conditions.

III. The use (or not) of statistical tests to evaluate changes in energy output has no major impact when a sufficient quantity of data is gathered (e.g. WTG#3 = 3.4% in Table 6-5 vs. WTG#3 = 3.3% in Table 6-7), while it can have a more significant impact with smaller data sets (ex.: WTG#5 = 1.8% in Table 6-6 vs. WTG#5 = 3.0% in Table 6-8).

IV. The side-by-side methodology is greatly affected by wake sectors, as shown by the comparison of Table 6-9 and Table 6-10 for both WTG#3 and WTG#5.

It is the author's opinion that in the actual context (i.e. no possibility to conduct a toggle test), the side-by-side methodology with the removal of waked sectors and including statistical tests is the most relevant method to use. Accordingly, the relative gain value of 2.3% +/-1.1% is therefore considered the most relevant value in that it includes statistical tests, consideration of wake, and have been obtained with a sufficient amount of data.

6.5 Conclusion

A side-by-side comparison of two turbines fitted with a power performance improvement package has been completed and has shown a significant increase in power output for one of the two tested turbines (WTG#3). The other tested turbine (WTG#5) did not show a significant increase in power output. It is the author's opinion that the poor result for WTG#5 is not related to the absence of a real gain but mainly due to the fact that only a very narrow sector of valid data was available and therefore did not allow for a comprehensive side-by-side test for this turbine.

The energy gains and uncertainties are presented in Table 6-13.

Table 6-13 Summary of energy gains

Description	WTG#3	WTG#5
AEP (w/o package) [MWh/yr]	8,369	8,352
AEP (w/ package) [MWh/yr]	8,564	8,368
AEP Gain [MWh/yr]	194.6	16.0
AEP Gain [%]	2.3	0.2
Uncertainty in AEP Gain [MWh/yr]	91.3	16.2
AEP Gain	2.3 +/- 1.1%	0.2 +/- 0.2%

CONCLUSION

The objective of this research was to improve the power performance of operational wind power plant. To this end, novel artificial neural networks (ANN) with up to six (6) inputs have been developed and used to evaluate the impact of Imposed Yaw Offset (IYO) on two operational wind turbines. A second testing involving the implementation of aerodynamic components on two other operational wind turbines has been conducted using a side-by-side statistical methodology. Noteworthy findings of this research and recommendations to both wind farm owners and future researchers interested in this field of investigation are summarized herein.

The present research project represented, by its nature, technical and commercial challenges in terms of project management, database implementation, aerodynamics, metrology, statistical testing, learning techniques, etc. Particularly delicate in this highly multi-disciplinary effort was ensuring that the various parties involved agreed to participate in the project when research and operational objectives were at times divergent and confidentiality requirements restrictive. Despite these challenges, the project was successfully completed with the research leading to the following noteworthy findings:

I. The implementation of a high-resolution (1 Hz) database that facilitated the gathering of nearly 5 years of data from three wind farm (totalling over 200 operating WTGs and several met masts) is inarguably a unique database for the research world. This database has made possible new innovative investigations and will certainly foster advanced research in the future.

II. Modeling with ANN has demonstrated that the incorporation of six (6) inputs in a multi-stage modeling technique showed the highest accuracy for the two wind turbines studied. A journal article on these findings has been proposed and accepted (Pelletier et al., Submited date: March 2013, Under revision).

III. It has been illustrated that the IEC61400-12-1 correction for air density might be turbine specific and that the 1/3 factor might not be appropriate for all turbine types. Further validations are needed.

IV. To our knowledge, the yaw testing conducted in the context of this project has never been completed in such an exhaustive manner. Neither the testing methodology nor the quantity of data obtained were found anywhere in the review of literature.

V. Imposed Yaw Offset (IYO) testing has been conducted and has demonstrated, on the two tested turbines, a potential energy gain of 1% to 2% at an IYO of approximately +7°.

VI. Results of the IYO have also demonstrated the importance and the sensitivity of measuring the wind vane alignment with a high level of precision. A tool has been developed, patented and commercialized with this objective. See Annex I for more details.

VII. Results obtained in this research have demonstrated that the wind turbine power curve comparison method has some limitations when applied in different meteorological conditions, particularly when it is not possible to apply a toggle testing.

VIII. Statistical tools have been developed to compare changes in turbine performance during side-by-side testing.

It is unfortunate that logistic and temporal constraints have required the termination of this project. The findings of this research have demonstrated the need to further investigate the potential impact of power performance modelling and yaw offsets on operational wind turbines. In this context, the following recommendations are offered to the wind farm owner as well as researchers who might be interested in further pursuing the research presented herein.

I. In order to properly verify whether the results presented herein can be generalized to more than two turbines, further testing on other multi-megawatt

turbines should be conducted. Should the results repeat themselves, such tests would allow the conclusions presented herein to be corroborated.

II. The incorporation of more than six (6) inputs is possible in the multi-stage modelling technique. Further investigation should be conducted with additional inputs that were not available for this testing such as higher-than-hub-height wind speed measurements using LIDAR or SODAR technology.

III. If possible, it may be of value to conduct new testing for angles closer to the optimal IYO found in this research. For example, investigation for IYO of +5°, +6°, +7°, +8°, +9°, and +10° would provide relevant information about the steep decrease in power output at these critical angles.

IV. The author makes the following recommendations to the wind farm owner:

   A. A yaw offset of +5° should be imposed on both of the tested turbines. The offset should be fixed through a software parameter or with a precise calibration tool if the wind vane needs to be physically rotated.

   B. Once re-oriented, side-by-side testing for these two turbines should be completed in order to assess the true energy gain.

   C. If satisfactory results are obtained, the owner could gradually measure the orientation of the wind vanes on all its turbines and impose a proper offset. This should be done gradually in order to gain confidence in the offset value and the evaluation of the true energy gain.

It is worth mentioning that throughout the course of this research project, a number of results, studies, experiences or applications have been applied to an industrial context. For instance, the author of this document has been requested by wind farm owners to support them in implementing or improving control rooms, performing energy yield follow-up and package improvement validation of operating wind assets, etc. Some power performance improvement testing has been conducted.

Lastly, the reader might notice that several questions remain unanswered and that further research remains necessary in order to more properly understand the phenomena related to the yaw offset of operational wind turbines and its impact on power performance. Due to logistic and temporal constraints it was necessary to conclude the investigations and complete the present report. It is hoped that the findings presented herein adequately addressed the objective of this research as proposed in the Introduction.

ANNEX I

ALIGNMENT SYSTEM AND METHOD, E.G. FOR WIND TURBINES (PATENT, US 61/720,145)

During the course of this research, given that the importance of wind vane alignment had been demonstrated, it was decided to develop an alignment system for nacelle-mounted wind vanes. This alignment tool has therefore been developed with the objective of ensuring high levels of precision and repeatability.

This tool has been designed to be compatible with several models of wind turbines and to achieve alignment *in situ*. The calibration alignment system has been realized in keeping with isostatic principles to ensure the highest level of repeatability while minimizing distortions due to thermal variations. Its aluminum alloy composition ensures an excellent resistance to corrosion, good rigidity and light weight (<18 kg). The assembly is retractable in less than a minute and can be lifted in a certified bag for wind turbines (F.T.M.S., ASME B30:9). Using a high precision laser, this instrument projects two lines directly on the nacelle: one for the center line of the WTG and one for the 0 deg of the wind vane. A procedure has been developed in order to precisely identify the systematic error of alignment between the wind vane and the centre line of the main shaft. This value is used as a correction factor in order to minimize the error in the wind direction estimate.

The competitive advantages of this invention are:

- Higher precision than current methods (+/- 1° full chain of measurement),
- Enables wind vane alignment for any desired angle (e.g. to compensate for rotor impact on the wind vane),
- Rapid execution (< 30 min.),
- Enables alignment of other components,
- Light weight of equipment (fully contained in one bag).

Patent requests for this invention have been submitted for Canada, the United States and Mexico.

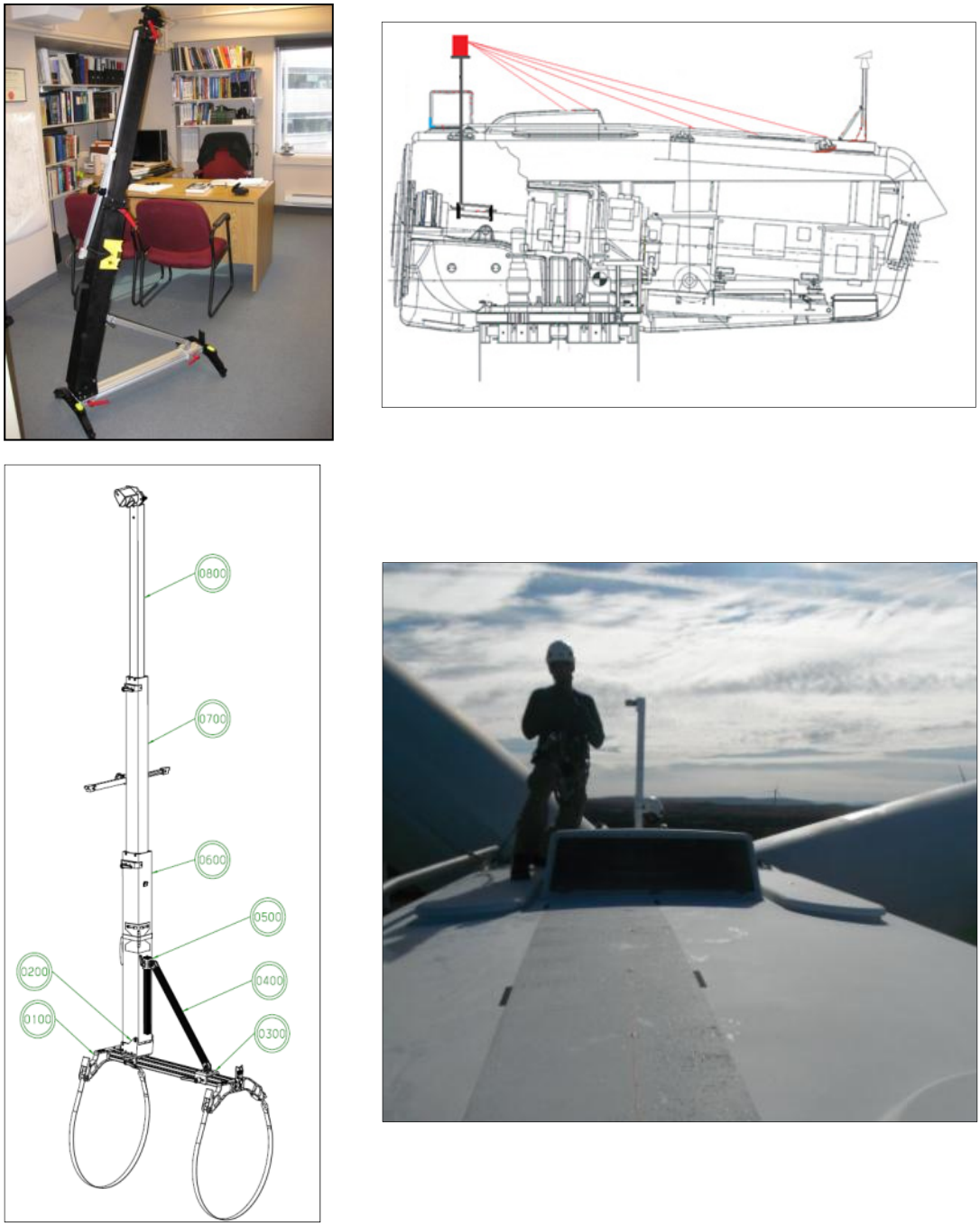

Figure-A I-1 Photos and drawings of the patented wind vane alignment tool

ANNEX II

TESTED INPUTS FOR ARTIFICIAL NEURAL NETWORK MODELLING

1. Variables dépendantes

Variables	Unité	Plage	Description
Pmoy	kW	0-2000	Puissance active moyenne [10min] de l'éolienne

2. Variables indépendantes

2.1 Variables incontrôlables

2.1.1 Éolienne de référence

Variables	Unité	Plage	Description
Pmin	kW	0-2000	Puissance active min [10min] de l'éolienne
Pmax	kW	0-2000	Puissance active max [10min] de l'éolienne
Pstd	kW	0-2000	Puissance active écart-type [10min] de l'éolienne
Pskew	kW	-10-+10	Puissance active skew [10min] de l'éolienne
Vmoy	m/s	0-30	Vitesse du vent à la nacelle moyenne [10min]
Vmin	m/s	0-30	Vitesse du vent à la nacelle min [10min]
Vmax	m/s	0-30	Vitesse du vent à la nacelle max [10min]
Vstd	m/s	0-30	Vitesse du vent à la nacelle écart-type [10min]
Vskew	m/s		Vitesse du vent à la nacelle skew [10min]
Vkurto	m/s		Vitesse du vent à la nacelle kurtosis [10min]
Dmoy	deg	0-360	Direction du vent à la nacelle moyenne[10min]
Dmin	deg	0-360	Direction du vent à la nacelle min[10min]
Dmax	deg	0-360	Direction du vent à la nacelle max[10min]
Dstd	deg	0-360	Direction du vent à la nacelle écart-type[10min]
Dskew	deg		Direction du vent à la nacelle skew[10min]
Dyawmoy	deg	0-360	Orientation de la nacelle moyenne[10min]
Dyawmin	deg	0-360	Orientation de la nacelle min[10min]
Dyawmax	deg	0-360	Orientation de la nacelle max[10min]
Dyawstd	deg		Orientation de la nacelle écart-type[10min]
Dyawskew	deg		Orientation de la nacelle écart-type[10min]
Tyawdroite	sec	0-600	Temps de rotation de la nacelle clockwise
Tyawgauche	sec	0-600	Temps de rotation de la nacelle anti-clockwise
STATEmoy	sec	0-600	State and Fault-moyenne[10min] 2=turbine on grid

OSmoy	sec	0-600	Operational Status-Moyenne[10min]16=load operation

2.1.2 Éolienne voisine

Variables	Unité	Plage	Description
P2moy	kW	0-2000	Puissance active moyenne [10min] de l'éolienne
P2min	kW	0-2000	Puissance active min [10min] de l'éolienne
P2max	kW	0-2000	Puissance active max [10min] de l'éolienne
P2std	kW	0-2000	Puissance active écart-type [10min] de l'éolienne
P2skew	kW	-10-+10	Puissance active skew [10min] de l'éolienne
V2moy	m/s	0-30	Vitesse du vent à la nacelle moyenne [10min]
V2min	m/s	0-30	Vitesse du vent à la nacelle min [10min]
V2max	m/s	0-30	Vitesse du vent à la nacelle max [10min]
V2std	m/s	0-30	Vitesse du vent à la nacelle écart-type [10min]
V2skew	m/s		Vitesse du vent à la nacelle skew [10min]
D2moy	deg	0-360	Direction du vent à la nacelle moyenne[10min]
D2min	deg	0-360	Direction du vent à la nacelle min[10min]
D2max	deg	0-360	Direction du vent à la nacelle max[10min]
D2std	deg		Direction du vent à la nacelle écart-type[10min]
D2yawmoy	deg	0-360	Orientation de la nacelle moyenne[10min]
D2yawmin	deg	0-360	Orientation de la nacelle min[10min]
D2yawmax	deg	0-360	Orientation de la nacelle max[10min]
D2yawstd	deg		Orientation de la nacelle écart-type[10min]
STATE2	sec	0-600	State and Fault-moyenne[10min] 2=turbine on grid
OS2	sec	0-600	Operational Status-Moyenne[10min]16=load operation

2.1.3 Mât météo

Variables	Unité	Plage	Description
V80moy	m/s	0-30	Vitesse moyenne [10min] à l'anémo primaire-mât de mesure
V80min	m/s	0-30	Vitesse min [10min] à l'anémo primaire-mât de mesure
V80max	m/s	0-30	Vitesse max [10min] à l'anémo primaire-mât de mesure
V80std	m/s	0-30	Vitesse écart-type [10min] à l'anémo primaire-mât de mesure
V80skew	m/s		Vitesse skew [10min] à l'anémo primaire-mât de mesure

V40moy	m/s	0-30	Vitesse moyenne [10min] à l'anémo primaire-mât de mesure
V40min	m/s	0-30	Vitesse min [10min] à l'anémo primaire-mât de mesure
V40max	m/s	0-30	Vitesse max [10min] à l'anémo primaire-mât de mesure
V40std	m/s	0-30	Vitesse écart-type [10min] à l'anémo primaire-mât de mesure
V40skew	m/s	0-30	Vitesse skew [10min] à l'anémo primaire-mât de mesure

D78moy	deg	0-360	Direction du vent moyenne[10min] à 78m-mât de mesure
D78min	deg	0-360	Direction du vent min[10min] à 78m-mât de mesure
D78max	deg	0-360	Direction du vent max[10min] à 78m-mât de mesure
D78std	deg	0-360	Direction du vent écart-type[10min] à 78m-mât de mesure

D40moy	deg	0-360	Direction du vent moyenne[10min] à 40m-mât de mesure
D40min	deg	0-360	Direction du vent min[10min] à 40m-mât de mesure
D40max	deg	0-360	Direction du vent max[10min] à 40m-mât de mesure
D40std	deg	0-360	Direction du vent écart-type[10min] à 40m-mât de mesure

T80moy	° C	+/-30	Température de l'air à 78m au mât de mesure
T40moy	° C	+/-30	Température de l'air à 40m au mât de mesure
T5moy	° C	+/-30	Température de l'air à 5m au mât de mesure
HRm80moy	%	0-100	Humidité relative à 78m au mât de mesure
Pm80moy	Kpa	0-105	Pression atmosphérique à 78m au mât de mesure

2.2 Variables calculées

Variables	Unité	Plage	Description
RHOmoy80			Densité de l'air au mât de mesure
IT80moy			Intensité Tubulence
ITmoy			Intensité Tubulence lue à la nacelle
WS8040			Cisaillement V80/V40
YAWerreur			Erreur de yaw: Direction vent nacelle - Orientaion nacelle
YAWerreur2			Erreur yaw2: Direction vent mât - Orientation nacelle
Derreur			Écart entre direction du mât et de la nacelle
Tyaw	sec	0-600	Nombre de seconde où l'éolienne s'est orientée
WV7860	deg		Wind veer

2.3 Autres variables testées mais sans effet

Variables	Unité	Plage	Description
$V^2$80			Vitesse du vent au carré
$V^3$80			Vitesse du vent au cube
V^n80			Vitesse du vent à puissance n
V80/V70			Ratio de vitesse
V80/V60			Ratio de vitesse
V80/V50			Ratio de vitesse
log(V80)			Logarithme de la vitesse
Racine(V80)			Racine de la vitesse
G			Cisaillement selon Albers 2007

2.4 Variables inconnues (non testés dans le modèle)

Variables	Unité	Plage	Description
Vitesse >80m			Vitesses au dessus du moyeu
Vitesse rotor			Vitesses sur l'ensemble du rotor (vertical et horizontal)
Composantes verticales du vent			
Vitesse entre les niveaux de mesure			

ANNEX III

VALIDATION OF THE NACELLE WIND SPEED TRANSFER FUNCTION

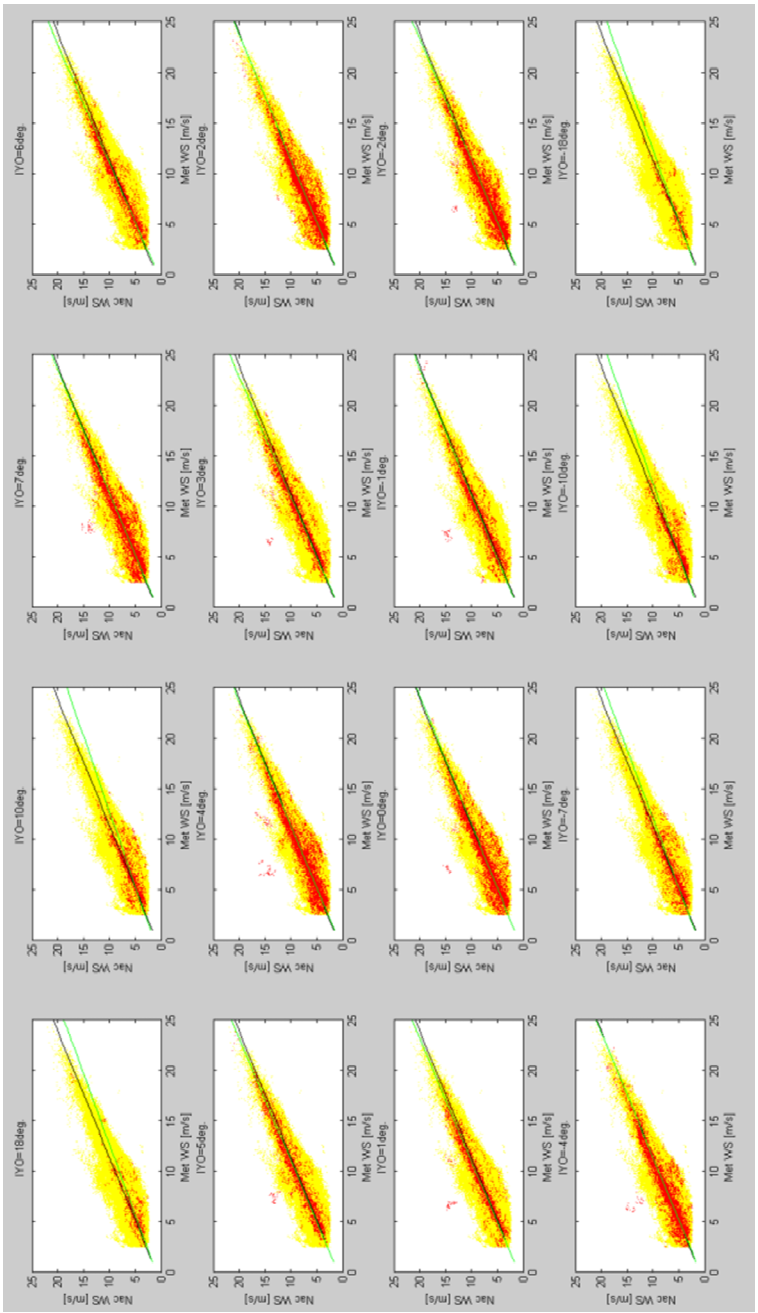

Figure-A III-1 WTG#1 – Nacelle transfer function before (black line) and after (green line) the IYO implementation

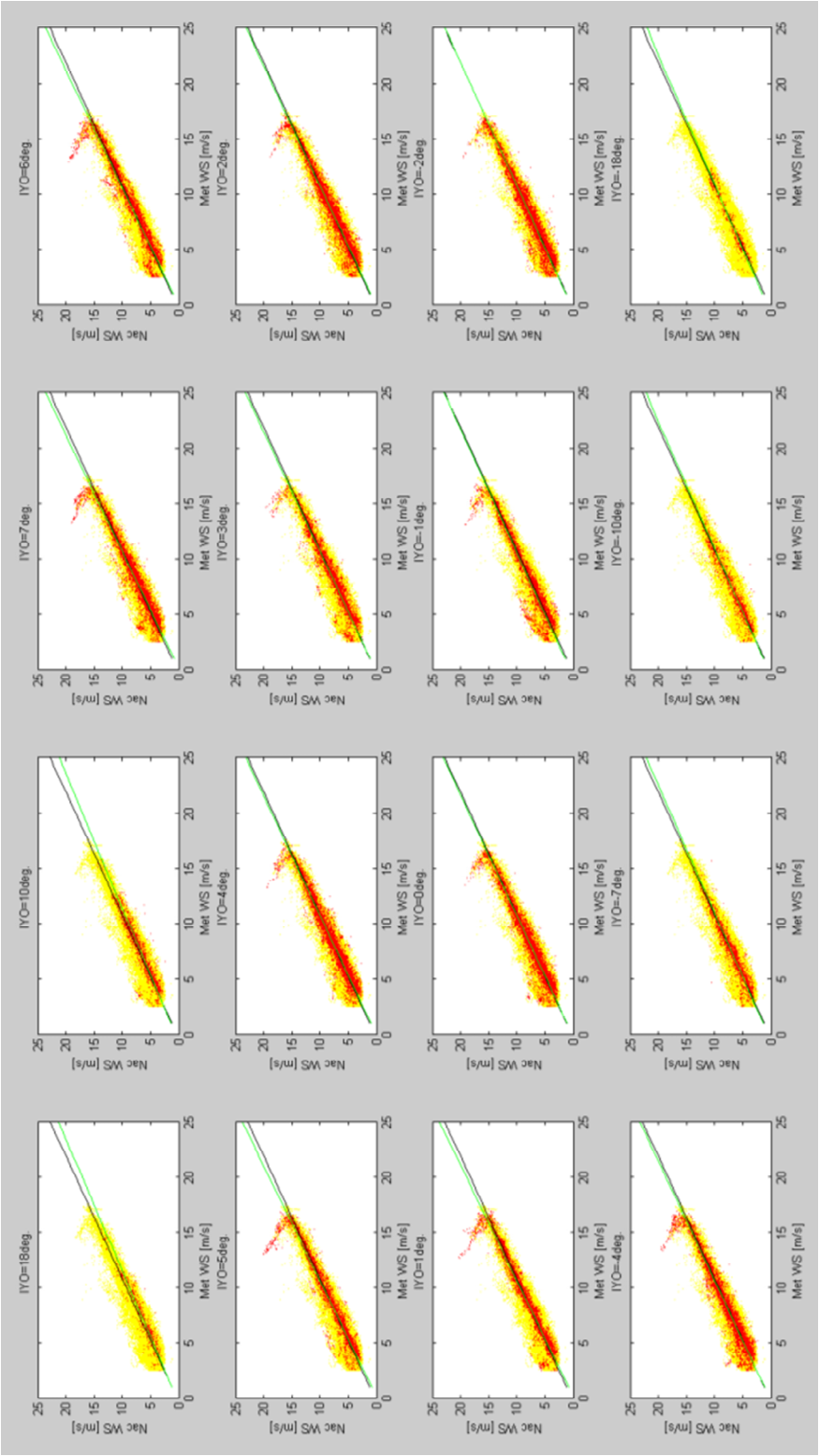

Figure-A III-2 WTG#2 – Nacelle transfer function before (black line) and after (green line) the IYO implementation

ANNEX IV

DATA DISTRIBUTION

WTG#1

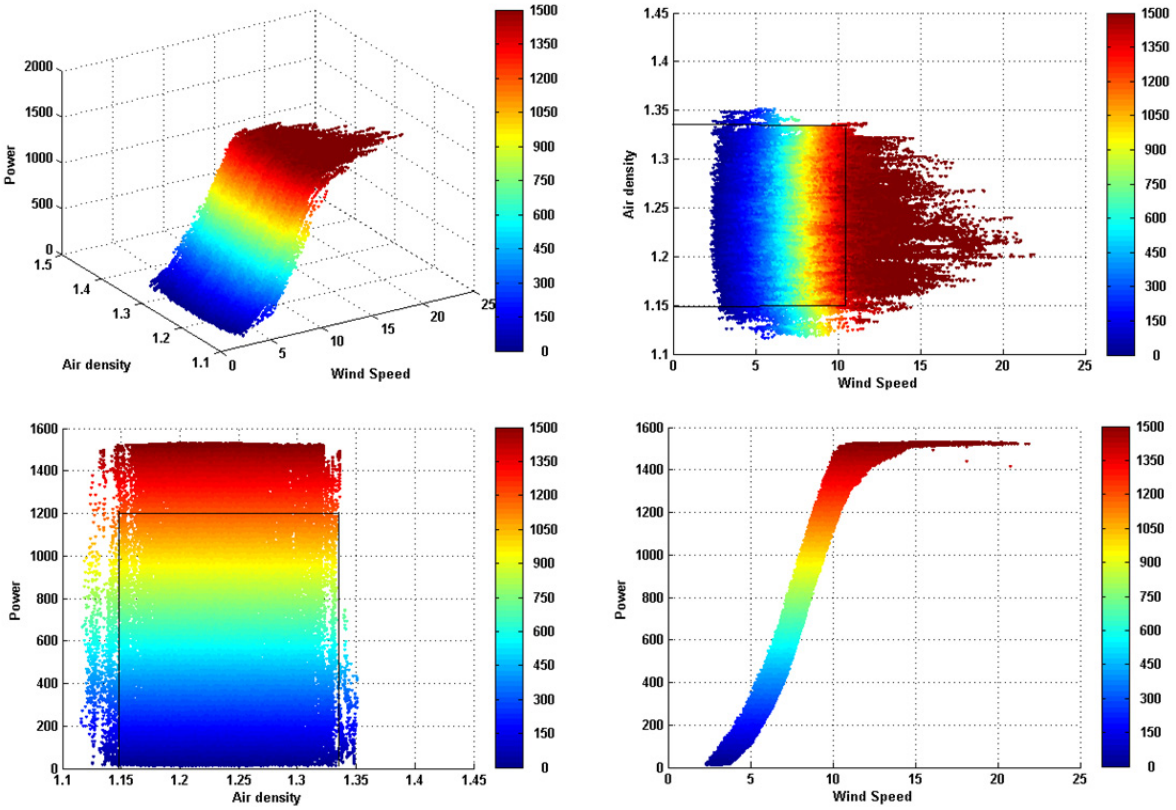

Figure-A IV-1 WTG#1 – Power vs. wind speed and air density

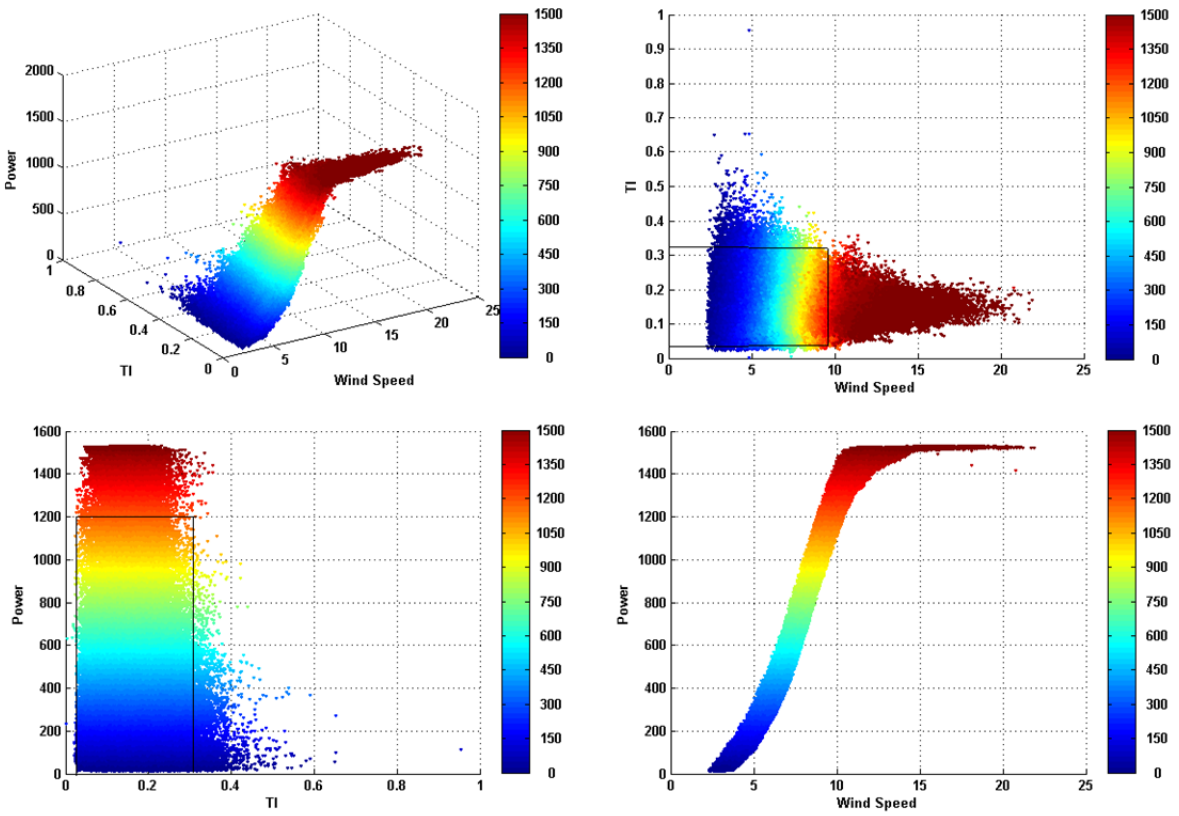

Figure-A IV-2 WTG#1 – Power vs. wind speed and TI

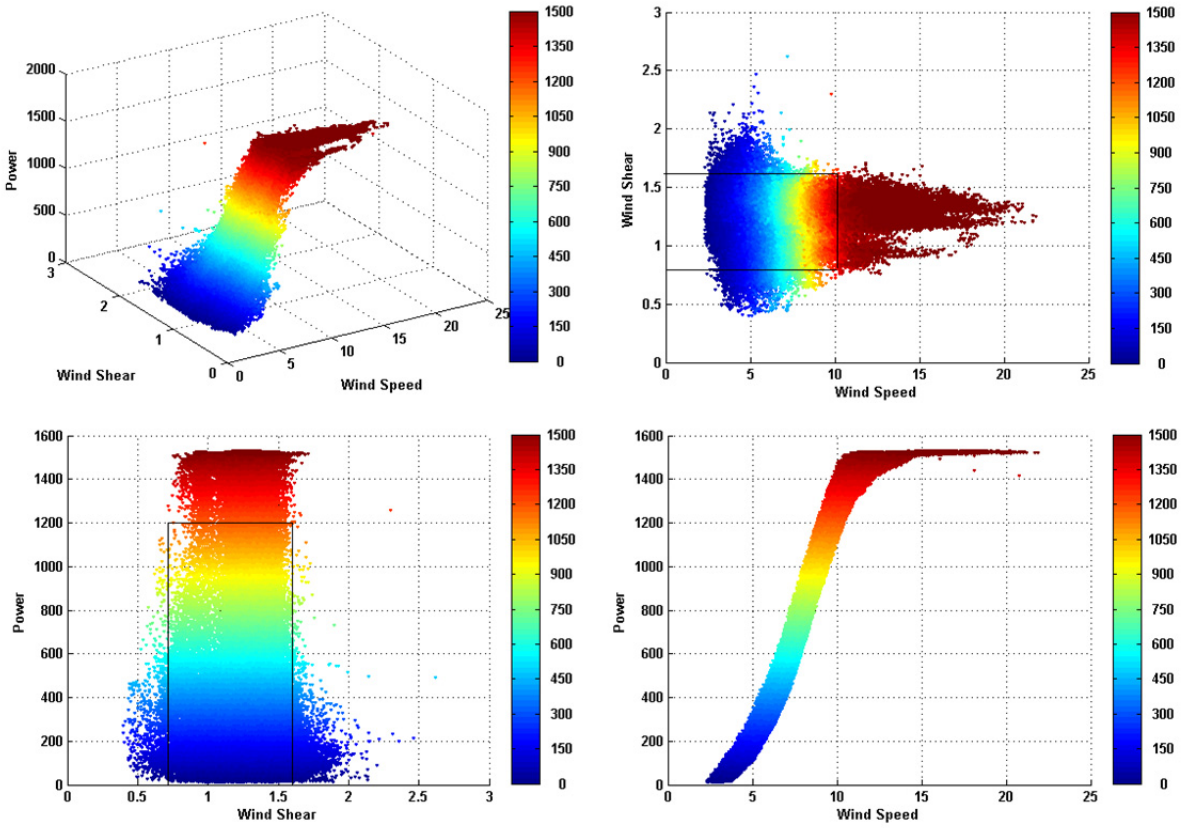

Figure-A IV-3 WTG#1 – Power vs. wind speed and WS8040

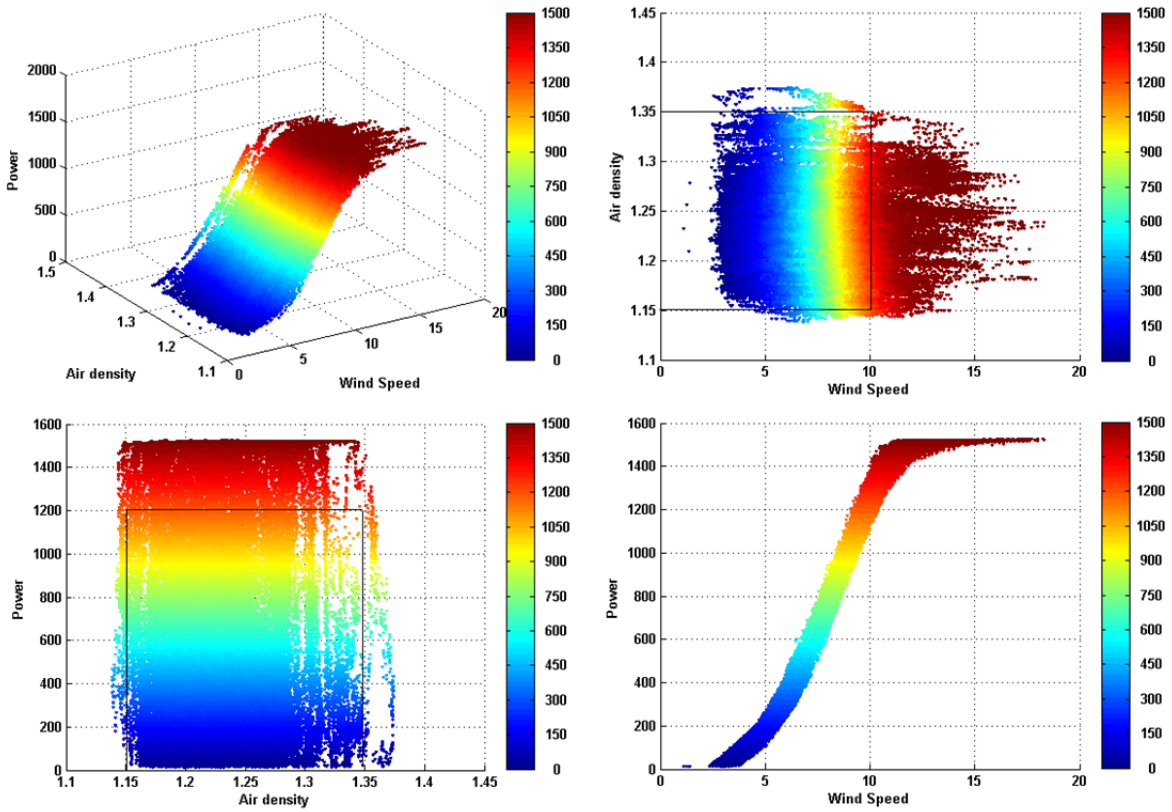

Figure-A IV-4 WTG#2 – Power vs. wind speed and air density

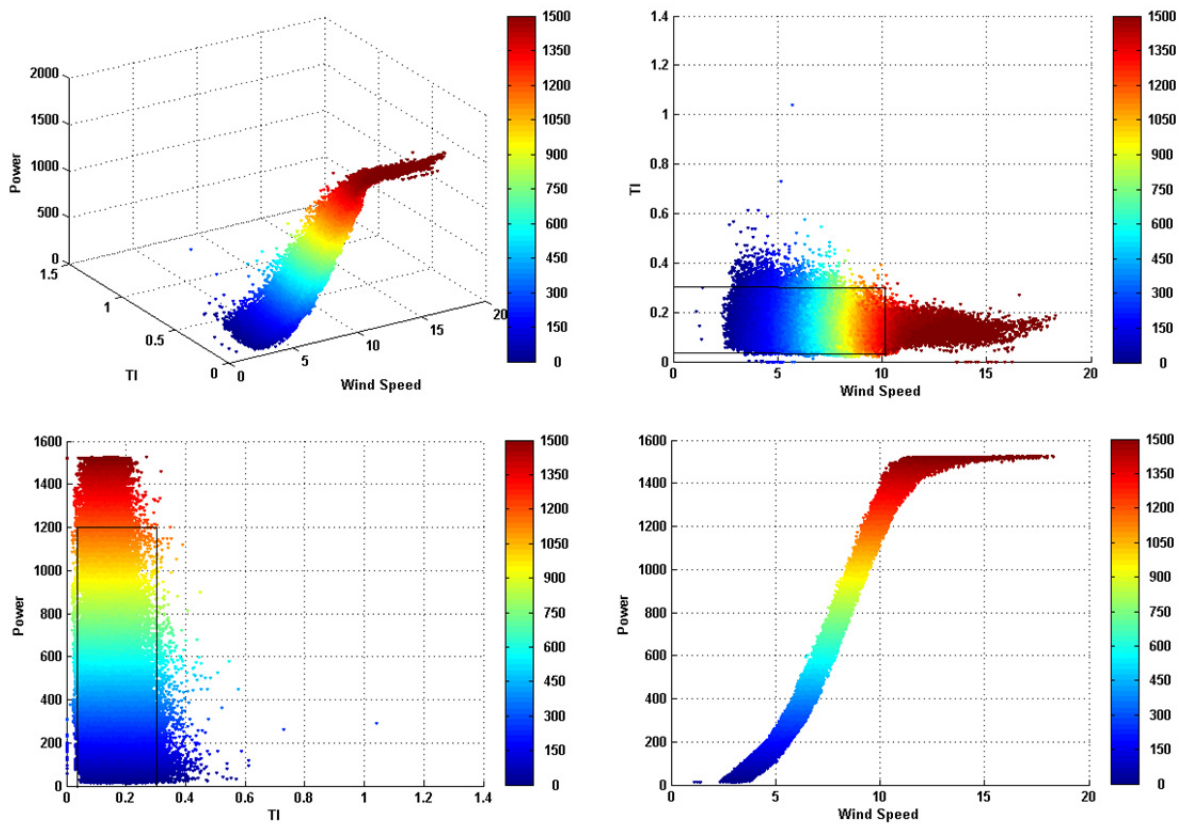

Figure-A IV-5 WTG#2 – Power vs. wind speed and TI

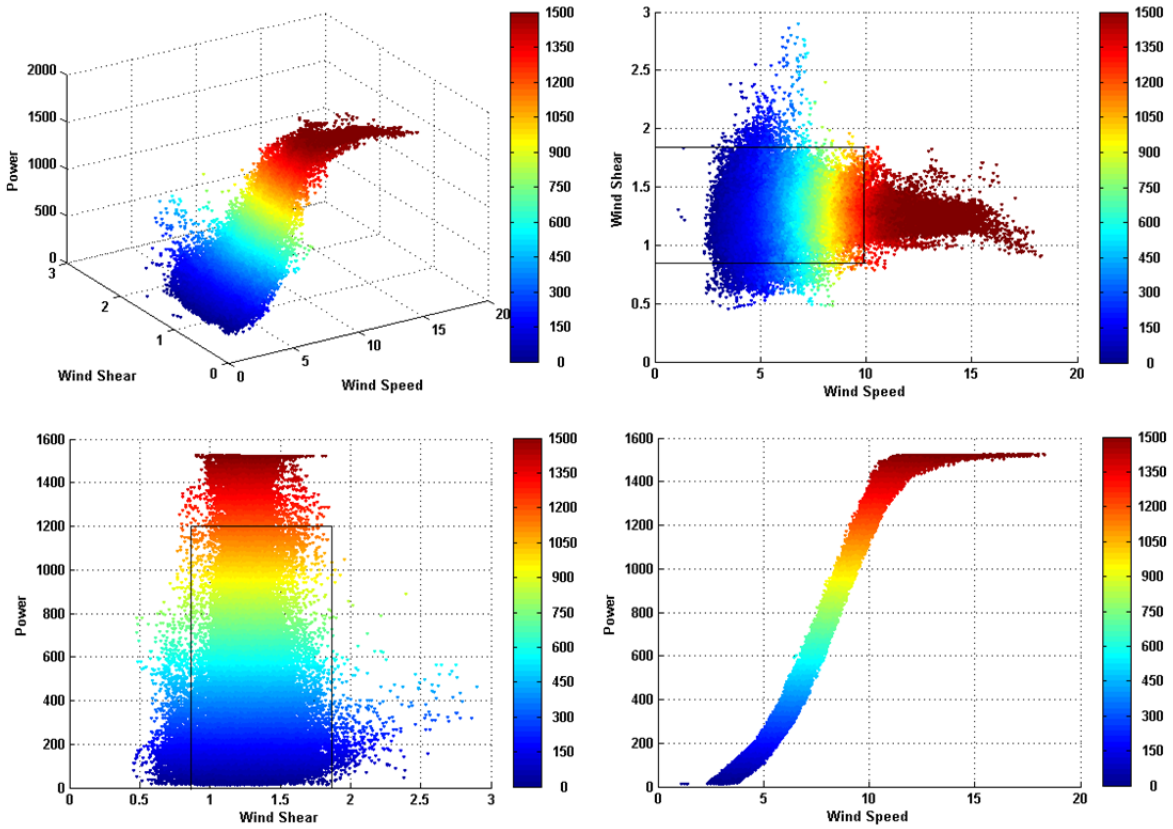

Figure-A IV-6 WTG#2 – Power vs. wind speed and WS8040

ANNEX V

STATISTICAL TEST RESULTS FOR THE SIDE-BY-SIDE COMPARISON

During the side-by-side testing, the use of several statistical tests proved to be necessary. This annex will summarize the theory of the statistical tests used and the results obtained for the two side-by-side tests completed.

STATISTICAL TESTS

Statistical tests are used to provide a quantitative result that facilitates decision-making with respect to a process. These tests are applied to data samples and are usually stated in terms of both a condition that is doubted (null hypothesis) and a condition that is believed (alternative hypothesis). A common format for a hypothesis test is:

H_o: Statement of the null hypothesis, (e.g.: the means of the two samples are equivalent)
H_1: Statement of the alternative hypothesis, (e.g.: the means of the two samples are not equivalent)

The statistical significance of a result is the probability that the result of a statistical test is true. Statistical significance reflects the degree to which the result is "true" (in the sense of being "representative of the population"). The α value is generally used to assess the level of significance desired. This level of confidence imposed on α value will depend on the context of the study. However, typical values for α are between 0.05 and 0.01, meaning that there is a 5% to 1% chance of rejecting the null hypothesis while it is in fact true. This is known as the Type I error. Conversely, Type II error is defined as the probability of accepting the null hypothesis when the alternative hypothesis is in fact true. Table-A V-1 summarizes Type I and I errors.

Table-A V-1 Type I and Type II errors

		Situation	
		H_0 is true	H_1 is true
Decision	Do not reject H_0	Good decision	**Type II error**
	Reject H_0	**Type I error**	Good decision

Statistical tests can be applied to a number of comparison processes such as the comparison of the means of two samples, standard deviation or even distribution. Various specific statistical tests have been developed depending on the validation requested. The following sections present the various types of tests which were required in the course of this research.

P-VALUE

While statistical tests can provide what is referred to as a critical value which represents the value at which the H_0 hypothesis begins to be rejected for a given α value, a more practical alternative is to report the results of a hypothesis test through the use of the p-value. The p-value is the probability of the test statistic will take on a value at least as extreme as the observed value when the null hypothesis is true. More technically, the p-value represents a decreasing index of the reliability of a result. The higher the p-value, the less we can believe that the observed relation between variables in the sample is a reliable indicator of the relationship between the respective variables in the population. More specifically, if the P-value is less than or equal to α, then H_0 is rejected, whereas if the p-value exceeds α, we would fail to reject H_0. Therefore, the p-value is an indication of the probability to reject H_0 while it is true in fact.

NORMALITY TESTS

A sampling distribution is assumed to be normally distributed (or Gaussian) if it exhibits the following probability density function:

$$f(x) = \frac{1}{\sigma\sqrt{2\pi}} e^{-\frac{(x-\mu)^2}{2\sigma^2}} \quad \text{(A V-1)}$$

where:

μ is the average,

σ is the standard deviation of the distribution.

Normality tests are used to determine whether a data sample is properly represented by the normal distribution with given μ and σ values. Several authors have developed various techniques in order to complete normality tests.

While visual methods can be used to validate the normalization of a sample (through simple histogram visualization or the use of the Henry line), these techniques are not particularly convenient for obtaining automatic numerical results for the acceptance or rejection of the normality hypothesis. Through the MALTLAB application, two normality tests have been applied: i) the lillieTest and ii) the jbTtest. Both of these tests use the following hypothesis:

H_0: the sample comes from a normally distributed population

H_1: the sample does not come from a normally distributed population

The lillieTest and jbTest are 2-sided goodness-of-fit tests that return a value of 1 if they reject the null hypothesis at a pre-defined level of confidence α (0.05), and a value of 0 if the null hypothesis cannot be rejected. In the present research, if either one or both of the results returned a value of 1, then it was assumed that the tested sample was not from a normally distributed population with a confidence level of 95%.

Determination of the normality (or not) of a sample is important since it will impact which statistical tests to use for the comparison of means and medians. It has been found that in the side-by-side testing, the vast majority of the 10-minute power outputs in a power bin were not distributed according to a normal distribution.

DISTRIBUTION TESTS (OR GOODNESS OF FIT)

Distribution tests are generally used to validate whether or not a sample is following a given statistical distribution (e.g. normal, Weibull, exponential, binary, etc.) or to verify whether or not two samples have the same type of distribution, which would indicate that they were obtained from the same population.

The χ^2 test is used to validate whether observations from a sample are distributed according to a given family of distribution. The validation consists mainly of comparing the theoretical frequencies of the Probability Density Function (PDF) of the expected distribution with the one observed from the data sample. The χ^2 value is calculated per the following formula:

$$\chi^2 = \sum_{i=1}^{n} \frac{(O_i - E_i)^2}{E_i} \qquad \text{(A V-2)}$$

where:

χ^2 is the Khi-square value

O_i is the observed frequency in the ith class interval

E_i is the expected frequency for the given distribution for the ith class interval

n is the numbers of intervals

The obtained χ^2 value is then compared to the χ^2 probability table and the H_0 hypothesis is rejected if the value is below the table value at the given confidence level.

While the χ^2 methodology is simple to apply, its effectiveness is highly dependent on the number of intervals established and the quantity of data in each interval. Alternatively, the Kolmogorov-Smirnov test (KS-test) is based on the comparison of the Cumulative Density

Function (CDF). This testing has been programmed in the MATLAB application under the KS-test and KS-test2 functions. KS-test returns a test decision for the null hypothesis that the data from the sample are from a standard normal distribution. The KS-test2 function returns a test decision for the null hypothesis that the data in Sample 1 and Sample 2 are from the same distribution. In the case of the present research, since the objective was to compare the reference sample with the sample obtained during testing (after implementation of the improvement package), the KS-test2 function was used.

TESTS ON THE EQUALITY OF TWO MEANS

For samples with demonstrated normal distributions, the two-sample Z-test (or T-test when sampling size is lower than 30) can be used to assess if the difference in the two means from two samples is significant.

Difficulty arises when the two investigated samples exhibit non-normal distribution and are of different sizes. Fortunately, Lumley (Lumley et al., 2002) demonstrated that for this particular case, the t-student test is probably the most appropriate statistical test to use to validate whether or not the two means of two samples are significantly different. Therefore, for all data samples that were demonstrated to be not normally distributed (i.e. most of the cases), the ttest2 function from MATLAB has been used to validate whether or not the difference in means for each sample of the power output obtained in the side-by-side testing was significant.

TESTS ON THE EQUALITY OF TWO MEDIANS

The ranksum function in MATLAB is the application of the Wilcoxon ranksum test. This function tests the null hypothesis that data coming from both samples are of equal medians (H_0) as opposed to not being of equal medians (H_1). The rejection of H_0 with a proper level of confidence is another indication that two samples are from two different populations.

While statistical tests with the proper level of confidence (α) can provide a good indication whether or not two samples are from different populations, they are not infallible. Therefore, it is always good practice to complete multiple tests in order to increase the reliability of the obtained results (acceptance or rejection of the H_0 hypothesis). In the context of this research, differences in two samples (before and after the change in performance) were accepted as significant only if *all* of the statistical tests conducted (distribution, mean and median) were conclusive.

The following tables present all results obtained through the series of statistical tests performed in the comparison of WTG#3 vs. WTG#4 and WTG#5 vs. WTG#6.

Table-A V-2 Statistical Tests for WTG#3 and WTG#4

Bin no.	Plage de puissance		Pref	ÉcartREF	ÉcartTST	No. of data		Test_Dist		Test_median		Test_Normal		Test_sigma		Test_moyenne	
	Pinf	Psup				Reference	Test	h	p	h	p	h	p	h	p	h	p
1	0.0	101.0	51.8	3.0	6.7	2096	221	0	0.133	0	0.053	1	0.001	1	0.016	1	0.049
2	101.0	200.1	150.2	4.9	18.5	2187	189	1	0.000	1	0.000	1	0.019	1	0.017	1	0.000
3	200.1	299.6	250.1	3.8	21.4	1890	193	1	0.000	1	0.000	1	0.001	1	0.003	1	0.000
4	299.6	398.7	349.2	4.4	25.4	1750	234	1	0.000	1	0.000	1	0.022	1	0.031	1	0.000
5	398.7	499.3	448.2	2.9	24.2	1521	192	1	0.001	1	0.000	1	0.001	0	0.334	1	0.000
6	499.3	599.6	550.4	3.2	31.2	1339	171	1	0.002	1	0.000	1	0.001	0	0.689	1	0.000
7	599.6	699.3	648.9	2.4	41.5	1292	176	1	0.000	1	0.000	1	0.116	1	0.000	1	0.000
8	699.3	799.3	749.8	7.1	34.6	1155	170	1	0.002	1	0.004	1	0.003	1	0.006	1	0.010
9	799.3	899.6	848.9	18.2	5.7	1097	165	1	0.001	1	0.045	1	0.049	1	0.001	0	0.303
10	899.6	999.7	950.3	15.5	52.6	1023	194	1	0.000	1	0.000	1	0.049	1	0.013	1	0.003
11	999.7	1098.7	1049.0	-0.7	55.9	925	173	1	0.000	1	0.000	1	0.009	1	0.000	1	0.000
12	1098.7	1197.6	1148.3	12.9	85.0	819	144	1	0.000	1	0.000	1	0.210	1	0.000	1	0.000
13	1197.6	1298.6	1246.8	0.3	79.5	759	154	1	0.000	1	0.000	1	0.500	1	0.000	1	0.000
14	1298.6	1399.2	1350.5	5.9	74.0	700	133	1	0.001	1	0.000	1	0.347	1	0.023	1	0.001
15	1399.2	1498.9	1448.0	2.5	83.4	686	109	1	0.000	1	0.001	1	0.500	1	0.000	1	0.003
16	1498.9	1599.8	1549.9	-13.5	71.3	657	111	1	0.000	1	0.001	1	0.448	1	0.000	1	0.001
17	1599.8	1700.8	1649.7	8.4	56.3	558	79	0	0.119	0	0.053	1	0.500	0	0.310	0	0.055
18	1700.8	1800.2	1751.9	3.5	1.6	596	80	0	0.083	0	0.428	1	0.031	1	0.020	0	0.943
19	1800.2	1899.8	1848.5	1.9	64.4	584	99	1	0.000	1	0.001	1	0.024	1	0.002	1	0.016
20	1899.8	2002.1	1951.1	8.2	78.0	641	87	1	0.000	1	0.000	1	0.001	0	0.182	1	0.002
21	2002.1	2102.5	2053.1	-10.5	30.1	727	102	1	0.031	1	0.032	1	0.023	0	0.968	1	0.036
22	2102.5	2215.4	2151.8	-25.6	4.7	920	155	1	0.023	1	0.006	1	0.001	0	0.325	1	0.031
23	2215.4	2279.1	2279.1	-16.4	-8.9	3677	604	1	0.000	1	0.000	1	0.001	0	0.163	1	0.029

Bin no.	Plage de puissance		Pref	Écart Moyenne	LCI	UCI	Analyses des gains énergétiques			Incertitudes			
	Pinf	Psup					Weibull [hr]	Weibul [%]	Gain [kWh]	u1(Type A) [kW]	u2(Type B) [kW]	u(Combinée) [kW]	(FiSi)^2
1	0.0	101.0	51.8	3.8	0.0	7.5	2003.6	0.2	0.0	3.74	0.08	3.74	0.00
2	101.0	200.1	150.2	13.6	8.3	19.0	679.0	0.1	9260.1	5.35	0.22	5.36	0.17
3	200.1	299.6	250.1	17.6	9.3	26.0	508.4	0.1	8960.5	8.36	0.37	8.36	0.24
4	299.6	398.7	349.2	21.0	12.3	29.7	444.3	0.1	9329.6	8.73	0.51	8.75	0.20
5	398.7	499.3	448.2	21.3	10.6	32.0	373.3	0.0	7942.0	10.70	0.65	10.72	0.21
6	499.3	599.6	550.4	28.0	14.8	41.2	358.5	0.0	10038.9	13.20	0.80	13.22	0.29
7	599.6	699.3	648.9	39.1	22.0	56.2	269.7	0.0	10541.9	17.06	0.95	17.09	0.28
8	699.3	799.3	749.8	27.5	6.7	48.4	264.6	0.0	7285.0	20.85	1.09	20.87	0.40
9	799.3	899.6	848.9	-12.5	-36.3	11.4	258.3	0.0	0.0	23.85	1.24	23.88	0.00
10	899.6	999.7	950.3	37.1	13.0	61.2	200.6	0.0	7449.4	24.08	1.39	24.12	0.31
11	999.7	1098.7	1049.0	56.6	26.9	86.3	189.9	0.0	10746.1	29.74	1.53	29.78	0.42
12	1098.7	1197.6	1148.3	72.1	36.9	107.4	184.2	0.0	13288.3	35.23	1.68	35.27	0.55
13	1197.6	1298.6	1246.8	79.2	39.6	118.8	182.3	0.0	14444.0	39.57	1.82	39.62	0.68
14	1298.6	1399.2	1350.5	68.1	28.8	107.4	155.8	0.0	10609.3	39.32	1.97	39.37	0.49
15	1399.2	1498.9	1448.0	80.9	28.9	132.9	147.6	0.0	11936.0	51.99	2.11	52.03	0.77
16	1498.9	1599.8	1549.9	84.8	35.6	133.9	144.2	0.0	12225.4	49.15	2.26	49.20	0.66
17	1599.8	1700.8	1649.7	48.0	-1.0	97.0	139.3	0.0	0.0	49.01	2.41	49.07	0.00
18	1700.8	1800.2	1751.9	-1.9	-55.2	51.3	151.1	0.0	0.0	53.27	2.56	53.33	0.00
19	1800.2	1899.8	1848.5	62.6	11.7	113.5	180.7	0.0	11312.6	50.90	2.70	50.97	1.11
20	1899.8	2002.1	1951.1	69.7	26.1	113.4	174.5	0.0	12170.2	43.62	2.85	43.71	0.76
21	2002.1	2102.5	2053.1	40.5	2.7	78.3	190.6	0.0	7725.1	37.81	3.00	37.93	0.68
22	2102.5	2215.4	2151.8	30.3	2.8	57.8	337.0	0.0	10216.6	27.51	3.14	27.69	1.13
23	2215.4	2279.1	2279.1	7.5	0.8	14.2	1221.1	0.1	9154.7	6.71	3.33	7.49	1.09

Table-A V-3 Statistical Tests for WTG#5 and WTG#6

Bin no.	Plage de puissance		Pref	ÉcartREF	ÉcartTST	No. of data		Test_Dist		Test_median		Test_Normal		Test_sigma		Test_moyenne	
	Pinf	Psup				Reference	Test	h	p	h	p	h	p	h	p	h	p
1	0.0	99.2	49.8	4.1	4.4	1480	109	0	0.611	0	0.416	1	0.058	0	0.655	0	0.922
2	99.2	198.2	148.7	10.8	14.3	1219	65	1	0.001	1	0.022	1	0.019	0	0.688	0	0.502
3	198.2	298.1	247.7	11.9	17.6	925	86	0	0.105	0	0.134	1	0.186	0	0.434	0	0.410
4	298.1	398.5	348.6	9.8	8.5	723	55	0	0.421	0	0.790	1	0.355	0	0.415	0	0.908
5	398.5	499.0	448.4	9.7	12.0	613	90	0	0.270	0	0.784	1	0.005	1	0.000	0	0.888
6	499.0	597.9	549.5	9.8	17.6	524	67	0	0.222	0	0.665	1	0.017	1	0.000	0	0.722
7	597.9	698.1	646.4	17.8	-27.7	417	65	1	0.006	0	0.172	1	0.500	1	0.000	0	0.135
8	698.1	799.7	749.9	14.7	7.6	348	57	1	0.008	0	0.487	1	0.500	1	0.000	0	0.872
9	799.7	898.7	849.4	7.4	-19.8	289	54	0	0.055	0	0.432	1	0.159	1	0.000	0	0.479
10	898.7	998.1	947.9	1.7	60.2	256	46	1	0.004	1	0.005	1	0.060	1	0.000	0	0.188
11	998.1	1099.2	1048.3	-14.9	71.0	206	63	1	0.001	1	0.000	1	0.301	1	0.013	1	0.007
12	1099.2	1196.8	1150.2	10.5	27.7	183	44	0	0.687	0	0.496	1	0.471	0	0.445	0	0.623
13	1196.8	1297.9	1243.5	0.6	36.4	168	40	0	0.734	0	0.580	1	0.500	0	0.513	0	0.303
14	1297.9	1401.2	1352.3	38.8	51.9	138	39	0	0.840	0	0.922	1	0.500	0	0.880	0	0.763
15	1401.2	1497.9	1450.0	18.9	100.5	139	24	0	0.000	0	0.000	0	0.000	0	0.000	0	0.000
16	1497.9	1598.1	1545.8	-32.6	-108.5	122	13	0	0.000	0	0.000	0	0.000	0	0.000	0	0.000
17	1598.1	1700.9	1650.5	-13.0	67.6	102	7	0	0.000	0	0.000	0	0.000	0	0.000	0	0.000
18	1700.9	1805.2	1751.3	-36.3	-60.6	72	11	0	0.000	0	0.000	0	0.000	0	0.000	0	0.000
19	1805.2	1903.2	1859.1	-57.8	-146.0	76	8	0	0.000	0	0.000	0	0.000	0	0.000	0	0.000
20	1903.2	1999.9	1947.2	-32.8	-122.4	88	9	0	0.000	0	0.000	0	0.000	0	0.000	0	0.000
21	1999.9	2101.7	2052.6	-63.2	-128.5	74	14	0	0.000	0	0.000	0	0.000	0	0.000	0	0.000
22	2101.7	2210.9	2150.9	-36.0	-101.4	85	20	0	0.000	0	0.000	0	0.000	0	0.000	0	0.000
23	2210.9	2270.9	2270.9	-44.0	-29.9	214	99	1	0.000	1	0.001	1	0.001	0	0.913	0	0.334

Bin no.	Plage de puissance		Pref	ÉcartREF	Écart Moyenne	LCI	UCI	Analyses des gains énergétiques			Incertitudes			
	Pinf	Psup						Weibull [hr]	Weibull [%]	Gain [kWh]	u1(Type A) [kW]	u2(Type B) [kW]	u(Combinée) [kW]	(FiSi)^2
1	0.0	99.2	49.8	4.1	0.2	-4.5	5.0	1991.6	0.2	0.0	4.78	0.07	4.79	0.00
2	99.2	198.2	148.7	10.8	3.5	-6.8	13.9	681.2	0.1	0.0	10.32	0.22	10.32	0.00
3	198.2	298.1	247.7	11.9	5.7	-7.9	19.4	510.4	0.1	0.0	13.66	0.36	13.67	0.00
4	298.1	398.5	348.6	9.8	-1.3	-22.6	20.1	451.4	0.1	0.0	21.34	0.51	21.34	0.00
5	398.5	499.0	448.4	9.7	2.2	-28.8	33.2	372.8	0.0	0.0	31.03	0.65	31.04	0.00
6	499.0	597.9	549.5	9.8	7.8	-35.7	51.3	355.1	0.0	0.0	43.47	0.80	43.48	0.00
7	597.9	698.1	646.4	17.8	-45.5	-105.5	14.5	271.0	0.0	0.0	60.00	0.94	60.00	0.00
8	698.1	799.7	749.9	14.7	-7.1	-94.8	80.6	268.7	0.0	0.0	87.70	1.09	87.70	0.00
9	799.7	898.7	849.4	7.4	-27.3	-103.9	49.4	255.2	0.0	0.0	76.64	1.24	76.65	0.00
10	898.7	998.1	947.9	1.7	58.5	-29.5	146.4	199.9	0.0	0.0	87.95	1.38	87.96	0.00
11	998.1	1099.2	1048.3	-14.9	85.9	24.5	147.3	194.0	0.0	16668.6	61.39	1.53	61.41	1.85
12	1099.2	1196.8	1150.2	10.5	17.3	-51.8	86.3	181.8	0.0	0.0	69.07	1.68	69.09	0.00
13	1196.8	1297.9	1243.5	0.6	35.8	-32.5	104.2	182.4	0.0	0.0	68.37	1.81	68.40	0.00
14	1297.9	1401.2	1352.3	38.8	13.2	-73.0	99.3	160.0	0.0	0.0	86.14	1.97	86.16	0.00
15	1401.2	1497.9	1450.0	18.9	0.0	0.0	0.0	143.1	0.0	0.0	0.00	2.12	2.12	0.00
16	1497.9	1598.1	1545.8	-32.6	0.0	0.0	0.0	143.4	0.0	0.0	0.00	2.26	2.26	0.00
17	1598.1	1700.9	1650.5	-13.0	0.0	0.0	0.0	141.8	0.0	0.0	0.00	2.41	2.41	0.00
18	1700.9	1805.2	1751.3	-36.3	0.0	0.0	0.0	160.3	0.0	0.0	0.00	2.56	2.56	0.00
19	1805.2	1903.2	1859.1	-57.8	0.0	0.0	0.0	177.3	0.0	0.0	0.00	2.71	2.71	0.00
20	1903.2	1999.9	1947.2	-32.8	0.0	0.0	0.0	164.9	0.0	0.0	0.00	2.84	2.84	0.00
21	1999.9	2101.7	2052.6	-63.2	0.0	0.0	0.0	191.9	0.0	0.0	0.00	3.00	3.00	0.00
22	2101.7	2210.9	2150.9	-36.0	0.0	0.0	0.0	326.9	0.0	0.0	0.00	3.14	3.14	0.00
23	2210.9	2270.9	2270.9	-44.0	14.1	-14.6	42.8	1233.6	0.1	0.0	28.68	3.31	28.87	0.00

ANNEX VI

UNCERTAINTY ANALYSIS OF THE SIDE-BY-SIDE TESTING

The present appendix presents the details of the uncertainty analysis related to the side-by-side methodology. It first presents the mathematical reasoning for the Type A uncertainties; Type B uncertainties are presented afterwards.

The side-by-side methodology mainly consists of the comparison of a test turbine (WTtest) (for which changes in performance are expected) and a reference turbine (WTref) (whose power performance is assumed to remain unchanged for the duration of the testing). This method is completed over two different time periods, namely:

I. Period 1, corresponding to the period preceding the anticipated change in performance of WT_{test};

II. Period 2, corresponding to the period following the said change in performance of WT_{test}.

[1] Type A Uncertainty

Assuming turbines WT_{ref} and WT_{test} and the two periods of the side-by-side testing (Period 1 and Period 2), the power differences $(P_{WTtest} - P_{WTref})_{Period1}$ and $(P_{WTtest} - P_{WTtest})_{Period2}$ can be re-written as:

$$Y = (P_{WTtest} - P_{WTref})_2 - (P_{WTtest} - P_{WTref})_1 \qquad \text{(A VI-1)}$$

where:

Y is the energy gain for the tested turbine (WT_{test})

P_{WTtest} is the power output of the tested turbine (WT_{test})

P_{WTref} is the power output of the reference turbine (WT_{ref})

In order to further simplify Equation A IV-1, a change in variables has been applied to represent the power differences between the two turbines for the two time periods.

$$Z_1 = (P_{WTtest} - P_{TWref})_1 \quad \text{(A VI-2)}$$

$$Z_2 = (P_{WTtest} - P_{WTref})_2 \quad \text{(A VI-3)}$$

According to the GUM (2008) and the preceding changes in variables, the uncertainty in the power increase is expressed as:

$$u^2(Y) = u^2(Z_1) + u^2(Z_2) + 2u(Z_1,Z_2) \quad \text{(A VI-4)}$$

Equation 4 describes the Type A uncertainty in the difference in power for a given bin of power. The third term of Equation A IV-4 represents the uncertainty related to the covariance of the two terms (Z1 and Z2). Since the measurements for the two terms (Z1 and Z2) have taken place at different time periods, the observations between the two terms are therefore non-correlated and the covariance is expected to be zero. The remaining terms of Equation 4 are re-written as follows:

$$u^2(Z_1) = u^2(P_{WTtest,period1}) + u^2(P_{WTref,period1}) + 2u(P_{WTtest,period1},P_{WTref,period1}) \quad \text{(A VI-5)}$$

$$u^2(Z_2) = u^2(P_{WTtest,period2}) + u^2(P_{WTref,period2}) + 2u(P_{WTtest,period2},P_{WTref,period2}) \quad \text{(A VI-6)}$$

The final term in each of Equations A IV-5 and A IV-6 is the covariance of the corresponding measurements, and are expressed as:

$$u(P_{WTtest,period1}, P_{WTref,period1}) = r(P_{WTtest,period1}, P_{WTref,period1})u(P_{WTtest,period1}, P_{WTref,period1)} \quad \text{(A VI-7)}$$

$$u(P_{WTtest,period2}, P_{WTref,period2}) = r(P_{WTtest,period2}, P_{WTref,period2})u(P_{WTtest,period2}, P_{WTref,period2)} \quad \text{(A VI-8)}$$

The correlation coefficient (r) of the power signals of the two turbines is actually an indication of the level of concordance between the power output of the test and reference

turbines. Figure-A VI-1 presents the level of correlation between the power output of WTG#3 and WTG#4.

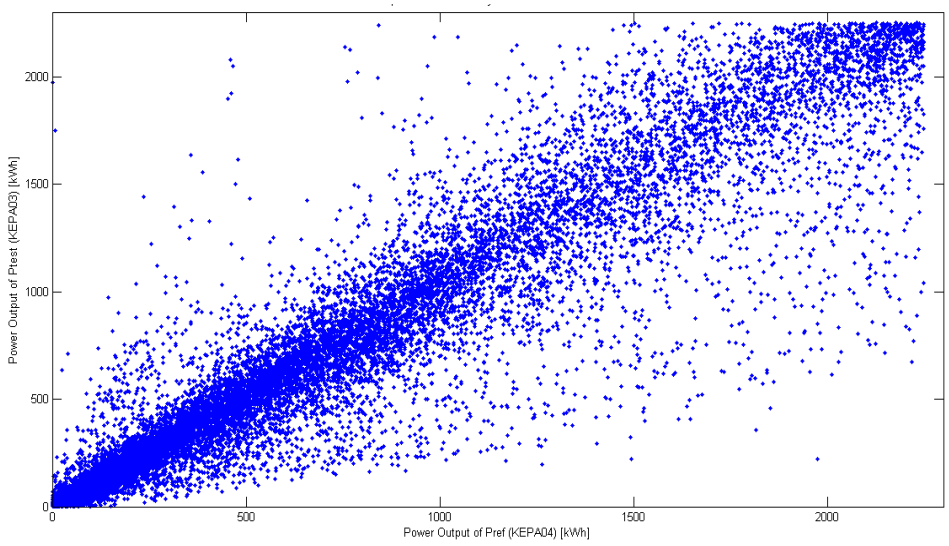

Figure-A VI-1 Power Output Correlation Analysis between WTG#3 & WTG#4

The correlation coefficient for the preceding figure has a value of 0.9368. The level of correlation will depend on the turbine separation distance and the complexity of the terrain. Thus the uncertainties expressed in Equations 5 and 6 are reduced as the correlation of the power outputs of the two turbines under study is improved.

6.5.1.1 Type B Uncertainty

According to the (GUM, 2008), Type B uncertainties are usually evaluated based on means other than statistical analysis of the observed data series. These types of uncertainties are generally obtained from an assumed probability distribution based on available information (i.e. previous measurements, calibration reports, manufacturer's specifications, references from handbooks or professional judgment). Generally, Type B uncertainties need to be evaluated for sensors such as anemometers, thermometers, power transducers, etc.

In the side-by-side evaluation only the Type B uncertainty for the power transducers is needed since other instruments are not involved in this type of analysis.

Assuming the use of Class 02 current transformers (as suggested by the Manufacturer), the uncertainty limit at 20% load is +/-0.35% for a rectangular distribution, which gives an uncertainty of 0.2% (GUM 2008).

$$u_{ct,i} = \frac{0.35\%\ P_i[kW]}{\sqrt{3}} = 0.2\%\ P_i[kW] \qquad \text{(A VI-9)}$$

Likewise, for Class 05 power converters (again, as suggested by the manufacturer), and assuming a rectangular distribution, the uncertainty in measurement is expressed as follows:

$$u_{pc,i} = \frac{0.5\%\ P_i[kW]}{\sqrt{3}} = 0.29\%\ P_i[kW] \qquad \text{(A VI-10)}$$

The combined uncertainty in the power measurement system of a given wind turbine can now be determined using the following equation:

$$u_{p,i} = \sqrt{{u_{ct,i}}^2 + {u_{pc,i}}^2 + 2u(P_{ct}, P_{pc})} \qquad \text{(A VI-11)}$$

The last term of this equation can be assumed to be equal to zero since no correlation exists between these two components of the power transducer.

The total uncertainty in the measurement of Y (Equation A IV-1) can now be obtained by combining the uncertainties according to the following equation which considers the fact that two power transducers are installed on two different turbines and that a difference in power is calculated between a reference and a testing period:

$$u_{P,i} = \sqrt{4(0.2\%P_i)^2 + 4(0.29\%P_i)^2} = 0.7\%P_i \text{ [kW]} \quad \text{(A VI-12)}$$

Lastly, Equation A IV-13 provides the level of uncertainty for a single measurement of the power increase for a given bin. Since the present analysis pertains to the evaluation of the average difference in power output for a given bin, the uncertainty in the mean should be considered. The following formula will provide this estimate:

$$\overline{u_{p,i}} = \frac{u_{P,i}}{\sqrt{N_i}} \quad \text{(A VI-13)}$$

where:

N_i is the number of data available for each power bin

REFERENCES

Albers, Axel. 2004. « Relative and Integral Wind Turbine Power Performance Evaluation ». In *European Wind Energy Conference & Exhibition*. (London, UK, 22-25 November). EWEA.

Albers, Axel. 2010. « Turbulence and Shear Normalisation of Wind Turbine Power Curve ». In *European Wind Energy Conference*. (Warsaw, Poland, 21-22 April).

Albers, Axel, Tim Jakobi, Rolf Rohden et Jurgen Stoltenjohannes. 2007. « Influence of Meteorological Variables on Measured Wind Turbine Power Curves ». In *European Wind Energy Conference*. (Milan, Italy, 2007).

Alinot, Cédric, et Christian Masson. 2002. « Aerodynamics of Wind Turbines in Thermally Stratified Turbulent Atmospheric Boundary Layer ». In *10th Annual conference of the CFDSC*. (Windsor, June 2002), p. 553-559.

Anahua, E., St. Barth et J. Peinke. 2008. « Markovian power curves for wind turbines ». *Wind Energy,* vol. 11, n^{o} 3, p. 219-232.

Anahua, Edgar. 2007. « Stochastic Analysis of Wind Turbine Power Curves ». Oldenburg, Russia, Carl Von Ossietzky Universitat.

Angelou, N., Jakob Mann, M. Courtney et M. Sjoholm. 2010. *Doppler lidar mounted on a wind turbine nacelle - UPWIND deliverable D6.7.1*. National Laboratory for sustainable Energy, Risoe DTU.

Antoniou, Ioannis, Rozenn Wagner, Søren M. Pedersen, Uwe Paulsen, Helge A. Madsen, Hans E. Jørgensen, Kenneth Thomsen, Peder Enevoldsen et Leo Thesbjerg. 2007. « Influence of wind characteristics on turbine performance ». In *European Wind Energy Conference & Exhibition*. (Milan, Italy).

Asension-Cuesta, S., J.A. Diego-Mas et J. Alcaide-Marzal. 2010. « Applying generalised feedforward neural netwoks to classifying industrial jobs in terms of risk of low disorders ». *Elsevier,* vol. 40, n^{o} 6, p. 629-635.

Auld, V., R. Hill et T.J. Taylor. 2003. *Uncertainty in deriving dispersion parameters from meteorological data*. UK atmospheric Dispersion Modelling Liaison Committee.

Bailey, Bruce, Scott McDonald, Daniel Bernadett, Michael Markus et Kurt Elsholz. 1997. *Wind Resource Assessment Handbook: Fundamentals for Conducting a Successful Monitoring Program*.

Baléo, J.-N., B. Bourges, Ph. Courcoux, C. Faur-Brasquet et P. Le Cloirec. 2003. *Méthodologie Expérimentale - Méthodes et outils pour les expérimentations expérimentales scientifiques*. École des mines de Nantes.

Beattie, Andrew. 2001. « Wind Turbine Power Performance Assessment Under Real conditions ». Loughborough University.

Bell, Benjamin. 2008. « Individual Wind Turbine and Overall Power Plant Performance Verification ». In *AWEA Asset Management Workshop*. (San Diego, January 17-18 2008). AWEA.

Boettcher, Frank, J. Peinke, D. Kleinhans et R. Friedrich. 2007. « Handling systems driven by different noise sources: Implications for Power Curve Estimations ». In *Wind Energy*, sous la dir. de Heilelberg, Springer Berlin. p. 179-182.

Bunse, U., et H. Mellinghoff. 2008. « Assessment of Wind Profile Effects for a Set of Site Calibration Measurments following IEC 61400-12-1 ». *Dewi-Magazin,* vol. February 2008, p. 27-31.

Carolin, Mabel, M. 2008. « Analysis of wind power generation and prediction using ANN: A case study ». *Renewable Energy,* vol. 33, n^{o} 5, p. 986-992.

Cattin, René. 2012. *Icing of Wind turbines - Windforsk projects, a survey of the development and reasearch needs*. Elforsk report 12:13.

Clifton, A., L. Kilcher, J.K. Lundquist et P. Fleming. 2013. « Using machine learning to predict wind turbine power output ». *Environmental Research Letters, 8(2), 024009*.

Curvers, et P.A. Werff. 2001. *Identification of Variables for Site Calibration and Power Curve Assessment in Complex Terrain*. ECN-C-02-102.

Dakin, E.A. 2009. *Boosting Power Production - Project Report on Nebraska Public Power Disctrict - Vindicator LWS Field Trial*. Catch the Wind.

Dakin, Elizabeth Anne, Avishekh Pal, Frederick Belen et Michael Kupper. 2010. *Boosting Power Production Update*. Catch the Wind.

Dalili, N., A. Edrisy et R. Carriveau. 2007. « A review of surface engineering issues critical to wind turbine performance ». *ScienceDirect*, p. 428-438.

Dreyfus, G., J.-M. Martinez, M. Samuelides, M. B. Gordon, F. Badran, S. Thiria et L. Hérault. 2004. *Réseaux de neurones - Méthodologies et applications*. 375 p.

Frandsen, S., I. Antoniou, J.C. Hansen, L. Kristensen, Madsen, B. Chaviaropoulos, D. Douvikas, J.A. Dahlberg, A. Derrick, P. Dunbabin, R. Hunter, R. Ruffle, D.

Kanellopoulos et G. Kapsalis. 2000. « Redefinition power curve for more accurate performance assessment of wind farms ». *Wind Energy,* vol. 3, n^{o} 2, p. 81-111.

Fugon, Lionel, Jérémie Juban et George Kariniotakis. 2008. « Data mining for wind power forecasting ». In *European Wind Energy Conference*. (Brussels, Belgium, April 2008).

G.P., Van den Berg. 2008. « Wind Turbine Power and Sound in Relation to Atmospheric Stability ». *Wind Energy,* vol. 11, p. 151-169.

Gaumond, M., P.-E. Réthoré, S. Ott, A. Pena, A. Bechmann et K.S. Hanse. 2013. « Evaluation of the wind direction uncertainty and its impact on wake modeling at the Horns Rev offshore wind farm ». *Wind Energy doi: 10.1002/we.1625*.

Gottschal, J., et J. Peinke. 2008. « Power curves for wind turbines - a dynamical approach ». In *European Wind Energy Conference*. (Brussels, Belgium).

Graves, Anne-Marie, et Keir Harman. 2007. « Operating Wind Farm Monitoring and Performance Optimization - Sandia ». In *2nd Wind Turbine Reliability Workshop*. (September 17-18).

GUM, I.S.O. 2008. *Évaluation des données de mesure - guide pour l'expression de l'incertitude de mesure*. BIPM, IEC, IFCC, ISO, IUPAP, IUPAC, OIML.

Hannah, P. 1997. *Investigation of upflow on escarpments*. ETSU-W--36/00281/35/REP: Energy Technology Support Unit (ETSU).

Harman, K.D., et P.G. Raftery. 2003. « Analytical Techniques for Understanding the Performance of Operational Wind Farms ». In *European Wind Energy Conference*. (Madrid, Spain, 16-20 June).

Honhoff, Saskia. 2007. « Power curves: The effect of environmental conditions ». In *American Wind Energy Association Workshop*. (Portland, USA, 12-13 January).

Hunter, R., Troels Friis Pedersen, P. Dunbabin, I. Antoniou, S. Frandsen, Helmut Klug, Axel Albers et Kong Wai Lee. 2001. *European Wind Turbine Testing Procedure Developments - Task 1: Measurement Method to Verify Wind Tubine Performance Characteristics*. Risoe.

International Electrotechnical Commission. 2005. *IEC61400-12-1: Wind Turbines - Part12-1: Power performance measurements of electricity producing wind turbines*. 1st PPUB edn (Geneva, Switzerland: International Electrotechnical Commission).

International Electrotechnical Commission. 2012. *IEC61400-12-2 : Power performance of electricity producing wind turbines based on nacelle anemometry*. 1st PPUB edn (Geneva, Switzerland: International Electrotechnical Commission).

Kaiser, K., W. Langreder, H. Hohlen et J. Hojstrup. 2003. « Turbulence Correction for Power Curves ». In *European Wind Energy Conference*. (Madrid, Spain, 16-18 May).

Khalfallah, Mohammed. 2007. « Suggestions for improving wind turbines power curves ». *Elsevier*, n° 209, p. 221-229.

Klug, Helmut. 2007. « Wind Farm Performance Verfication ». In *23rd Canadian Wind Energy Association*. (Québec, October 1-3).

Kragh, K.A. 2013. « Performance Enhancement and Load Reduction on Wind Turbines Using Inflow Measurements ». DTU Institut for Vindenergi, 175 p.

Kusiak, Andrew, et Wenyan Li. 2011. « The Prediction and Diagnosis of Wind Turbine Faults ». *Renewable Energy,* vol. 36, n° 1, p. 16-23.

Kusiak, Andrew, Haiyang Zheng et Zhe Song. 2009a. « Models for monitoring wind farm power ». *Renewable Energy,* vol. 34, p. 583-590.

Kusiak, Andrew, Haiyang Zheng et Zhe Song. 2009b. « Power Optimization of Wind turbines with Data Mining and Evolutionary Computation ». *Renewable Energy,* vol. 35, p. 695-702.

Li, Shuhui. 2003. « Wind power prediction using recurrent multilayer perceptron neural networks ». In *Power Engineering Society General Meeting, 2003, IEEE*. Vol. 4, p. 2330 Vol. 4.

Li, Shuhui, Edgar O'Hair, Michael G. Giesselmann et Don C. Wunsch. 1998. « Comparative analysis of regression and neural network models for wind power ». In. (St.Louis, MO, USA) Vol. 8, p. 675-681. Coll. « Intelligent Engineering Systems Through Artificial Neural Networks »: ASME, Fairfield, NJ, USA.

Li, Shuhui, D. Wunsch, E. O'Hair et M. A. Glesselmann M. Glesselmann. 2001a. « Using neural networks to estimate wind turbine power generation ». In *Power Engineering Society Winter Meeting, 2001. IEEE*. sous la dir. de Wunsch, D. Vol. 3, p. 977 vol.3.

Li, Shuhui, Don C. Wunsch, Edgar O'Hair et Michael G. Giesselmann. 2001b. « Comparative analysis of regression and Artificial neural network models for wind turbine power curve estimation ». vol. 123, p. 327-332.

Lindahl, Staffan, et Keir Harman. 2012. « Analytical techniques for performace monitoring of modern wind turbines ». In *European Wind Energy Conference*. (Copenhagen, Danemark, 16-19 April).

Llombart, A., S.J. Watson, J.M. Fandos et D. Llombart. 2005a. « Power Curve Characterization II: modelling using polynomial regression ». In *International conference on renewable energies and power quality*. (Zaragoza Spain, 16,17,18 of March, 2005).

Llombart, A., S.J. Watson, D. Llombart et J.M. Fandos. 2005b. « Power Curve Characterization I: improving the bin method ». In *International conference on renewable energies and power quality*. (Zaragoza Spain, 16,17,18 of March, 2005).

Lumley, T., P. Diehr, S. Emerson et L. Chen. 2002. « The Importance of the Normality Assumption in Large Public Health Data Sets ».

Lydia, M., I. Selvakumar, S. Kumar et temp. 2013. « Advanced Algorithms for Wind Turbine Power Curve Modelling ».

Madsen, HA. 2000. « Yaw simulation using a 3D actuator disc model coupled to the aeroelastic code HAWC. ». In *IEA Joint Action, Aerodynamics of Wind Turbines*. (Stockholm), sous la dir. de Symposium, 13th, p. 133-146.

Maier, H.R., et G.C. Dandy. 2000. « Neural Networks for the prediction and forecasting of water resources variables: a review of modelling issues and applications ». *Elsevier*, p. 101-124.

Mamidipudi, Priyavadan, Elizabeth Anne Dakin et Andrew Hopkins. 2011. *Yaw Control - The Forgotten Controls Problem*. Catch the Wind.

Marvuglia, A. 2011. « Learning a wind farm power curve with a data-driven approach ». In *World Renewable Energy Congress*. (Linkoping, Sweden, 8-13 May).

Mikkelsen, Robert, Jens Sorensen, Stig Oye et Niels Troldborg. 2007. « Analysis of Power Enhancement for a Row of Wind Trubines Using the Actuator Line Technique ». *Journal of Physics: Conference Series 75*.

Montes, Estibaliz, Alberto Arnedo, Ruth Cordon et Rafael Zubiaur. 2009. « Influence of wind shear and seasonality on the power curve and annual energy production of wind turbines ». In *European Wind Energy Conference and Exhibition*. (Marseille, France, 16-19 March).

Parkes, Jeremy, Luis Munoz, Jack Wasey et Andrew Tindal. 2006. « Wind Energy Trading Benefits Through Short Term Forecasting ». In *European Wind Energy conference*. (Milan, Spain, 27feb-2March).

Pedersen, T. F. 2004. « On wind turbine power performance measurements at inclined airflow ». *Wind Energy,* vol. 7, n° 3, p. 163-176.

Pedersen, Troels Friis, Soren Gjerding, Peter Ingham, Peder Enevoldsen, Kjaer Jesper Hansen et Kanstrup Henrik Jorgensen. 2002. *Wind Turbine Power Performance Verification in Complex Terrain and Wind Farms*. Risoe.

Pelletier, F., et C. Masson. 2008. « Meteorology Based Maintenance ». In *Canadian Wind Energy Association*. (Vancouver, Canada).

Pelletier, F., C. Masson et A. Tahan. Submited date: March 2013, Under revision. « Wind Turbine Power Curve Modelling Using Artificial Neural Network ». *Renewable Energy*. .

Pelletier, Francis. 2007. « Planning for Wind Farm Performance Verification ». In *CanWEA - Wind Turbine Operations & Maintenance Seminar*. (Montréal, 21-22 novembre 2007).

Pelletier, Francis, Christian Masson et Antoine Tahan. 2010. « Modelling Through High Frequency Data Sampling and Other Advantages ». In *European Wind Energy Conference*. (Warsaw, Polland, 20-23 April).

Perovic, Srdjan, Ed Wilkinson, Glynn Lloyd, Paul Bridges et Mark Osborne. 2010. « Wind Turbine Yaw Misalignment Cost-effective Detection and Correction ». In *The Windpower 2010 Conference & Exhibition*. (Dallas, USA, 3-5 May). American Wind Energy Association.

Pinson, P., H.A. Nielsen et H. Madsen. 2007. *Robust Estimation of Time-varying Coefficient Functions - Application to the Modeling of Wind Power Production*. Lyngby, Denmark: Technical University of Denmark.

Radecke, Van H. 2004. « Turbulence Correction of Power Curves ». *Dewi-Magazin,* vol. February 2004, p. 56-62.

Randal, Gordon. 2008. « Scada Data Mining and IT Needs to Improve Plant Operation and Downtime ». In *AWEA Asset Management Workshop*. (San Diego, January 17-18 2008). AWEA.

Roeth, Jacques. 2010. *Wind Resource Assessment Handbook*. New York State Energy Research and Development Authority. NYSERDA9998.

ROMO. 2013. « ROMO Wind ». < www.romowind.com >. Consulted 7 March 2013.

Sainz, E., A. Llombart et J.J. Guerrero. 2009. « Robust filtering for the characterization of wind turbines: Improving its operation and maintenance ». *Energy Conversion and Management,* vol. 50, p. 11.

Sumner, Jonathon, et Christian Masson. 2006. « Influence of Atmospheric Stability on Wind Turbine Power Performance Curves ». *Journal of Solar Energy Engineering,* vol. 128, n^{o} 4, p. 531-538.

TC88WG6, International Electrotechnical Commission / IEC. 2004. *IEC61400-12-3 : Wind Turbines - Part12-3: Wind Farm Power Performance Testing (DRAFT) - version 4*.

Technocentre Éolien. 2012. < https://www.eolien.qc.ca/ >. Consulted April 9, 2012.

Tukey, J.W. 1977. *Exploratory Data Analysis*. Addisson-Wesley.

Wagner, Rozenn. 2010. « Accounting for the Speed Shear in Wind Turbine Power Performance Measurement ». Risoe-DTU - National Laboratory for Sustainable Energy, 124 p.

Wagner, Rozenn, M. Courtney, J. Gottschal et P. Lindelow-Marsden. 2010a. « Improvement of power curve measurement with lidar wind speed profiles ». In *EWEC2010*. (Warsaw, Poland).

Wagner, Rozenn, M. Courtney et Torben Larsen. 2010b. *Simulation of shear and turbulence impact on wind turbine performance*. RISO-R-1722(en).

Wilkinson, M., B. Darnel, T. Vand Delft et K D Harman. 2013. « Comparison of Methods for Wind Turbine Condition Monitoring with Scada Data ». In *European Wind Energy Conference*. (Vienna, Italia).